Injectable Chondroitin Sulfate-Based Hydrogel Drug Delivery Systems

A Major Qualifying Quarterly Project Report submitted to the faculty of

WORCESTER POLYTECHNIC INSTITUTE

in partial fulfillment of the Degree of Bachelor Science.

Submitted By:

Camila Carvalho

Camila Carvalho

Brianna McCuaig

Brianna McCuaig

Nicole Racca

Nicole Racca

Corinne Saucier

Corinne Saucier

April 27th, 2022

Professor Jeannine M. Coburn, Ph.D., Advisor

Department of Biomedical Engineering

Table of Contents

Table of Figures

Table of Tables

Abstract

Neuroblastoma is the most common extracranial solid tumor diagnosed in children ages 10 years and younger. The current gold standard treatment for neuroblastoma is systemic chemotherapy, which results in the death of both healthy and malignant cells and has adverse effects that negatively impact development in children. Localized delivery of chemotherapeutics with the ability for sustained release is therefore desirable to reduce off-target complications. One method that has been recently explored to achieve this localized delivery and sustained release is hydrogel-based drug delivery systems. This project aims to design, fabricate, and validate a hydrogel-based drug delivery system that has an acceptable injection force profile for the localized intra-tumoral delivery of chemotherapeutics. The final hydrogel formulation will be evaluated for efficacy via a dimethyl-methylene blue assay, injection force testing, and daunorubicin loading and release assays. After evaluating three design approaches the team concluded on using 10% 4 h methacrylated chondroitin sulfate hydrogels that are UV-A light cured, to produce a hydrogel drug delivery system that is compatible with the loading of the chemotherapeutic agent daunorubicin. Upon further testing it was found that the hydrogel system was able to provide reproducible drug loading, remain insoluble and provide a sustained drug release profile over 30 days. When the system was further tested with injection force testing using a 2 kN Instron, it was found that the hydrogel had a non-reproducible injection for and an average force of 38 N, showcasing that this system did not meet the target for reproducibility and target injection force. Although these targets were not met, further conclusions were made to generate a fabrication technique that can meet these requirements.

Acknowledgements

The team would like to thank the Coburn Lab at the Gateway Biomedical Engineering Department of WPI for supervision during lab experiments and answering the many questions asked by the team. A special thanks goes to advisor Dr. Jeannine M. Coburn, for her guidance and thorough feedback on all aspects of the project. Additionally, the team would like to thank Kate Mistretta for her mentorship and providing valuable feedback. Lastly, the team would like to thank Lisa Wall for her help in gathering necessary project materials.

Authorship

All authors contributed equally to this work.

Glossary

C

CGT

Critical Gelation Temperature

CH

Chitosan

CH-DA

Chitosan-Grafted-Dihydrocaffeic Acid

CNS

Central Nervous System

CS

Chondroitin Sulfate

CS-MA

Methacrylated Chondroitin Sulfate

D

DDS

Drug Delivery System(s)

DMMB

Dimethyl-Methylene Blue

DNR

Daunorubicin

DOX

Doxorubicin

DS

Degree of Substitution

E

ECM

Extracellular Matrix

EULAR

European League Against Rheumatism

F

FRP

Free-Radical Polymerization

F127

Pluronic F127

G

GA

Glycolic Acid

GAG

Glycosaminoglycan

Glc-NAc

N-acetylglucosamine

GMA

Glycidyl Methacrylate

H

HA

Hyaluronic Acid

L

LA

Lactic Acid

LCGT

Lower Critical Gelation Temperature

LCST

Lower Critical Solution Temperature

LLC

Lyotropic Liquid Crystalline

M

MQP

Major Qualifying Project

N

NB

Neuroblastoma

O

OA

Osteoarthritis

OARSI

Osteoarthritis Research Society International

OP

Oxidized Pullulan

OW

Oil-in-Water

OWO

Oil-in-Water-in-Oil

P

PEC

Polyelectrolyte Complexes

PECE or PEG-PCL-PEG

Poly(ethylene glycol)-poly(caprolactone)-poly(ethylene glycol)

PECT

Poly(ε-caprolactone-co-1,4,8-trioxa[4.6]spiro-9-undecanone)-poly(ethylene glycol)-poly(ε-caprolactone-co-1,4,8-trioxa[4.6]spiro-9-undecanone)

PEG

Polyethylene Glycol

PEI-Lys

Polylysine-Modified Polyethylenimine

PEO

Polyethylene Oxide

PEO-PPO-PEO

Polyethylene oxide-polypropylene oxide-polyethylene oxide

PLGA

Poly(lactic acid-co-glycolic acid)

PLGA-PEG-PLGA

Poly(dl-lactide-co-glycolide-b-ethylene glycol-b-dl-lactide-co-glycolide)

PNIPAM

Poly(N-isopropylacrylamide)

PWC

Pairwise Comparison Chart

S

SNS

Sympathetic Nervous System

SOP

Standard Operating Procedure

U

UCGT

Upper Critical Gelation Temperature

W

WO

Water-in-Oil

WOW

Water-in-Oil-in-Water

WPI

Worcester Polytechnic Institute

#

3D

3-Dimensional

I. Introduction

Neuroblastoma (NB) is a cancer derived from the sympathoadrenal progenitor cells of the neural crest (Matthay et al., 2016). The neural crest is part of the sympathetic nervous system (SNS) meaning that NB can present itself anywhere along the SNS (Johnsen et al., 2019). With 90% of tumors occurring in patients 10 years or younger, NB is the most common extracranial solid tumor diagnosed in children. The current gold standard treatment for high-risk NB is cytotoxic chemotherapy, which is inherently systemic. While this method is effective in killing cancerous cells, chemotherapeutic agents are unable to differentiate between healthy and malignant cells, resulting in the undesirable death of healthy cells. This is especially detrimental in children because the death of healthy cells can negatively impact development. One method to reduce systemic exposure is to administer the therapeutics locally into the tumor site. An example of this local administration involves the use of hydrogel drug delivery systems (DDS).

A hydrogel is a 3-dimensional (3D) non-water soluble network of hydrophilic polymers that swell in water (Fan et al., 2019). Hydrogels loaded with chemotherapeutics have been researched for their applications in drug delivery systems to allow for a controlled release of biologically active compounds that possess desired local effects and minimize systemic exposure (Elias et al., 2015; Ma et al., 2015; Pan et al., 2018; Wang et al., 2013; Bu et al., 2017). Hydrogels may be used for direct delivery into targeted sites to allow for a local release of a biologically active compound which decreases toxicity to only where the tumor cells lie (Fan et al., 2019). While the focus of this project is the treatment of NB, other cancer types such as osteosarcoma have seen increased benefits during animal trials of the direct introduction of therapeutics to the tissue system that the cancer effects via hydrogel DDS. Professor Jeannine M. Coburn's Lab at Worcester Polytechnic Institute (WPI) has developed a chondroitin sulfate-based hydrogel that is capable of the loading and slow release of cationic chemotherapeutics. This is intended to provide a more localized approach to anti-cancer therapeutics where the chondroitin sulfate (CS) hydrogels make possible the sustained release of positively charged therapeutics over the course of days or weeks. This hydrogel is intended to be injected directly into the tumor site; however, the injection force required to extrude 20 μL of the hydrogel through a 27 G needle is too great to allow for applications in a clinical setting.

The goal of this project is to fabricate CS drug delivery vehicles loaded with chemotherapeutics for the treatment of NB that can be injected with a force that is feasible for clinical application. Various techniques can be used to decrease injection force, including but not limited to, mechanical changes to the injection system, mechanical methods of decreasing viscosity, and chemical changes to the hydrogel to decrease viscosity. Each of these techniques will be discussed in detail in Section 2.6.

II. Literature Review

2.1 Neuroblastoma

2.1.1 Characteristics

NB is an embryonal tumor that develops in the SNS and is derived from the neural crest (Matthay et al., 2016). Because of its derivation from the sympathoadrenal progenitor cells of the neural crest, NB can present itself anywhere along the SNS (Johnsen et al., 2019). The neuronal cell bodies of the central nervous system (CNS) form their sympathetic innervations at the thoracic and lumbar regions of the spinal cord and the efferent nerve fibers leave the spinal cord and make their first synaptic connections in the abdomen, with the prevertebral sympathetic ganglia (Wood, 2004). Although primary tumor locations also include the chest, neck, and pelvis; the abdomen accounts for approximately 65% of primary NB sites (Chu et al., 2011).

Two common genetic mutations have been associated with NB, MYCN amplification and ALK mutation. Although MYCN amplification is only identified in 20 to 30% of NB patients, the overall survival rate of patients with this mutation is less than 50%, making MYCN amplification a strong predictor of overall risk in NB patients (Otte et al., 2021). ALK mutations are slightly less common, with presence in only about 9% of primary NB tumors and approximately 14% in high-risk tumors; this mutation is also considered a strong predictor of poor prognosis in high-risk patients (Trigg & Turner, 2018). In a 2012 study by Zhu et al., it was found that when comparing zebrafish with either MYCN or ALK and zebrafish with both MYCN and ALK, those expressing both genes had a higher probability, and rate, of tumor induction than those expressing only one gene (Otte et al., 2021).

2.1.2 Patient Demographics

NB is a unique tumor that has a tendency for spontaneous tumor regression when diagnosed <18 months of age, an early age of onset compared to other cancers, and a high frequency of metastatic disease at diagnosis (Matthay et al., 2016). With 90% of tumors occurring in patients 10 years or younger; NB is the most common extracranial solid tumor diagnosed in children. The median age of diagnosis is 18 months, with 40% of patients diagnosed at infancy. The age of diagnosis is very telling of the patients' likely outcome, with patients 18 months and younger more likely to undergo spontaneous regression, and lower survival rates associated with patients diagnosed when older than 18 months. The location of the

primary tumor can also be highly prognostic, with tumors located in the medulla of the adrenal glands associated with lower survival rates in comparison to other primary tumor sites. In addition to age and the location of the primary tumor, clinical presentation of NB is also dependent on the sites of metastasis. Metastatic disease is identified in approximately 50% of patients most frequently in the regions of the lymph nodes, bone marrow, and bone. Liver and skin metastases are also common in infants younger than 18 months.

2.1.3 Current Treatment Methods

Progression of NB is commonly characterized based on stages 1-4, which correlate to low (Stage 1), intermediate (Stage 2), and high risk (Stage 3 & 4) assessments which dictates the level of treatment/intervention per patient (Insitute, 2021). Patients with NB are placed into these risk assessment groups which also depends on other prognostic factors such as age, tumor histology, specific changes in chromosome 11 in present tumor cells, the number of chromosomes present in tumor cells, and the presence or absence of MYCN gene amplification (Society, 2021b). Stage 1 patients tend to have tumors that are central to one area and can be removed in full via surgery. Patients with stages 2-4 refer to those whose cancer may have already spread to other regions or to patients in situations where the full extent of the tumor is not able to be removed via surgical intervention. These risk assessments help determine treatment plans for the patients depending on the severity of their disease.

For patients classified as low risk NB, surgical intervention is the first line of treatment, and it is highly likely that due to its centralized location, the tumor can be completely removed (Pinto et al., 2015). As touched upon previously, some infants with these localized tumors do not require any surgery or plan of intervention and will still see a spontaneous tumor regression. Patients diagnosed with stage 1 NB have an overall survival rate of 96% and are often cured from NB following surgery alone. Patients with stage 2 NB tend to have a tumor in one central location but portions of it may not be visible during surgery, or only part may be removed as it is in close contact to other vital tissues. These patients tend to receive surgical intervention, but without clear margins, the complete solid tumor mass may not be removed. Surgical intervention for these patients can be supplemented with cytotoxic chemotherapy or radiotherapy. Patients with Stage 2 NB have a 96% survival rate 3 years after the treatment intervention. Other patients classified under Stages 3 & 4 NB are due to the growth and migration of cancer cells to additional regions of the body and the proximal growth of the solid tumor in areas of highly

sensitive tissues, with stage 4 including the migration of cancer cells to distant lymph nodes. Patients of high risk have tumors that may not be completely removed through surgical intervention and additional regions of the body where the cancer has metastasized. These patients go through surgical intervention where the initial solid tumor mass may be removed, and then the surgical treatment is supplemented with 5 to 6 rounds of chemotherapy. Stage 3 and 4 patients have the worst prognosis despite the multitude of treatment combinations.

Chemotherapy, a treatment in which a drug is administered for the primary purpose of irradicating cancer cells, is commonly administered following surgical intervention when the entire tumor mass cannot be removed. This compound may also be administered to consolidate the patient's tumor before removal of the tumor through surgery. The chemotherapy treatment regimen consists of multiple rounds, administered on consecutive days, with a break for the body to recover before subsequent rounds. One rotation tends to last 3 to 4 weeks, depending on the patient's identified risk level. Higher risk patients endure longer treatment durations. Treatment length is also dependent on the therapeutic being administered, the cancerous cells of interest, and the rate of mass loss of the tumor during chemotherapy treatment (Society, 2021c). Commonly used chemotherapeutic drug compounds include cyclophosphamide, doxorubicin (DOX), carboplatin, and etoposide for the treatment of NB tumors (Davidoff, 2012).

Chemotherapy is a standard treatment for all types of cancers. Chemotherapeutic agents are administered in various ways depending on the dosage control needed, efficacy, and toxicity profile. The six common routes of administration for chemotherapy are oral delivery, subcutaneous injection, intravenous delivery, topical treatments, intraperitoneal treatment, and intra-arterial treatment (Clinic, 2021). Some chemotherapeutics are not available to be administered orally because they are pH sensitive and are degraded in the highly acidic environment of the stomach.

Chemotherapeutic drugs also have their own disadvantages where the drug compounds cannot differentiate between healthy cells and those causing cancer, leading to cell death in healthy cells as well as metastatic (Society, 2021a). The lack of ability to differentiate between the healthy and cancerous cells causes damage to healthy tissues. Other common side effects patients may endure include shortness of breath, mouth sores, infection, hair loss, abdominal pain, back pain, diarrhea, tightness in the chest, bladder irritation, and low platelet counts. More severe side effects include fertility issues, loss of endocrine function, hearing loss for pediatric

patients, central neurotoxicity, peripheral neuropathy, and decrease in ability of heart pumping. To reduce the side effects and systemic exposure of chemotherapy, the drug compound may be delivered intratumorally to target the affected area directly and increase efficacy with increased intertumoral concentrations.

2.2 Chondroitin Sulfate

2.2.1 Chemistry and Properties

CS, as seen in Figure 1, is sulfated glycosaminoglycan (GAG) composed of a chain of alternating sugars, specifically repeating disaccharide units of β-1,3-linked *N*-acetyl galactosamine (GalNAc) and β-1,4-linked *D*-glucoronic acid (GlcA) with sulfates in certain positions (Zhao et al., 2015). CS is identified with a different letter according to the different positions of sulfation: chondroitin-4-sulfate (CS A), chondroitin-6-sulfate (CS C), chondroitin-2,6-sulfate (CS D), and chondroitin-4,6-sulfate (CS E). The average molecular weight for CS found in animal tissues is 20 kDa, which encompasses over 100 individual sulfated sugar units at various positions in the molecular chain. Typically, this naturally occurring biomaterial can be found in the cartilage of mammals including but not limited to bovine, porcine, shark, and squid cartilage. Depending on the type of CS, it may also be found in abundance in skin, extracellular matrix (ECM), nerve tissue, and blood vessels of mammals.

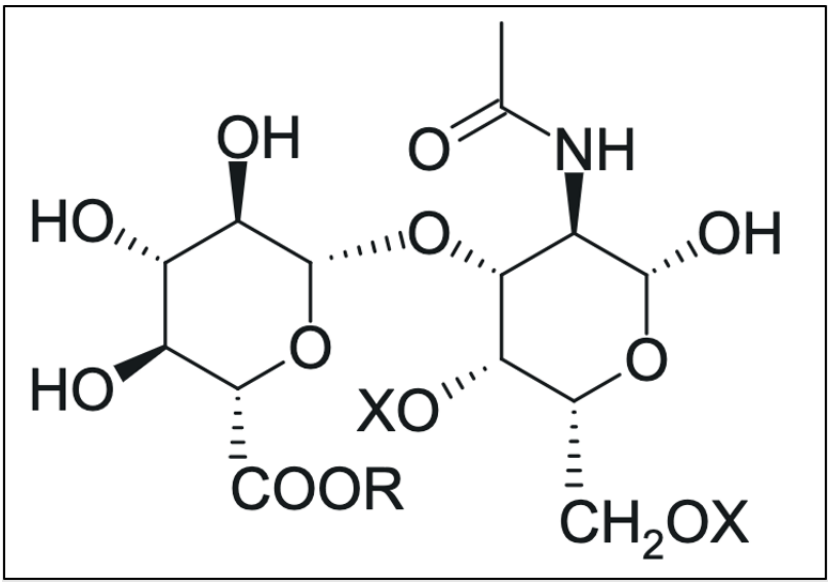

Figure 1: Chemical structure of CS, where R is Na or H and X is SO3R or H.

CS is a vital structural component of connective tissues and cartilage as it forma a network with collagen found in connective tissue, allowing for the transport of macromolecules like globular proteins (Wang et al., 2003). Additionally, in the biomedical field, many studies have addressed the therapeutic effects CS has on osteoarthritis patients, improving their articular function and reducing their overall pain (Wang et al., 2003). It is also imperative to note that natural CS is readily water-soluble, and consequently, many studies have pointed out how it might not have a sustained drug release profile. However, CS can be modified to allow for crosslinking into an insoluble biopolymer network, or hydrogel.

One successful technique of modifying CS to achieve a water insoluble hydrogel is completed in two steps: methacrylation and crosslinking (Fajardo et al., 2013; Li et al., 2003). For a GAG to become photo-crosslinkable it must first be methacrylated by functionalizing the hydroxyl groups with vinyl groups as shown in Figure 2. In the case of this project, the reagent used for this methacrylation process is glycidyl methacrylate (GMA). According to Fajardo et al. (2013), this reaction between CS and GMA can occur via two routes, a transesterification reaction or an epoxide ring-opening reaction. In the case of our project, this reaction is completed through the ring opening reaction where the GMA reacts with both functional groups in CS (carboxyl and hydroxyl) allowing methacrylate insertion into two different positions on the polysaccharide backbone: 3-methacryloyl-1-glycerol ester and 3-methacryloyl-2-glyveryl ester.

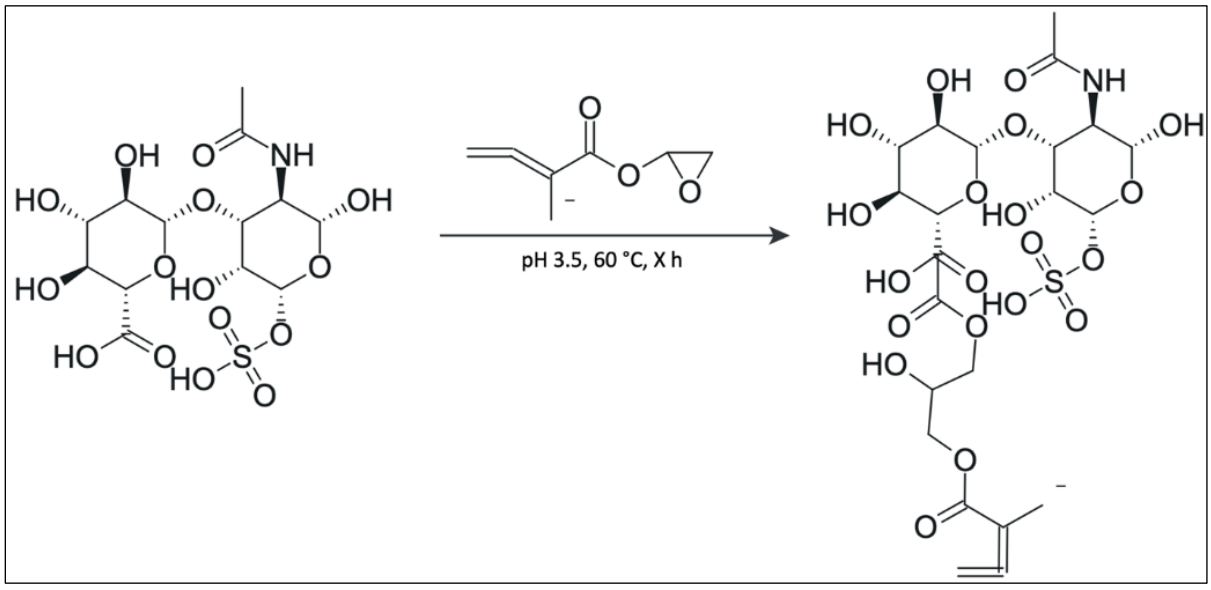

Figure 2: Mechanism for methacrylation of CS with GMA, where the methacrylation time, X, may vary.

Free-radical polymerization (FRP) is another method where a polymer forms through the formation of free-radical groups (Betancourt et al., 2010). For hydrogels, FRP is used to crosslink acrylate groups on water-soluble polymer chains. This allows for the binding of polymer groups due to the unpaired electron in their orbit (Coburn). Radical groups can be formed on methacrylated chondroitin sulfate (CS-MA) via the use of an initiator, e.g., Irgacure®2959, and UV light exposure. The Irgacure®2959 undergoes photolysis when exposed to UV light forming radical groups that are transferred to the methacrylate group within the CS-MA chains. When two radical groups on CS-MA chains react, they form a bond. As this reaction proceeds, a CS-MA hydrogel is formed, as shown in Figure 3.

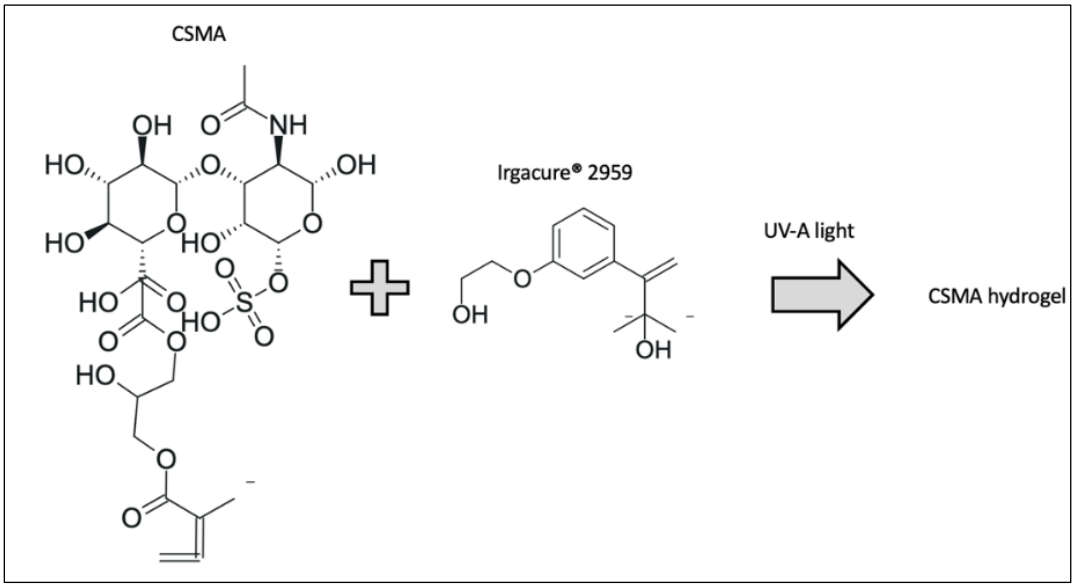

Figure 3: CS-MA chemical structure and the effect of Irgacure®2959 for hydrogel formation (Keutgen et al., 2021).

2.2.2 Chondroitin Sulfate Uses

There are several uses and applications for CS in the biomedical field. Its first, and major use, is related to the most common form of arthritis, osteoarthritis (OA). OA is a disease characterized by the progressive degradation of joint tissues, mainly cartilage, and the inflammation of synovial membrane (Henrotin et al., 2010). Treatment of OA involves various forms of therapeutic intervention and drugs that may slow or even stop joint degradation. CS, as previously defined, is a major component of cartilage, and is responsible for many of its biomechanical properties, including resistance and elasticity. CS assists in repair and formation

of bone, cartilage, and tendon, and helps tissues maintain their structural integrity; this also plays a role in modulating anti-inflammatory effects. (Bishnoi et al., 2016). Given these properties, CS is favorable in the treatment of OA and is one of the most widely used symptomatic slow acting orally administered drug for this purpose, though not approved by the FDA. CS has shown evidence of slowing down the development of OA when used as a treatment method and has been recommended by the Osteoarthritis Research Society International (OARSI) and the European League Against Rheumatism (EULAR) (Henrotin et al., 2010). An additional advantage of CS for OA is that CS is not reactive, allowing it to be paired with other treatment drugs with minimal risk of adverse events.

Beyond OA treatments, in preclinical testing, CS has proved useful in improving wound healing and cartilage repair. Healing and repair in the body occurs mainly through cells working to fabricate new, or fix damaged, tissues. CS can increase cellular migration, attachments, and proliferation, which are ideal capabilities for this purpose (Pezeshki-Modaress et al., 2017). In a 2004 *in vitro* study using rabbit palatal fibroblasts, CS was supplemented in some sample sets (Zou et al., 2004). It was found that the samples treated with CS experienced an increase in cell adhesion and proliferation, while samples with no CS treatments led to reduced cell adhesion and proliferation with a slower wound closure rate. Additionally, CS can be used in combination with compounds like hyaluronan and *N*-acetylglucosamine (GlcNAc) or chitosan (CH) to repair cartilage after surgery to increase the synthesis of hyaluronan, glucosamine and collagen-II, while also inhibiting ECM degrading enzymes (Muzzarelli et al., 2012).

In recent years, CS has become a popular component in many DDS. Various properties, many of which have already been stated, contribute to this growth in demand. These include the strong biocompatibility, biodegradability, and low toxicity that CS possesses (Zhao et al., 2015). Additionally, CS has various derivable groups, including carboxylates, sulfates, and hydroxyls that increase its ability to be modified. These characteristics make CS a desirable addition to DDS.

2.3 Doxorubicin and Daunorubicin for Use in Hydrogel Drug Delivery Systems

Various chemotherapy drugs exist and are utilized today, both within traditional cancer treatment and the field of DDS. Some of the most common chemotherapeutic drugs are DOX, and another drug in the same family, daunorubicin (DNR).

DOX and DNR are both anthracyclines, antibiotics stemming from strains of *Streptomyces* bacteria (McGowan et al., 2017). Anthracyclines work to treat cancer by intercalating with DNA grooves through ionic and hydrogen bonds, preventing the enzyme topoisomerase II from binding properly (Marinello et al., 2018). Topoisomerase II introduces double strand breaks in the DNA helix to manage tangles and supercoils and introduces new strands for the purpose of DNA replication. Blocking the ability of topoisomerase II to stabilize the DNA leaves the strands broken and leading to eventual cell apoptosis once the strands are cut in genomic regions of active DNA synthesis.

The structure of an anthracycline includes a tetracyclic aglycone structure of four cyclohexane chains with a daunosamine sugar moiety at the carbon C7 in ring-A, adjacent quinone-hydroquinone groups in ring-B and ring-C, a methoxy substituent carbon C4 in ring-D, a carbonyl group at C13, and a short side chain in C9 (McGowan et al., 2017). DOX and DNR only differ in their side chains, where DOX includes a primary alcohol and DNR includes a methyl group, as shown in the structures depicted in Figure 4.

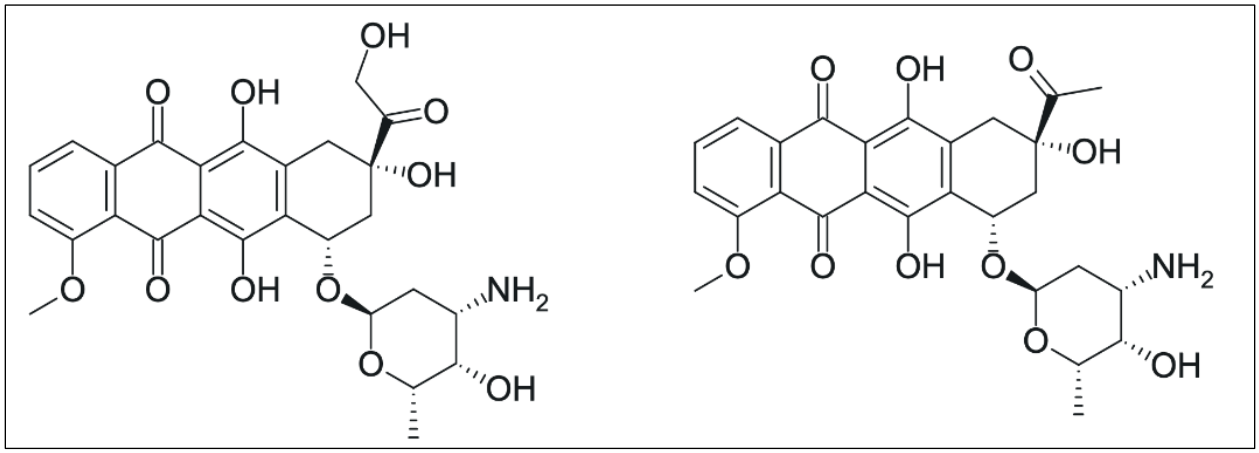

Figure 4: Chemical structures of DOX, left, and DNR, right (McGowan et al., 2017).

While they are both anthracyclines, DNR and DOX have some differences. DNR is chemotherapy used mostly in acute lymphoblast and myeloblastic leukemias (Shin et al., 2010). DOX is one of the most common chemotherapy drugs on the market for various cancer types, specifically carcinomas, such as breast or lung cancer, and sarcomas, such as liposarcoma and leiomyosarcoma. In general, more research has been performed on the usage of DOX in the drug delivery field in comparison to DNR.

Examples of DOX in various DDS are wide and numerous, some of which were summarized in a review study on hydrogel types (Fan et al., 2019). In a 2016 study, DOX was utilized in an injectable, thermosensitive hydrogel system in which DOX was encapsulated in a poly (ε-caprolactone-co-1,4,8-trioxa [4.6] spiro-9-undecanone) (PECT) hydrogel through self-polymerized nanoparticles (Huang et al., 2016). This hydrogel is thermosensitive, so it exhibited an increase in viscosity as the temperature was raised, before transitioning from a solution to a gel at 37°C. Overall, this system of intracellular chemical drug release enhanced anti-tumor effects of DOX. Another DOX-loaded thermosensitive hydrogel is from a 2014 study, in which DOX was paired with PLK1shRNA/polylysine-modified polyethylenimine (PEI-Lys) complexes to improvement treatment of osteosarcoma (Ma et al., 2014). This study showed similar benefits of injectability and body temperature gelling that the 2016 study did.

For pH-sensitive hydrogels, a 2019 study can serve as an example. A pH-sensitive hydrogel was created from chitosan-grafted-dihydrocaffeic acid (CH-DA) and oxidized pullulan (OP), and was loaded with DOX to monitor its ability to release drug with pH decreases in tumoral environments (Liang et al., 2019). This study yielded great results, as a decrease in pH triggered DOX release, with over 80% being released in 60 hours at a pH value of 5.5. Additionally, an example of photosensitive hydrogels utilizing DOX is also relevant. A 2011 study loaded DOX into a DNA polyacrylamide conjugate hydrogel for lymphocytic leukemia (Kang et al., 2011). This hydrogel sought application for the controllable release of DOX, and their results showed a DOX release rate of 65% within 10 minutes, verifying DOX's ability to maintain its therapeutic effect.

2.4 Current Models Using Chondroitin Sulfate

2.4.1 Chondroitin Sulfate Methacrylate Particles for Drug Release

A 2018 Major Qualifying Project (MQP) at WPI utilized CS for the purpose of improved NB treatment. In this project, the team sought to develop a microfluidics device to fabricate CS-MA microparticles. CS-MA was chosen as a material for the microparticles due to its drug release capabilities, biocompatibility, cost-effectiveness, and adaptability (Loaisa et al., 2018).

This project resulted in a soft lithography-based co-flow microfluidics device with a flow focusing inlet aperture and serpentine channels that has a 100 µm width and produced particles with diameters less than 100 µm. From this system, CS-MA microparticles were fabricated. The

sizes of these microparticles varied slightly between the four trials run, with 1-week post-swelling sizes of 98.44 ± 23.26 μm, 96.15 ± 38.11 μm, 95.59 ± 38.48 μm and 82.79 ± 20.6 μm. These showed no significant difference in particle diameter, thus asserting that this process yields reproducible CS-MA microparticles.

In addition to their fabrication, the team also loaded the microparticles with DOX. Approximately 385 μg of DOX was loaded per mg of particles, and the sustained release of the drug was evaluated over the course of one week. At one week, the length of time an intravenous chemotherapy treatment cycle usually takes, the CS-MA microparticles had released an average of 12.7 ± 3.37% of the total loaded DOX. A biocompatibility test revealed that the DOX-loaded microparticles were active over time, which is imperative for a DDS.

While this study yielded promising results, various recommendations for future directions were made, three being of high importance. Three of these were of high importance to this study. First, alterations to the channel size of the microfluidic device, or another fabrication method, should be explored to create smaller microparticles. Second, a more long-term drug release study is necessary to better understand the degradation rates of the CS-MA microparticles and the release rates of DOX. Lastly, other chemotherapeutic drugs, besides DOX, should be considered in future studies to potentially yield better drug release results.

2.4.2 Chondroitin Sulfate Injectable Hydrogels with Long-Term Release Profiles

Hydrogel DDS, as previously explained, have shown promising potential for local cancer treatment (Ornell et al., 2019). Though previous work with biopolymer hydrogels such as silk fibroin, salecan, and CH have shown potential for drug delivery purposes, CS based hydrogels are most commonly explored for tissue engineering applications. In this study, CS-MA with a range of degrees of substitution (DS) were fabricated and characterized for loading and release of chemotherapeutics drugs, as well as the physical and structural properties of the hydrogels. This was the first study to report photo crosslinked CS-MA hydrogels without any copolymers for drug delivery purposes.

CS-MA was fabricated using a heterogeneous phase reaction of CS with GMA at pH 3.5. The reaction time for methacrylation varied from 2 h to 24 h, with a plateau between 12 h and 24 h. Regarding how the DS affected the physical properties of the hydrogels, the swelling decreased as DS increased, which was observed for both 10% and 20% CS-MA hydrogels. There was no difference in swelling between 8 h, 12 h, and 24 h for both concentrations of CS-MA

hydrogels. It is important to note that swelling studies were not performed with the 2 h CS-MA at 10% hydrogels as these hydrogels did not retain their physical form and disintegrated during the swelling process. Regarding drug loading and release, two drugs were tested: sunitinib and DOX. For sunitinib, a cancer therapeutic that targets several receptor tyrosine kinases to block intracellular signaling, varying the DS from 0.05 to 0.28 altered the drug release profile. For example, CL20 and CH20, hydrogels with 20% CS-MA concentration and 2 h and 24 h reaction time respectively, had a linear drug release from day 4 to 14 with a R^2 value of 0.99. Moreover, CL20 hydrogels released all the loaded sunitinib and/or lost their mechanical integrity by an average of 21 days, while CH20 hydrogels continued releasing the drug for approximately 42 days. A summary of the sunitinib release can be found in Table 1.

Table 1: Summary of sunitinib release from CS-MA DDS.

Label	Burst Release (mg) Day 1	Linear Region (Day 4-14) mg per Day	Total Release (mg) Day 21
CL20	30 ± 7	18 ± 3	313 ± 68
CH20	21 ± 7	9 ± 1	211 ± 20

The same drug loading and release analysis was performed on CL20 and CH20 hydrogels using DOX. Like sunitinib, there was no significant difference in DOX-loading between the two types of hydrogels tested, which released 71 ± 15 mg and 61 ± 6 mg in 30 days, respectively. Overall, a burst release of DOX was observed in the first 7 days, followed by a sustained linear release, which extended until the completion of the study for both CL20 and CH20 hydrogels. The CL20 hydrogels exhibited a release rate of 1.2 ± 0.3 mg per day, with an R^2 value of 0.99, and the CH20 hydrogels had a release rate of 1.1 ± 0.1 mg per day, with an R^2 value of 0.98. The main differences between sunitinib and DOX were that hydrogels loaded with DOX did not lose mechanical integrity after 21 days and showed a slower release profile as compared to the sunitinib-loaded hydrogels, only releasing between 20 to 30% of the loaded DOX in a month.

In this study, researchers used CS-MA with different ranges of methacryloyl substitutions to form hydrogels for in-tumor drug delivery. There were no differences in drug loading, but significant differences in drug release for different DS with matched CS-MA concentrations. Therefore, by controlling both DS and CS-MA concentration, drug loading and release of different drugs used in cancer therapy can be achieved. The study proved, for the first time, the ability of CS-MA-based hydrogel to be used for sustained drug release. These CS hydrogels bind to positively charged molecules and slowly release the molecules over days to weeks, while

maintaining *in vitro* drug cytotoxicity. However, even though injectability was addressed during the research, it was concluded that these hydrogels require a very high injection force, which is not favorable for clinical settings.

2.5 Injection Forces

2.5.1 Objective and Subjective Measures of Injectability

Injection force is dependent on both the mechanical properties of the injection system and the rheological properties of the material. By assuming the needle acts as a pipe, the Hagen-Poiseuille equation can be adapted to model the movement of fluid through a needle (Thomas E Robinson, 2020).

$$Hagen - Poiseuille\ Equation = \ F = \frac{8*R_S^2*L*Q*\eta}{R_n^4} + F_f \quad \textbf{(Equation 1)}$$

Equation 1 shows the Hagen-Poiseuille equation that can be used to model the behavior of an injection of different parameters. In this equation, F is injection force (N), R_s is the internal syringe radius (m), R_n is the internal needle radius (m), L is the length (m), Q is the fluid flow rate (m^3/s), η is dynamic viscosity (Pa s) and F_f is the friction force between the plunger and barrel wall. As seen in Equation 1, an increase in viscosity correlates to an increase in required injection force. Hydrogels often require much greater injection forces than typical injectable fluids such as vaccines because of their high viscosity. In a study by Robinson et al. (2020), researchers aimed to understand the correlation between the force required to inject various biomaterials as determined through mechanical testing and as determined through a subjective measure by both female and male participants. To complete this study, a mechanical tester similar to our set up shown in Figure 5, was used to measure the force (N) required to compress the plunger of a syringe filled with 5 mL at a set velocity for hydrogels of varying viscosities.

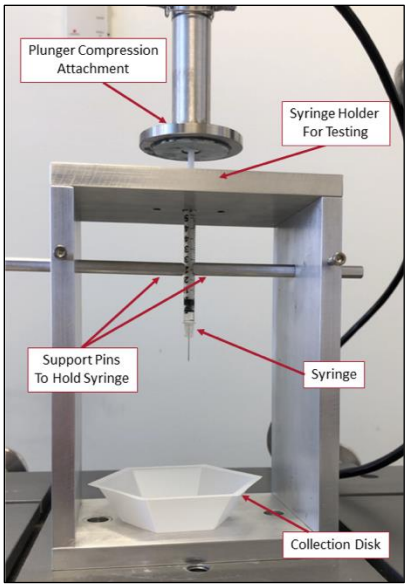

Figure 5: Mechanical testing setup used to determine injection forces.

Subjects were then asked to depress the plunger for syringes containing hydrogels of the same viscosities and volume and rate the effort required on a scale of 1 to 5, with 1 being easily injectable and 5 being entirely non-injectable. This was repeated with a total of 50 participants. By plotting the objective injection force (N) against the five-point subjective injection difficulty a linear correlation was discovered that suggests participants can easily inject 5 mL for forces less than 12 N, whereas considerable effort is required for 12-38 N, and great effort is required to inject less than 5 mL for 38-64 N.

Based on this result, a 3-way ANOVA was performed to understand the effect of each of the three variables: needle gauge, material, and compression rate, on each other as well as the outcome. The results of this ANOVA suggested that needle diameter had the greatest effect on injection force, then material, followed by compression rate.

2.5.2 Current Injection Forces

Professor Coburn's lab at WPI has developed a CS-MA hydrogel capable of sustained release of cationic therapeutics; however, the current injection forces required are considered unfavorable in a clinical setting (Ornell et al., 2019). In order to evaluate the syringeability of different concentrations of CS-MA with varying DS, a compressive test was performed comparable to the mechanical testing performed by Robinson et al. (Thomas E Robinson, 2020). The three CS-MA variations tested included 20% CS-MA with 2 h and 24 h reaction times and

10% 24 h CS-MA. This compressive testing was performed at a rate of 4 mm/min on 50 µL CS-MA hydrogels with a 27 G 0.5 mL 0.5 in needle, and a 3.5 mm inner diameter. It was found that 10% 24 h had an injection force of 38.6 N ± 14.1 N, 20% 2 h was 17.6 N ± 5.7 N, and 20% 24 h was 94.3 N ± 16.9 N. While the 10% 24 h and the 20% 2 h hydrogels may have what would be considered acceptable injection forces according to Robinson et al. (2020), these formulations were not considered to be desirable by the authors because they were not easily reproducible (Ornell et al., 2019; Thomas E Robinson, 2020). Thus, although they require a much greater injection force, 20% 24 h CS-MA hydrogels are the more desirable formulation.

There are various mechanical and material options for decreasing injection force including, but not limited to: decreasing needle gauge, decreasing injection speed, decreasing syringe barrel diameter, and decreasing hydrogel viscosity. The effect of a change in each of these parameters can be modelled by Equation 1.

2.6 Methods of Reducing Hydrogel Viscosity

2.6.1 Smart Hydrogel Drug Delivery Systems

A hydrogel is a 3-dimensional network of hydrophilic polymers that swell in water while maintaining their mechanical structure due to crosslinking of different polymer chains (Fan et al., 2019). These hydrogels have been researched for their use in DDS as they allow for a localized therapy that prevents healthy cells from being harmed by the systemic approach of traditional cancer treatment. Hydrogels are loaded with chemotherapy drugs and then injected directly into, or adjacent to the tumor site. Their soft and moist surface provides a high affinity with the native tissue, which significantly reduces adverse reactions of the human body. The 3D network of the hydrogel localizes drug toxicity within the area of the injection site. Another benefit of hydrogels is their high-water absorption capacity, although they are insoluble in water. This means that hydrogels can have similar water content as native body tissues, potentially allowing them to transport nutrients and waste.

Hydrogels can be divided into two subcategories: ordinary hydrogels, which are not sensitive to environmental changes, and smart hydrogels, which are affected by pH, temperature, or photoelectricity. A visual representation of the changes in state in a hydrogel solution due to changes in temperature can be seen in Figure 6.

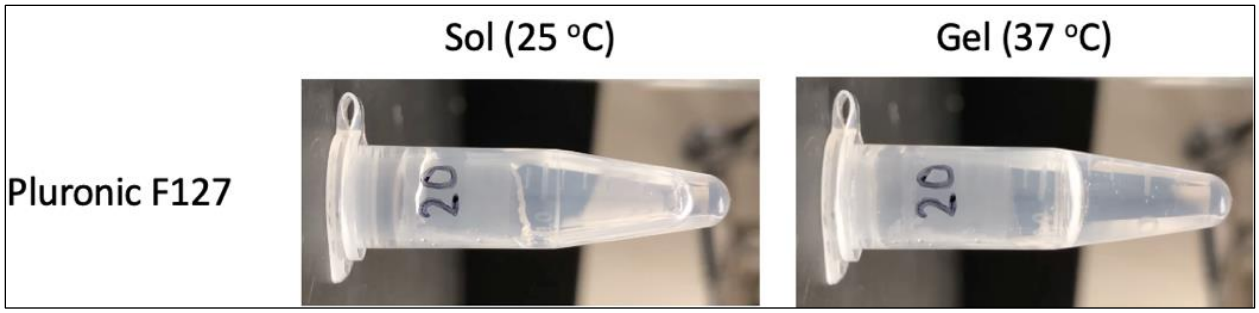

Figure 6: State of a thermosensitive hydrogel at different temperatures (25°C and 37°C).

Thermosensitive hydrogels change volume as the environment temperature changes (Fan et al., 2019). These temperature changes affect the hydrophobic groups within the chemical composition of the hydrogel, particularly the hydrogen bonding between the macromolecular chains. There are two forms of thermosensitive hydrogels: those that gel when cooled below the upper critical gelation temperature (UCGT) and those that gel when heated above the lower critical gelation temperature (LCGT) (Gioffredi et al., 2016). Specifically, for LCGT hydrogels, if the ambient temperature is above the LCGT, the hydrogel swells in aqueous solution. Common LCGT thermosensitive injectable hydrogels include compounds such as CH/glycerophosphate, Hyaluronic Acid (HA), PLGA, PEG, PECE and PECT.

Another type of well-researched smart hydrogels are pH-sensitive hydrogels, which change viscosity with changes in the pH of the external environment (Fan et al., 2019). Particularly, cancer cells undergo glycolysis more commonly than healthy cells, which release a lactic acid. This results in tumors with a lower pH than healthy tissue. The hydrogels take advantage of the tumor environment in order for the solution to be liquid when inserted through a syringe and to gel as it reaches the pH of the tumor site, consequently increasing hydrogel viscosity. A pH-sensitive hydrogel contains a great number of carboxyl and amino groups that dissociate with changes in external pH, typically when the hydrogel hits the pH of the tumor site. When the pH drops below a compound's pKa, a measure of the concentration of hydrogen ions in an aqueous solution, the carboxyl groups in the hydrogel take an extra proton and become neutral (Oroojalian et al., 2018). The degree of dissociation of these groups causes the internal and external ion concentrations to change. In addition, the dissociation of the deprotonated carboxyl groups and protonated amino groups causes the corresponding hydrogen in the hydrogel to move freely in the solutions, which reduces the cross-linking point of the hydrogel network and the degree of swelling of the hydrogel. Consequently, the structure of the hydrogel network and the

degree of swelling of the hydrogel change, thus allowing for the rate of diffusion and release of drugs in the hydrogel to be controlled. One example of this type of hydrogel is based on CH-DA and oxidized pullulan (OP), which were loaded with DOX (Fan et al., 2019). At the tumor site, glycolysis decreased the environment's pH, which triggered drug release. It was concluded that DOX was stably released from the hydrogel between pH 5.5 and 7.4 and was effectively released for more than 3 days.

The final smart hydrogels are photosensitive hydrogels, another method to alter hydrogel viscosity (Fan et al., 2019). The formation of photosensitive hydrogels can be divided into two methods according to the properties of the photosensitive material. The first is to insert the photosensitive molecular material into temperature-sensitive gel, which consequently converts the light energy into heat energy to induce the temperature inside the hydrogel to reach the lower critical solution temperature (LCST). In this case, photosensitivity is produced within the hydrogel. For the second method, a chromophore-azobenzene, spiropyran, o-naphthoquinone, anthracene, nitrophenyl, or coumarin is introduced into the polymer backbone, and its physicochemical properties are changed when subjected to light stimulation. Regarding the gelation reaction, when some of these compounds are exposed to ultraviolet light or near-infrared light, the ester group is broken, causing a photosensitive reaction. Generally, photosensitive hydrogels can be formed in the presence of light-sensitive chemicals, photoinitiators, when exposed to light. When UV or visible light interacts with photoinitiators, free radicals are produced, causing polymerization to begin and eventually the formation of crosslinked hydrogel networks (Qin et al., 2014). Finally, with the increasing requirement for controlled DDS, multi-sensitive hydrogels have also been researched, particularly co-sensitive hydrogels for temperature and pH. A temperature-sensitive and pH-sensitive hydrogel consists of a two-part hydrophilic polymer network, usually formed with two or more monomers or polymers. Overall, the unique characteristics of a hydrogel DDS have been a crucial method for cancer therapy.

2.6.2 Microbeads Drug Delivery Systems

Another type of DDS includes the usage of microbeads composed of manufactured polyelectrolyte complexes (PEC) particles of less than one millimeter (Daley et al., 2015). These particles self-assemble and are biologically active, which makes them able to be utilized for different biology and medical applications. Particularly, many researchers have explored these particles for cell-based cartilage therapy. In this study, drug delivery was not addressed, but the

process of fabrication of PEC particles could be adapted to create a system for site-specific delivery of drugs.

In one of these studies, researchers developed and characterized materials designed to mimic the composition of the cartilage ECM (Daley et al., 2015). CS and CH were utilized to form a cross-linked macromolecular PEC without the use of additional crosslinkers. The goal was to create a stem cell delivery method that required minimal processing and that produced 3D modular microtissues, which maintained cell viability and advanced chondrogenic differentiation of embedded stem cells. Researchers used rat-bone marrow-derived stem cells because of their ability to differentiate *in vitro* when cultured in biomaterial scaffolds. The microbeads formed were able to support high stem cell viability while preserving a round cell morphology, which was a targeted goal of the study (Daley et al., 2015). Differentiation was supported particularly with the 10:1 CS-CH microbead formulation. From the healing standpoint, microbeads could be used in developing next-generation cell-based therapies for cartilage repair. Using this system enables researchers to control *in vitro* preconditioning of stem cells in a microenvironment for delivery to the wound site as an injectable material. Even though there are no studies using this type of CS microbeads for drug delivery for cancer therapy, the methodology behind using them for cell-based cartilage therapy can be applied for the purpose of this MQP project.

2.6.3 Methods of Particlization

A third method of decreasing hydrogel injection force includes the fabrication of drug-loaded microparticles. The microfluids device explored by a 2018 MQP, mentioned in Section 2.4.1, utilized this approach of creating drug-loaded microparticles. Outside of microfluidics devices, these particles can be created in a variety of ways, including additional methods such as emulsification systems and mesh-based systems.

An emulsion is a multiphase system in which a dispersed phase forms droplets in a continuous phase (van der Graaf et al., 2005). A single emulsion can occur in two ways, oil-in-water (OW), in which oil is dispersed in a continuous water phase, or water-in-oil (WO), in which water is dispersed in a continuous oil phase. Similarly, double emulsions can be distinguished into two main types: water-in-oil-in-water (WOW), in which a water-in-oil emulsion is dispersed in water, and oil-in-water-in-oil (OWO), in which an oil-in-water emulsion is dispersed in oil. For the case of this project, a WOW emulsion would be most beneficial for acquiring dispersions of hydrophobic hydrogel in a continuous water phase.

There are various means of preparing emulsions, but the conventional method includes two steps and two surfactants (van der Graaf et al., 2005). For the preparation of a WOW emulsion, the first step is prepared under high-shear conditions and requires a hydrophobic surfactant to stabilize the interface of the WO. The second step is prepared under low shear conditions, as to not rupture the droplets, and requires a hydrophilic surfactant to stabilize the external interface of the oil globules.

Some general techniques for emulsification include high shear mixers, high pressure homogenizers, microfluidization, and ultrasound emulsification (Taha et al., 2020). High shear mixers, or high shear homogenizers, create coarse emulsions with slow chemical reactions and hydrodynamic interactions between dispersed and continuous phases. It does so with mixer heads that generate rotational, longitudinal, and radial velocity slopes to break larger droplets into smaller ones. High shear mixers require low to moderate energy to complete and are manufactured with various sizes and speeds for both laboratory and industrial use. While good for rudimentary needs, these devices are limited in their pumping capacity and droplet size.

High pressure homogenizers are like high shear mixers. They first create coarse emulsions, which are compressed using turbulent flow, to form fine emulsions. High pressure homogenizers do this with the use of a small valve and high-pressure pump. These devices utilize a moderate amount of energy and are used in various manufacturing industries as continuous homogenizing devices. While beneficial for large-scale emulsions, high pressure homogenizers are also very expensive, bulky, and require excessive cleaning after each use (Network). Microfluidic devices also use a pump to push pre-emulsion through micro-channels, with increasing velocities as the emulsions move, which produce nano-sized emulsions (Taha et al., 2020). This device is made up of an air-driven intensifier pump and an interaction chamber. Microfluidization is a high-energy emulsion process, but while it has potential for scale-up from laboratory to manufacturing, it has yet to do so, thus limiting its current applications.

Lastly, ultrasound emulsification, or high intensity ultrasound, uses shock waves, known as acoustic cavitation, to form and collapse air bubbles. Air bubble collapsing promotes the release of reactive radicals for chemical reactions, which leads to the formation of small emulsions. To do so, large droplets from the dispersed phase are formed in the continuous phase, where the shock waves and physical shearing act to breakdown the droplets into small

emulsions. These devices are energy efficient, stable, and easy to operate, but have only been used in a laboratory setting, and tend to create emulsions with low stability.

In comparison to conventional emulsification methods, membrane emulsification provides better control of droplet size and distribution (van der Graaf et al., 2005). There are two main types of membrane emulsification, including pre-mix and crossflow membrane emulsification. Pre-mix emulsification occurs when a pre-mix is pushed through a membrane to create finer droplets as seen in Figure 7.

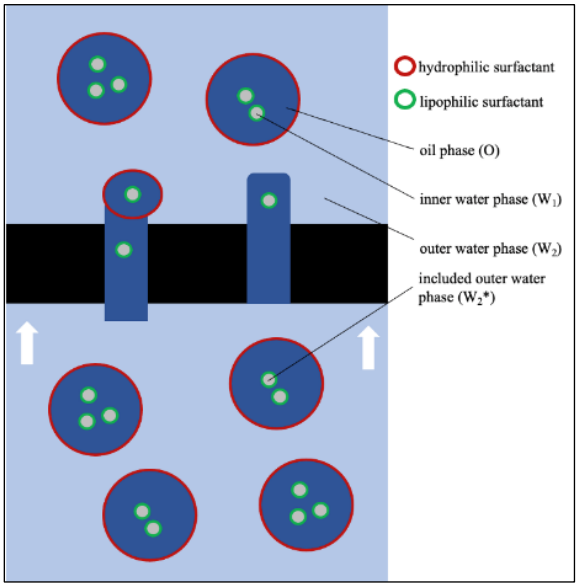

Figure 7: Pre-mix emulsification where arrows represent the direction of fluid flow. Adapted from, (van der Graaf et al., 2005).

As seen in Figure 7, to perform the pre-mix membrane emulsification the coarse WOW "pre-mix" emulsion created from conventional homogenization was forced through a cellulose acetone membrane. This action reduced the diameter of the oil droplets and forced the former outer water phase (W_2 *) out into the outer water solution (W_2). This outer water release was able to occur because (W_2 *) contains the hydrophilic surfactant that can wet the hydrophilic cellulose acetone membrane. Conversely, the inner water phase (W_1) was unable to leak out into the (W_2) because it contains the hydrophobic lipophilic surfactant. Like pre-mix, in crossflow membrane emulsification the phase to be dispersed is passed through a microporous membrane; however, instead of the continuous phase remaining stagnant, it is flowing along the membrane (Figure 8).

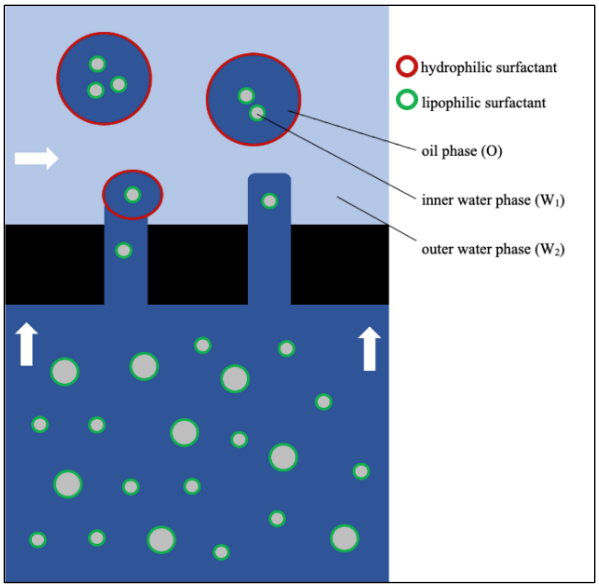

Figure 8: Double WOW emulsion by cross flow membrane emulsification. Where the arrow represents the direction of fluid flow. Adapted from (van der Graaf et al., 2005).

The size at which a particle breaks off at in crossflow membrane emulsification is dependent on the forces acting on it. As the particle is passed through the membrane, a pressure difference will occur between the to-be-dispersed phase and the droplet, causing the droplet to spontaneously detach due to the pressure difference. This detachment can also be affected by the velocity of the crossflow continuous phase; however, if the force at which the to-be-dispersed phase is being pushed through the membrane is the dominant force, the droplet size may not be affected by the velocity of the continuous phase.

In addition to emulsification techniques, mesh has been used for the creation of particles in drug delivery. There has been vast research on utilizing a mesh-based nebulizer system to decrease particle size for aerosol medicine. While the exact technique and purpose varies slightly, a 2018 study reports the basic methodology, where a liquid solution, which contains drug-loaded liposomes, is forced past a very small mesh through air-jetting or vibrations (Nimmano et al., 2018). Regardless of the means of force, this generates particles suitable for aerosols. This method has shown to have low damage to liposomes and its loaded drug, making it suitable for liposome drug delivery.

At this point, no studies have been done on how this mesh system could be adapted to hydrogels, but it could be possible for two main reasons. First, this mesh-nebulization system requires far smaller mesh sizes than a hydrogel particle would, as hydrogel particles must only be

suitable for injection, not nebulization. Second, both liposome and hydrogel drug delivery have used high intensity ultrasound, as discussed previously, for particle creation. Since they have both successfully used this similar technique, with the mesh-based system yielded better results for liposome drug delivery, it can be assumed that this process may also be plausible.

2.7 Thermosensitive Hydrogels

2.7.1 Thermosensitive Polymers for Hydrogel Injection

LCST thermosensitive hydrogels refer to hydrogels that go through the gelation process after reaching a critical solution temperature. The use of thermosensitive hydrogels enables a system to be injected as a solution into the site of interest, and then transition into a hydrogel after reaching body temperature, 37°C, or any temperature greater than the materials LCST. The use of these hydrogels allows for increased comfort of the patient during injection, and less force to be applied to the physician delivering the hydrogel.

Most hydrogels that display thermosensitive properties are developed by introducing a temperature sensitive polymer into a composite. Through this introduction, the composite adopts the properties of the polymer, including the LCST that dictates gelation. The most common polymers include Pluronic F127 (F127), Poly(N-isopropylacrylamide), and the triblock polymer poly(lactic acid-co-glycolic acid) and poly(ethylene glycol). These common polymers are commercially available, making them a feasible choice to create the injectable copolymer system.

2.7.2 Pluronic F127

Pluronics, also known as Poloxamers, is a PEO-based non-ionic surfactant (Shriky et al., 2020). These types of copolymers are among the most researched and commonly used substrates for injectable DDS. They are composed of polyethylene oxide-polypropylene oxide-polyethylene oxide (PEO-PPO-PEO) triblock copolymers. In general, Pluronics are utilized for their safety, bio-adhesiveness, stability, and ability to form hydrogels at low concentrations at body temperature. These types of block copolymers are diluted in a solvent to form micelles in solvents as soon as they reach a set temperature, as a result of PPO-block dehydration. If present in high concentrations, the triblock micelles associate above the critical gelation temperature (CGT) and assemble into a lyotropic liquid crystalline (LLC) phase, which refers to a liquid phase that has properties of both anisotropic crystalline solids and isotropic liquids. When used

in DDS, the polymeric matrices are exposed to shear forces that change the particles' crystal arrangement leading to a viscoelastic response. This type of shear-thinning responsive behavior is common for this class of biomaterials.

Pluronic F127, also known as Poloxamer 407, is used in biomedical applications due to its commercial availability and its consistency in undergoing a sol-gel transition, as a change from liquid state to gel state, near-physiological temperature and pH (Gioffredi et al., 2016). The chemical composition of F127 can be seen in Figure 9. F127 hydrogels have been widely researched as drug and cell carriers because of its low toxicity, reverse thermal gelation, high drug loading properties, and ability to gel in low concentrations and physiological conditions. Applications for these hydrogels include cell printing since they are biologically inert towards multiple cell types and able to show a broad range of viscosities due to temperature changes (Brunet-Maheu et al., 2009; Gilbert et al., 1986; Yang et al., 2009).

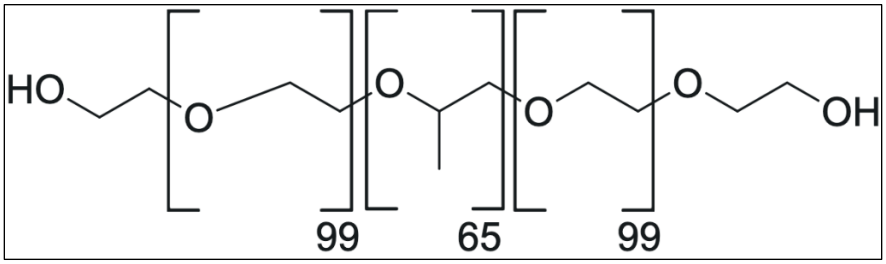

Figure 9: Chemical structure of F127.

A study was conducted to evaluate a thermosensitive F127 hydrogel DDS based on its gelation, microscopic and macroscopic structural changes at equilibrium and non-equilibrium in controlled environments (Shriky et al., 2020). Rheological measurements, performed in both rotational and oscillatory shear modes, were conducted to evaluate the sol-gel transition of the hydrogel. Samples were exposed to four tests with constant shear rate values of 10, 20, 50, and 100 s^{-1}. Hydrogels with low concentrations of F127 (1 to 5%) demonstrated reduced viscosity values as the temperature increased and, therefore, were considered as Newtonian fluids. As F127 concentrations increased, viscosity decreased until the environment temperature reached 22°C, and then a viscosity increase was observed up to a temperature of 31°C. This concluded that this DDS, at concentrations above 15%, undergoes a reversible thermal transition from micellar liquids to shear-thinning gels, which makes them ideal for injectable drug delivery applications. Moreover, a set of equations was determined to predict the gelling behavior of the

system of any F127 concentration above 20% during 3 stages it goes through (pre-gel, gel transition, and gelation point) as a function of temperature and shear rate.

2.7.3 Poly(N-isopropylacrylamide)

Poly(N-isopropylacrylamide) (PNIPAM) is a synthetic thermosensitive polymer that contains both hydrophilic amide groups (-CONH-) and hydrophobic isopropyl side chains (-CH $(CH_3)_2$) (Xu et al., 2020). PNIPAM has an LCST of 32^oC which makes it attractive as an injectable DDS as it takes on a solution state at room temperature and transitions to a gel state at a temperature lower than body temperature. At temperatures below the LCST, hydrogen bonds can form between the hydrophilic amide groups and water allowing the polymer to remain at a solution state. In this solution state, drugs can be directly dissolved into the solution. However, once the temperature is raised above the LCST, the hydrogen bonding is weakened and the hydrophobic interactions between isopropyl side chains are strengthened resulting in the formation of drug-loaded aggregates. Although PNIPAM possesses thermosensitive characteristics that are desirable for injectable drug delivery, there are three major shortcomings associated with the use of the polymer including: low biodegradability, relatively low drug loading capacity, and burst release of drug molecules. However, various studies have shown that by forming a composite hydrogel with new polymer blocks and taking advantage of the behaviors of the new polymer blocks it is possible to make up for these shortcomings. While studies have been shown to overcome this burst effect and low drug loading capacity, there are shortcomings in the current solution to increase biocompatibility of PNIPAM, as the only option is to choose a polymeric block with low toxicity and defined degrading routes.

Once the LCST is reached, the hydrophobic interactions strengthen which ultimately results in a demixing or syneresis phenomenon where the hydrogel separates into the shrunken gel and an aqueous phase (Andrei et al., 2016). As a result of this demixing, a burst effect can occur where a part of the drug is released very quickly at the beginning of the gelling process. In a study by Andrei et al., researchers found that by adding Dextran to PNIPAM they could increase the water retention of the hydrogel, which resulted in a more controlled and sustained drug release. Dextran is a naturally occurring biocompatible and biodegradable hydrophilic polysaccharide. Thus, by utilizing the hydrophilic properties of this material as well as the thermosensitive properties of PNIPAM researchers were able to create hydrogels with increased

water retention and drastically reduced burst effect. Pure PNIPAM had a water retention of about 12% whereas with the addition of Dextran the polymer had a water retention of about 40 to 55%.

Pure PNIPAM does not have the ability to effectively bind hydrophobic drugs because of a lack of hydrophobic binding sites (Xu et al., 2020). Various modifications have been made to overcome this challenge. In one study, researchers utilized nano-liposome micelles that could encapsulate hydrophobic species and embedded them into two copolymer PNIPAM systems including poly[(N-isopropylacrylamide)-co-chitosan] (PNIPAM-co-CS) and poly[(N-isopropylacrylamide)-co- (sodium alginate)] (PNIPAM-co-SA). This micellar encapsulation increased the loading capacity and protected the drug from oxidization. Another group overcame this drug loading dilemma by fabricating a PNIPAM hybrid hydrogel with the short peptide, I_3K (a three-isoleucine tail with one lysine head peptide), that has good drug loading abilities. As demonstrated in Figure 10 at temperatures above the LCST the I_3K fibrils form aggregates that entangle the PNIPAM. Because this process is driven by physical interactions including hydrogen bonding, hydrophobic interactions, and steric hinderance it is reversible with temperature change. The model drug used in this process was $G(IIKK)_3I\text{-}NH_2$, a peptide composed of glycine-$(isoleucine\text{-}isoleucine\text{-}lysine\text{-}lysine)_3\text{-}NH_2$, which is an amphiphilic cationic peptide. To load the drug, it was added to the I_3K-PNIPAM during its solution state. Overall, the composite system was able to take advantage of the drug loading ability of I_3K while maintaining the thermosensitive properties of PNIPAM.

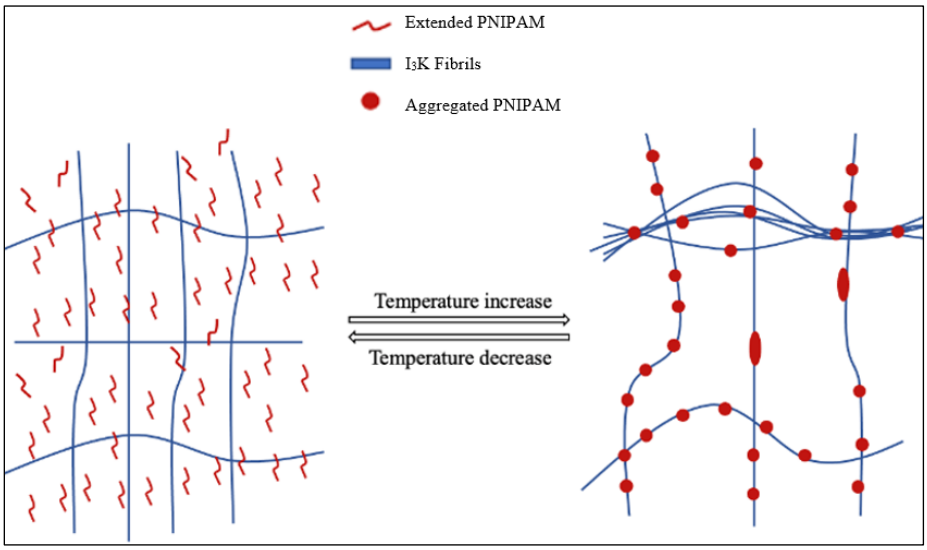

Figure 10: Schematic diagram of I3K/PNIPAM networks above (right) and below (left) the PNIPAM LCST. Adapted from (Xu et al., 2020).

2.7.4 Poly(dl-lactide-co-glycolide-b-ethylene glycol-b-dl-lactide-co-glycolide)

Poly(dl-lactide-co-glycolide-b-ethylene glycol-b-dl-lactide-co-glycolide) (PLGA-PEG-PLGA) is one of the most popular synthetic, thermo-gelling triblock copolymers (Yu et al., 2013). It is formed through the copolymerization of hydrophilic Polyethylene glycol (PEG) with hydrophobic poly(lactic acid-co-glycolic acid) (PLGA) to create a B-A-B triblock type (Wang et al., 2017). The structural formula of this copolymer is shown in Figure 11.

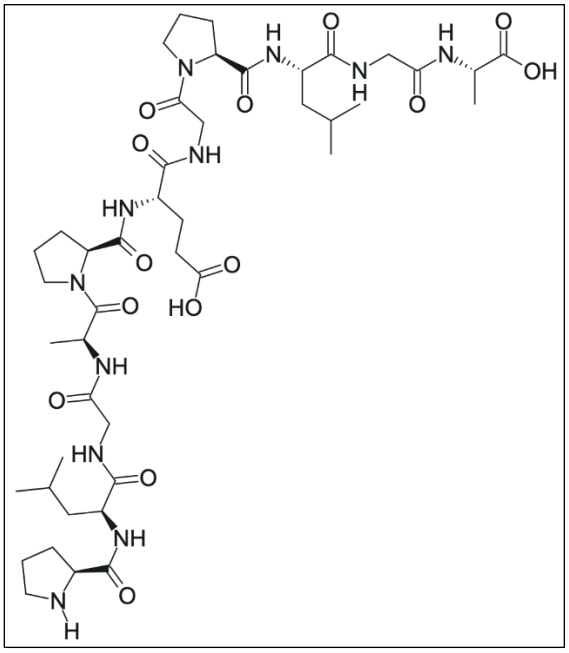

Figure 11: The structural formula of PLGA-PEG-PLGA (Polymers).

Thermo-reversible gelling polymers with PLGA/PEG blocks are highly researched, as both polymers have advantageous properties that are enhanced when copolymerized (Wang et al., 2017). PEG is nontoxic and lacks antigenic and immunogenic effects. PLGA is biodegradable and biocompatible. Together, PLGA-PEG-PLGA enhances the solubility of hydrophobic drugs, such as DOX, prolongs drug release, maintains biodegradable and biocompatible for long periods of time, and is highly injectable.

PLGA-PEG-PLGA takes on a solution state from 2°C to 15°C, and transitions to a water insoluble hydrogel at body temperature. Due to these properties, and its other characteristics, PLGA-PEG-PLGA is a desirable copolymer for an injectable DDS. There is, however, a major

limitation of PLGA-PEG-PLGA, which is that its solution viscosity increases when loaded with DOX, which lowers the injectability of the solution.

A study was completed using PLGA-PEG-PLGA block polymers for sustained release of DOX through a thermosensitive hydrogel. In this study, the triblock polymer was synthesized through bulk ring-opening copolymerization of lactic acid (LA) and glycolic acid (GA), with the presence of PEG and stannous octoate as the catalyst. This one-step synthetization process showcased highly reproducible results. During this study, varying concentrations of DOX were loaded onto the hydrogels and the properties of the hydrogels were then tested. By increasing the concentration of DOX, the viscosity of the polymer solution shows a significant increase. The viscosity (η) of the varying concentrations were analyzed in respect to temperature through the gelation process. From these experiments, it was shown that the increase in DOX concentration during loading does not affect the gelling rate for PLGA-PEG-PLGA but it does affect the viscosity of the solution. This is important for the use of an injectable hydrogel with thermosensitive properties as the system should have a low and reasonable viscosity at solution state during the injection process. A need for concentrations higher than 2 mg/mL for loading of the hydrogel will render the system uninjectable (Yu et al., 2013).

2.7.5 Example of a Thermosensitive Hydrogel Using Doxorubicin

As previously noted, thermosensitive hydrogels are one of the most widely used hydrogel DDS, and DOX and DNR are some of the most accepted chemotherapy drugs. Due to this, thermosensitive hydrogels loaded with DOX has been intensively researched and documented. A relevant study was completed in 2017, in which a thermosensitive hydrogel was formed using alginate-g-poly(N-isopropylacrylamide) (alginate-g-PNIPAM) (Liu et al., 2017). Alginate-g-PNIPAM was formed through the conjugation of PNIPAM to alginate, and from this a hydrogel with thermosensitive properties was fabricated. Figure 12 reflects this formation. The gelling standard of this material was a solution at room temperature and transitioned into a stable hydrogel upon injection into the body. This study monitored the controlled and sustained release of DOX for two hydrogel batches, Alg-PN_{48}-72% and Alg-PN_{46}-81%, where 48 and 46 represent the degree of polymerization, and 72 and 81 are the weight percentages of PNIPAM in the copolymer. These batches were released for 7 days and 20 days, respectively. In this time, no significant burst release was observed, while continuous release of DOX was observed. In addition, cytotoxicity testing indicated that alginate-g-PNIPAM copolymers formed micelles

after their dissolution from the hydrogel, encapsulating DOX molecules. These micelles were continuously released and served as a drug carrier, adequately delivering DOX to cells for treatment purposes. This study provides a promising example of the potential that injectable, thermosensitive hydrogels have for the sustained release and effective delivery of DOX, for the improved treatment of cancerous tumors.

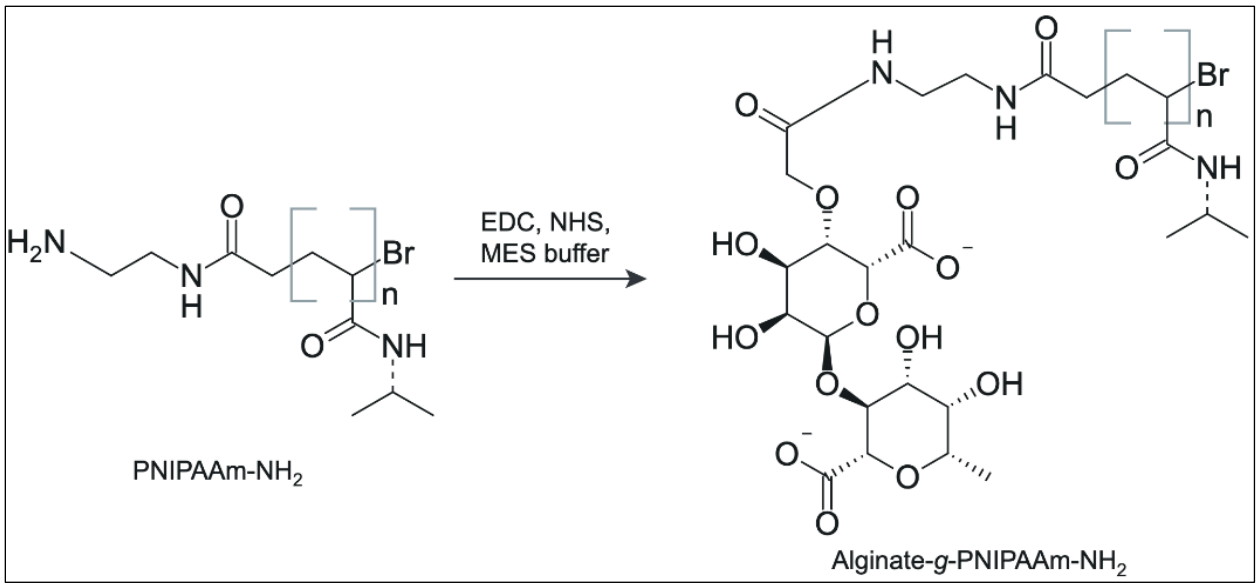

Figure 12: Synthetic schematic of the alginate-g-PNIPAM formation.

III. Project Strategy

3.1 Initial Client Statement

The initial client statement, given by Professor Jeannine M. Coburn, PhD is:

"Develop a fabrication technique to obtain water-insoluble, injectable chondroitin sulfate drug delivery vehicles and characterize the resulting chondroitin sulfate material."

As more knowledge was gained by the team, in addition to feedback from the advisor, a revised client statement has been crafted and is presented later, in Section 3.5.

3.2 Design Requirements

3.2.1 Design Objectives

The objectives of this project focus on the development of a fabrication technique to obtain an injectable CS-based drug delivery vehicle. This focus was determined based on the advisor needs and discussion during project team meetings. Four initial design objectives were developed based on the initial client statement, requirements to develop a DDS, as well as the limitations of the project. These objectives and their definitions can be seen in Table 2 through 5 with additional details in Section 3.3 Functions and Specifications.

Table 2: Consistent product and sub-objectives definitions.

Objective & Sub-objectives	**Definition**
Consistent Product	The output of the fabrication procedure must have repeatable and reliable characteristics.
Reproducibility of Injection Force	The force required to extrude the solution through the needle must be reproducible.
Reproducibility of Gelation Time	The gelling time for the hydrogels formulated are reliable and replicable.
Maintain Insolubility	The hydrogel must remain insoluble.

Table 3: User friendly and sub-objectives definitions.

Objective & Sub-objectives	**Definition**
User Friendly	The final product must be easy for users to use.
Safe to Handle	The final product should not cause physical harm to the handler.
Acceptable Injection Force	The injection force required to extrude the material through a needle must be acceptable.

Table 4: Competitive drug carrier properties and sub-objectives definitions.

Objective & Sub-objectives	**Definition**
Competitive Drug Carrier Properties	The final product should have comparable drug carrier properties.
Sustained Drug Release	The drug release profile should occur over a clinically acceptable time-period.
Physiologically Safe Material Degradation	Product materials beside drug should not elicit negative effects.
Reliable Drug Loading	The concentration of drug loaded should be repeatable.

Table 5: Industrial scalability and sub-objectives definitions.

Objective & Sub-objectives	**Definition**
Industrial Scalability	The prefilled syringe and hydrogel system must have the ability to be scaled up.
Capacity for Sterilization	The prefilled syringe system must be prepared in a sterile environment with a pre-sterilized syringe and filter sterilized drug product.
Consistent Syringe Filling	The syringe must be able to be filled to a precise and repeatable volume.

To prioritize objectives, the team used a Pairwise Comparison Chart (PWC) to identify what objectives and sub-objectives could be categorized as needs versus wants. For project management, only those identified as needs were considered in the design selection process. For the PWC, each sub-objective was compared individually with all other sub-objectives. For each individual comparison, the sub-objective deemed less important was assigned a value of 0 for that comparison, and the sub-objective deemed more important was assigned a value of 1. If the sub-objectives being compared were deemed of equal importance, a value of 0.5 was assigned to both sub-objectives. When all comparisons were complete, the values of each sub-objective were summed to give weights. The created PWC is in Appendix A, and Table 6 represents a summary of all subobjectives and their weight.

Table 6: Preliminary design sub-objective weights.

Main Objectives	Sub-Objective	**Weight**
Consistent Product	Reproducible Injection Force	6.5
	Reproducible Gelation Time	3.5
	Maintain Insolubility	7
User Friendly	Safe to Handle	2.5
	Acceptable Injection Force	8
Competitive Drug Carrier Properties	Sustained Drug Release	6.5
	Physiologically Safe Material Degradation	2
	Reliable Drug Loading	7
Industrial Scalability	Capacity for Sterilization	0.5
	Consistent Syringe Filling	1.5

From this PWC, the team decided that sub-objectives with a weight of 6 or less were considered wants and were removed from consideration for the purpose of this project. Therefore, 3 sub-objectives were removed from further consideration, in addition to the entire Industrial Scalability objective. The final sub-objectives the team utilized for the design selection process are shown in Table 7.

Table 7: Final design sub-objective weights.

Main Objectives	Sub-Objective	**Weight**
Consistent Product	Reproducible Injection Force	6.5
	Maintain Insolubility	7
User Friendly	Acceptable Injection Force	8
Competitive Drug Carrier Properties	Sustained Drug Release	6.5
	Reliable Drug Loading	7

3.2.2 Design Constraints

The constraints of this project are imperative to consider in the design process, as they influence what can be achieved and how possible methods are. Due to this, the team identified five major constraints, as described in Table 8.

Table 8: Design constraints definitions.

Constraints	**Description**
Money	The team has a budget of $250 per member, for a total of $1000.
Time	All project work must be completed by April 22, 2022; Gives the team approximately 8 months to complete all project work.
Material Availability	All materials must be purchasable at a reasonable cost and timeline, or available in the team advisor's lab space.
Equipment Availability	All equipment must already exist and be available to the team through WPI laboratory spaces.
CS Compatibility	The project design must be compatible with the incorporation of CS.

The constraints identified by the project team were money, time, material availability, equipment availability, and CS compatibility. Money is a constraint, as the WPI Biomedical Engineering Department provides $250 per team member for MQP projects resulting in a total allotted budget of $1000. This limitation requires the team to make very purposeful purchases for experimentation. Time is another constraint as the MQP is limited to completion in the 2021-2022 calendar school year, which runs from the end of August to mid-April, as the Project Presentation Day is April 22, 2022. This gives the team approximately 8 months to complete this study and therefore, the team must be mindful of such limits in the design and methodology.

The third constraint is material availability. Everything the team desires to purchase must not only be a reasonable cost due to the budget, but it also must be possible to purchase and receive in a timely manner. While some materials may be available for use in the team advisor's lab space, they cannot rely on this for all needs, so availability is a major consideration. Another constraint is equipment availability. In a similar manner to material availability, any experimentation that the team performs must be possible with the equipment currently available and accessible at WPI, as the budget is not vast enough to purchase new machinery. This equipment may be in Goddard Laboratories, Salisbury Laboratories, and Gateway Laboratories, as the team has access to these three facilities. The fifth, and final, constraint is CS compatibility. The project design that the team utilizes must be readily compatible with CS, as this material is a given requirement in the client statement and must be incorporated.

In the same way as the design objectives, the team used a PWC to give each design constraint a weight. Despite some constraints ending with larger weights than others, the team deemed all constraints to be pertinent to the project, so none were removed from consideration for the design selection process. The created PWC is found in Appendix A, and Table 9 represents a summary of all sub-objectives and their weight.

Table 9: Design constraint weights.

Constraint	Weight
Money	2.5
Time	1.5
Material Availability	3
Equipment Availability	0.5
CS Compatibility	2.5

3.3 Functions and Specifications

The team identified functions and specifications for the project. These functions and specifications are part of the design criteria to meet necessary objectives. Through the objective analysis conducted, the team identified six objectives as needs to guide the project design process, as listed in Table 10.

Table 10: Functions for the project.

#	Function
1	User friendly – Acceptable injection force
2	Consistent product – Reproducible injection force
3	Consistent product – Maintain insolubility
4	Competitive drug carrier properties – Sustained drug release
5	Competitive drug carrier properties – Reliable drug loading

3.3.1 Function 1. Product Must Have an Injection Force Within Acceptable Range

The first function is that the injection force of the product must not exceed 38N, as defined by literature (Thomas E Robinson, 2020). To verify this, the team must develop a Standard Operating Procedure (SOP) for quantifying the average injection force of the product.

3.3.2 Function 2. Product Must Have a Reproducible Injection Force

The second function is that the hydrogels must generate a reproducible injection force across batches. To verify this, the team must use the injection force SOP developed in Function 1 to ensure the injection force between all trials of the same formulation falls within a 5% range.

3.3.3 Function 3. Product Must Maintain Insolubility

The third function is for the CS product to maintain insolubility for at least 30 days, to ensure adequate time for sustained chemotherapeutic drug release. To verify this, the team must develop a dissolution study SOP to quantify the rate of dissolution in PBS at body temperature (37°C) and perform a 1,9-Dimethyl-Methylene blue (DMMB) assay to quantify CS releasing over time.

3.3.4 Function 4. Product Must Allow for Sustained Drug Release

The fourth function is that the hydrogel must successfully release the chemotherapeutic in a sustained manner. To verify this, the team must develop an SOP for measuring drug release to ensure that there has been at least 60% release *in vitro* of the chemotherapeutic over a 30-day

period, based on similar drug release studies in literature (Li et al., 2018). Spectrophotometry will be used for quantification of drug release in accordance with the SOP.

3.3.5 Function 5. Product Must Allow for Reproducible Drug Loading

The fifth function is that the product must be able to bind the chemotherapeutic drug and the drug loading must be quantifiable and repeatable. To verify this, the team must develop an SOP to test for the quantity of drug being loaded and ensure reproducibility of drug loaded after a 3-day period that falls within a 5% range.

3.4 Design Standard Requirements

In this section, the team outlines relevant industry, regulatory, and engineering standards and regulations for the final design. These standards would all need to be followed to receive FDA approval and be brought to industry. The categories of standards included are material characteristics, mechanical testing, cytotoxicity, and sterility. Relevant standards are outlined in Table 11.

Table 11: Standards for design requirements.

Category	Standard	Test	Purpose
Material Characteristics	ASTM F2150-19	Standard guide for characterization and testing of biomaterial scaffolds used in regenerative medicine and tissue-engineered medical products	Specifies available test methods to guide the characterization of bulk physical, chemical, mechanical, and surface properties of the scaffold construct.
	ASTM F2900-11	Standard guide for characterization of hydrogels used in regenerative medicine	Specifies test methods to assess biological properties, kinetics of formation, degradation and agent release, physical and chemical stability, and mass transport capabilities of hydrogels used in regenerative medicine.
Mechanical Testing	ISO 11040-6:2019	Syringe testing: Plastic barrels for injectables and sterilized sub-assembled syringes ready for filling	Specifies materials and product requirements, test methods for polymer barrels, and sterilized sub- assembled syringes ready for filling.
	ISO 11040-8	Syringe testing: Requirements and test methods for finished prefilled syringes	Specifies the quality, functional performance, and safety requirements for prefilled syringes, with relevant test methods.
Sterility	ISO 14160:2020	Sterilization of health care products	Specifies requirements for characteristics of liquid sterilizing agents that are used to sterilize single-use medical devices after the manufacturing process.
	ISO 10993-17	Biological evaluation of medical devices: Establishment of allowable limits for leachable substances	Specifies limits for the acceptable number of residues and sterilizing agents.
	ISO 13485	Medical device manufacturing	Specifies the entire manufacturing and sterilization process.

3.5 Revised Client Statement

After considering the requirements of the project, the revised client statement is to:

"Develop a fabrication technique to obtain a water-insoluble, injectable chondroitin sulfate-based hydrogel drug delivery system. Validate the loading of daunorubicin for the sustained release of the drug."

3.6 Project Approach

As the team created a strategic plan to assess the project and ensure success, major milestones were also identified. The major milestones were created, and a date of completion

was assigned in the hopes of addressing the issues stated in the client statement individually. The milestones were determined by how the team wanted to address the problem and was further divided between teammates to distribute workload throughout the 2021-2022 academic year.

3.6.1 Work Completed in A-Term (Sept-Oct 2021)

In A-Term, the team began working by defining the problem and the goals for the project. The team then further conducted a preliminary literature review which helped determine the significance of the work and the background to begin discussing project strategy. Through this the team gained knowledge regarding the project's subject matter and how it will advance the work done in the field. The literature review was continually added throughout the scope of the project to adjust based on additional needs and goals of the project. The team created a project strategy during this time which included determining the design objectives, constraints, and approaches for the project. The project strategy was completed by October 13, 2021, though would be edited in later terms. While creating the project strategy the team also developed a Gantt chart to build a timeline around deadlines, develop the breakdown of the project goals, and create a testing timeline for B-Term.

3.6.2 Work Completed in B-Term (Oct-Dec 2021)

In B-Term, the team completed preliminary fabrication and experimental work. The team developed CS hydrogels with copolymers PNIPAM and F127 and tested varying concentrations for proper fabrication techniques. To analyze these hydrogels and CS-MA hydrogels, with 4- and 24 h methacrylate times, the systems were subjected to testing procedures including injection force testing and gelation time. Loading studies were also completed for 24-h CS-MA hydrogels to further understand the loading process and to ensure proper loading. The team also began investigating the process of a DMMB assay to understand the potential leeching of CS from the hydrogels.

3.6.3 Work Completed in C-Term (Jan-Mar 2022)

In C-Term, the team completed a 30-day drug loading study on 20 μL 4 h CS-MA hydrogels from three batches of CS-MA produced by the Coburn lab. Alongside this study the team completed a DMMB assay to further identify one specific batch of 4 h CS-MA to use for the hydrogel system. Following the DMMB assay the team settled on a batch of 4 h CS-MA

synthesized in 2022 to further generate 50 μL hydrogels from and complete injection force testing, 30-day drug loading and release study, DMMB assay, and loaded hydrogel injection force testing. The team further continued to investigate their first thermosensitive polymer of choice by completing a dissolution study on F127 to showcase the polymer's solubility.

3.6.4 Work Completed in D-Term (Mar-May 2022)

Finally, in D-Term the team continued to complete final testing and further investigated the thermosensitive polymer PNIPAM and its properties for an injectable DDS by testing the feasibility of using PNIPAM to create CS based hydrogels for the delivery of DNR. The team made hydrogels with PNIPAM and CS in combination to test their gelation properties. Finally, the team finalized the final report and prepared for the final presentation at the end of the academic year. This report was completed and submitted for review by April 27, 2022 and the project was presented April 22, 2022.

IV. Design Process

4.1 Needs Analysis

Project sub-objectives defined as needs were given a percentage of importance and arranged in order from most important to least important for each main objective. Project wants were also identified; however, they were listed as last priority and were not given a percentage of importance. Table 12 lists the project needs, divided by main objective, in percentage from most important to least important.

Table 12: Ranked objectives and sub-objectives by percentage.

Main Objective	Sub-Objective	Percentage (%)
Consistent Product	Reproducible Injection Force	18.5
	Maintain Insolubility	20
	Reproducible Gelation Time	
User Friendly	Acceptable Injection Force	23
	Safe to Handle	
Competitive Drug Carrier Properties	Sustained Drug Release	18.5
	Reliable Drug Loading	20
	Physiologically Safe Material Degradation	
Industrial Scalability	Capacity for Sterilization	
	Consistent Syringe Filling	

As determined by the PWC detailed in Appendix A, the main objective needs for this project include consistent product, user friendliness, and competitive drug carrier properties. The main objective want for this project is the ability for industrial scalability. While these are the main objective needs, each of these main objectives also has its own wants and needs. For example, under user friendly, the product needs to have an acceptable injection force, whereas the want is for the product to be safe to handle.

4.2 Concept Map

To determine an initial conceptual design to fabricate an injectable DDS for the treatment of NB, several aspects need to be considered (Figure 13). For this project, the first selection is the fabrication method of the hydrogels as the client is looking to obtain an injectable hydrogel DDS. To generate the injectable hydrogel, multiple fabrication methods must be considered to obtain a system that fits the criteria given. The determination of fabrication will then help determine the polymers needed as certain polymers maintain specific mechanical properties that

limit the methods of fabrication. The fabrication system should be determined first, then a group of polymers may be considered, and a decision may be reached. The client also hopes to use CS in the system for its ability to bind to chemotherapeutic agents, which is also considered in the determination of the polymer. Following the determination of the polymer a conclusion shall be made on the chemotherapeutic agent of DOX versus DNR for its chemical and release properties. Following these choices, the hydrogels made with a polymer and CS will be fabricated and tested to ensure the fabrication method provides a system that shall result in a low injection force through a compression test on the Instron. Once the system has proven to have an acceptable injection force, the system will then be loaded with drug to ensure the capability to load chemotherapeutics.

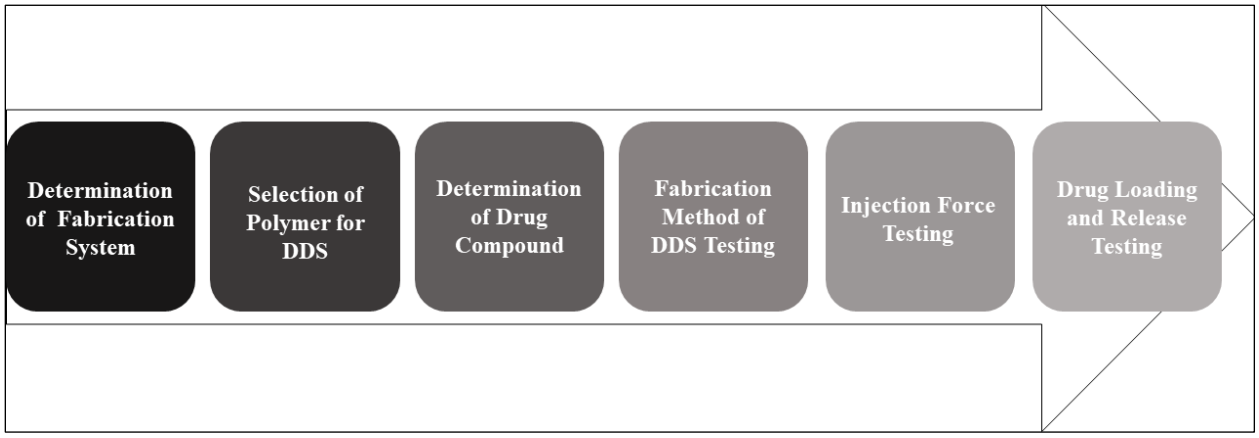

Figure 13: Conceptual flow diagram for fabrication of an injectable DDS for NB.

4.3 Design Approach Concepts

The following discusses the design approaches that were considered for the project to synthesize an injectable hydrogel. Those considered included F127, PNIPAM, and PLGA-PEG-PLGA to make thermosensitive hydrogels, CS-MA hydrogels with low methacrylation times, and microbeads generated by high pressure homogenization and microfluidics. These designs were compared in a selection matrix using the weighted design sub-objectives and constraints, which can be found in Section 4.4.

4.3.1 Thermosensitive Pluronic F127 Hydrogel

A thermosensitive hydrogel formation using F127 would allow for a solution to gel at body temperature and remain in a liquid state at temperatures below 37°C (Gioffredi et al.,

2016). Outside of its thermosensitive properties, F127 provides additional favorable characteristics such as safety of usage, bio-adhesiveness, stability, and the ability to form hydrogels at low concentrations at body temperature. Specifically, F127 has been researched as drug and cell carriers for its low toxicity, thermal gelation with reversible properties, and high drug loading properties. F127 is a thermosensitive polymer with a lower cost in comparison to other thermosensitive copolymers ($0.23 per gram), whose material is readily available in the lab. Previous studies have used a combination of F127 and CS due to its thermosensitive properties and its ability to bind to cationic drugs, respectively. According to such studies, CS was incorporated into the thermo-sensitive hydrogel through physical blend, which is the process of mechanically mixing various polymers together in a melt to create a polymer mixture (Li et al., 2018). Through studies the team will be able to evaluate the interactions between F127 and CS along with its properties for drug loading to determine a viable polymer solution.

4.3.2 Thermosensitive PNIPAM Hydrogel

A thermosensitive hydrogel formation using PNIPAM allows for a solution that would remain liquid at temperatures below 32°C and would gel above 32°C. PNIPAM naturally has low drug loading capacity; however, when crossed with CS, a polysaccharide with sufficient drug loading capacity, the polymer solutions would be able to take on the drug loading capacity of CS while maintaining the thermal transition temperature of PNIPAM. N-terminus PNIPAM is commercially available and the mechanism for synthesis of PNIPAM crosslinked to CS is well understood (Liu et al., 2017). Although the correct form of PNIPAM is commercially available, PNIPAM is expensive considering the budget of our project ($116 per gram).

4.3.3 Thermosensitive PLGA-PEG-PLGA Hydrogel

A thermosensitive hydrogel formed by using PLGA-PEG-PLGA allows for a hydrogel to be formed above 37°C and a solution to be maintained at all temperatures below. This will allow for a solution to be kept during storage and a hydrogel to be formed following the injection of the hydrogel. PLGA-PEG-PLGA has biodegradable capabilities and with the addition of PEG the copolymer is nontoxic and lack antigenic/immunogenic effects. With these properties and more PLGA-PEG-PLGA enhances solubility of hydrophobic drugs like DOX as well as prolonging drug release. One drawback of PLGA-PEG-PLGA is that with the load of DOX there is a potential of viscosity increase which can pose issues (Yu et al., 2013). Additionally, despite

PLGA-PEG-PLGA being commercially available, the polymer is expensive and unfeasible considering the budget for this project ($260 per gram).

4.3.4 Low-Methacrylation CS-MA Hydrogels

CS-MA hydrogels are readily used in Professor Coburn's lab at WPI, with methacrylation times up to 24 h and 10% Irgacure® 2959 stock, the CS-MA initiator, used at a ratio of 1:50, or 20 µL Irgacure® 2959 stock to 1 mL CS-MA solution. This hydrogel formulation is promising as it has well-documented success in its insolubility and drug carrier properties, and all the necessary materials and equipment are readily available to the team, with a cost of $377 per 5g for CS. The main limitation with the developed CS-MA hydrogel in its current form is that, though reproducible, its injection force is too high to be acceptable. To resolve this, the team has several proposed improvements to the CS-MA hydrogel design. First, it is believed that a lower CS-MA methacrylation time may lower the viscosity of the formulated hydrogel. Second, using less Irgacure®2959 would create less CS-MA chain bonds when exposed to UV light.

Thus, the team suggests a design using 4 h CS-MA, the lowest methacrylation time that has had consistent gelation success in Professor Coburn's lab, and 10% Irgacure® 2959 stock at a ratio of 1:100; half the amount that is called for in the current CS-MA protocol. The goal of these design alterations is to create a hydrogel with a lower, acceptable, injection force.

4.3.5 Microbeads by High-Pressure Homogenization

High-pressure homogenizers create coarse emulsions, which are compressed using turbulent flow to form fine emulsions, or microbeads. In this design, the team would create CS-MA hydrogels using the fabrication method already utilized in Professor Coburn's lab at WPI and would then use the high-pressure homogenizer to create CS-MA emulsions. In theory, this process would decrease the required injection force of this hydrogel material.

High-pressure homogenizers are readily available, such as by manufacturer Cole-Palmer, but they are expensive, ranging from $1000 to well over $4000, thus are outside the scope of this project. This would mean the team would have to rely on the high-pressure homogenizer, a Polytron PT-MR 2100, that is already available in Salisbury Laboratories. This device would produce consistent microbead sizes and works for small volumes ranging from 0.1 to 2000 mL (LabX, n.d.). A potential drawback of this method is that the device would require excessive

cleaning and the team would run the risk of microbead contamination, impacting cytotoxicity testing. This concern may be avoidable if the team was able to purchase a personal homogenizing device, but as noted, this is not possible due to the design constraints. Additionally, the team is not confident that the available high-pressure homogenizer could create CS-MA emulsions small enough to lower the required injection force to an acceptable rate.

4.3.6 Microbeads by Microfluidics

In general, microfluidic devices use a pump to push pre-emulsion through micro-channels that utilize increasing velocities to produce microbeads. This method was utilized by the 2018 MQP completed in the Coburn lab where the system contained syringe pumps that pushed the emulsions through an interaction chamber (Loaisa et al., 2018). While this method can successfully produce hydrogel microbeads for drug loading and release, it is difficult to create reproducible microbeads small enough for acceptable injection forces. Additionally, creating a microfluidic system can be costly and time consuming and operating the microfluidics system can be challenging due to back-pressure and leakage, which may be beyond the scope of this project.

4.4 Selection of Design Approaches

To compare the design approaches, the team created a design selection matrix. This matrix compared the 6 designs with the previously identified and weighted design criteria (sub-objectives and constraints). If the design was able to meet the criteria, it was assigned a value of 1. If the design could not meet the criteria, it was assigned a value of 0. If the team questioned if the design would or would not meet the criteria, it was assigned a value of 0.5.

To calculate a total score for each design approach, the values assigned for each criterion were multiplied by the weight of that sub-objective or constraint and totaled at the bottom of the matrix. The total score received for each design was out of 45 points. The design selection matrix can be found in Appendix B, and the total score associated with each design is represented in Table 13.

Table 13: Design approaches total scores.

Design Approaches	Total Score
Thermosensitive F127 Hydrogel	40.25
Thermosensitive PNIPAM Hydrogel	43.75
Thermosensitive PLGA-PEG-PLGA Hydrogel	38.25
Low-Methacrylation CS-MA Hydrogel	41
Microbeads by High-Pressure Homogenization	38.25
Microbeads by Microfluidics	33.5

To account for design failures and limitations, the team chose to pursue design verification on the three design approaches with the greatest scores. These designs were: a thermosensitive F127 hydrogel, a thermosensitive PNIPAM hydrogel, and a low-methacrylation CS-MA hydrogel. The experimentation that each design underwent is outlined next section.

Additionally, the team considered the two chemotherapeutic agents DNR and DOX as drug agents to be used as the agent in the DDS. DOX provides the ability to release drug over time whereas DNR has similar properties of release but has been found by the Coburn laboratory to exhibit a linear drug release profile over an extended period. The team chose to use DNR as the chemotherapy drug for design experimentation instead of DOX because due to its increased stability over the drug release profile and its natural saturated orange color.

V. Design Verification

5.1 Experimentation Summary

5.1.1 F127 and F127/CS Hydrogel Fabrication and Gelation

F127 hydrogels doped with CS were fabricated at various concentrations using the following protocol. First, calculations were performed in accordance with Appendix C to ensure the correct desired mass per mass concentration. The desired mass of F127, CS, and water were then combined in a glass vial and gently mixed with a magnetic stir bar at 4°C for 24 h. For control samples, the desired mass of F127 was dissolved in water only. Once the samples were completely dissolved, the glass vials were removed from the cold room and samples were allowed to warm to room temperature. Once warmed to room temperature, 500 µL samples were aliquoted into 1.5 mL Eppendorf tubes (see Figure 14) and gelation time was tested by placing the samples into a 37°C hot block. Several concentrations of F127 and CS were evaluated to determine the ideal formulation (see Table 14). Results of this study are found in Section 5.2.1.

Table 14: F127 formulations fabricated.

% F127	CS Percentage							
	0%	0.5%	1%	2%	3%	5%	8%	10%
10%	X							
15%	X					X	X	X
16%	X	X	X	X	X			
17%	X	X	X					
18%	X	X	X	X	X	X	X	X
20%	X	X	X	X		X		

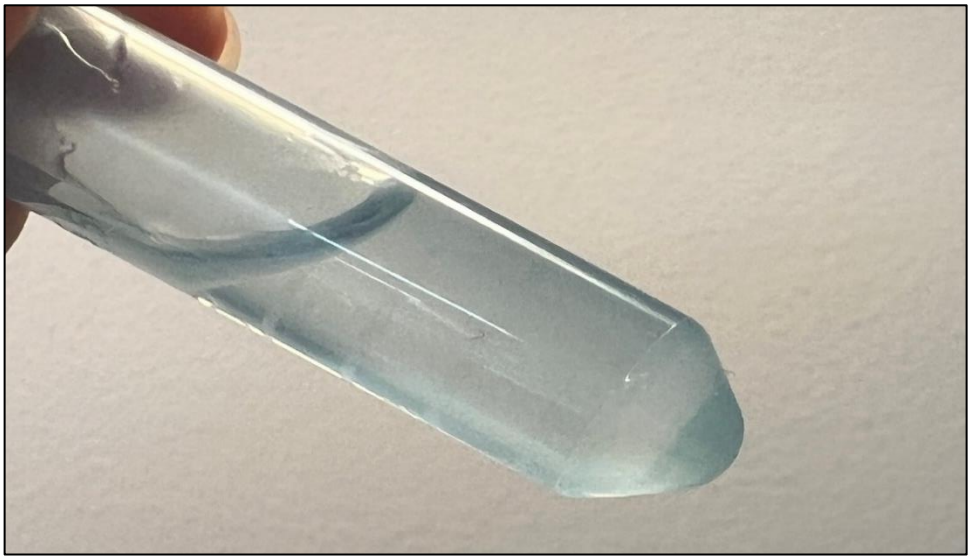

Figure 14: Pluronic F127 formulation at room temperature.

5.1.2 PNIPAM-CS Hydrogel Fabrication and Gelation

PNIPAM conjugated to CS was fabricated using the protocol outlined in Appendix D, which required 3 days of dialysis and 5 days of lyophilization. The product was added to PBS at the desired concentration and allowed to dissolve at 4°C. Once the samples were completely dissolved, 500 µL samples were aliquoted into Eppendorf tubes (see Figure 15) and allowed to warm to room temperature. Once warmed to room temperature, samples were placed into a 37°C hot block. Limited concentrations of the yield product were fabricated (10%, 20%, and 33%), and results can be found in Section 5.3.1.

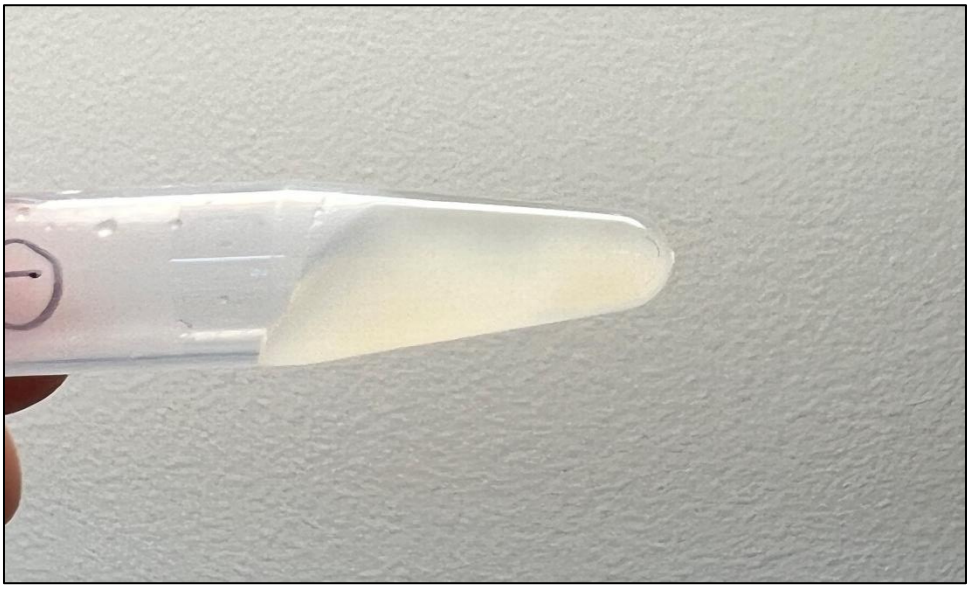

Figure 15: PNIPAM-CS formulation at room temperature.

5.1.3 Low-Methacrylation CS-MA Hydrogel Fabrication and Gelation

CS-MA was fabricated using the established protocol outlined in Appendix E. The product was utilized to fabricate CS-MA hydrogels, using an adapted version of the protocol used in Professor Coburn's lab, found in Appendix F. Table 15 outlines each of the CS-MA formulations that were fabricated using this protocol.

Table 15: CS-MA formulations fabricated.

CS-MA Formulations	**CS-MA Percentage & Hydrogel Size**			
	10% 20 µL	**20% 20 µL**	**10% 50 µL**	**20% 50 µL**
4 h	X	X	X	X
8 h				X
24 h				X

First, CS-MA and ultrapure water were combined, dissolved, and centrifuged to achieve the desired concentration and volume of hydrogel. Then, a 10% Irgacure® 2959 stock was created using Irgacure®2959 and 70% ethanol, and vortexed until fully dissolved. The 10% Irgacure® 2959 stock was then added, at a ratio of 1:100 to the 4 h CS-MA solution and 1:50 to the 8 h and 24 h CS-MA solutions. The solutions were then centrifuged. Gelation was performed using slight difference methods for the hydrogel volumes of 20 µL and 50 µL based on testing needs. Both volumes were placed under UV light for 10 to 20 minutes, depending on the duration required for gelation. This time varied depending on factors such as gel size, and hydrogel proximity to the UV light source. For the 20 µL hydrogels, the CS-MA solution was pipetted into droplets on parafilm, shown in Figure 16(A), and after gelation were moved to a well plate where they were washed 3 times with Mill-Q water and then allowed to swell for at least 3 days. For the 50 µL hydrogels, the CS-MA was pipetted into cutoff syringes, shown in Figure 16(B), and after gelation they were washed 3 times with ultrapure water directly in the syringe and remained there to swell for at least 3 days.

Figure 16: (A) The droplet on parafilm gelation set-up for the 20 µL hydrogels, and (B) the cutoff syringe gelation set-up for the 50 µL hydrogels.

5.1.4 Injection Force Testing of Hydrogels

To test the ability to inject the thermosensitive formulations and the photo-crosslinked CS-MA hydrogels, injection force testing was completed according to the protocol in Appendix G. These tests were completed using an Instron E1000 with a 2 kN load cell (Catalog # 2527-

129). A custom-made compression fixture was utilized to hold the syringe plunger at a 90° angle and minimize slippage when force is applied. This custom fixture further supported the syringe with two pins (Figure 17). Experiments were run using a compression based Bluehill script, at a rate of 4 mm/min that was programmed to terminate after travelling the distance of the full height of the hydrogel in the syringe. This hydrogel height was measured and input into the script for each sample. During the test, extension and load were sampled every 250 ms and was exported following the conclusion of the test. Following the conclusion of the test the data was analyzed utilizing the excel analysis Tool Pack and plotted using a moving average on an interval of 70 points. Additionally, the maximum force and average force over the plateau region were calculated. These tests allowed for the understanding of the force required to extrude the hydrogel through a 28 G needle with a volume of 0.5 mL and a needle length of 0.5 in. Results of these studies can be found in Section 5.2.2 for F127 hydrogels and Section 5.4.1 for CS-MA hydrogels.

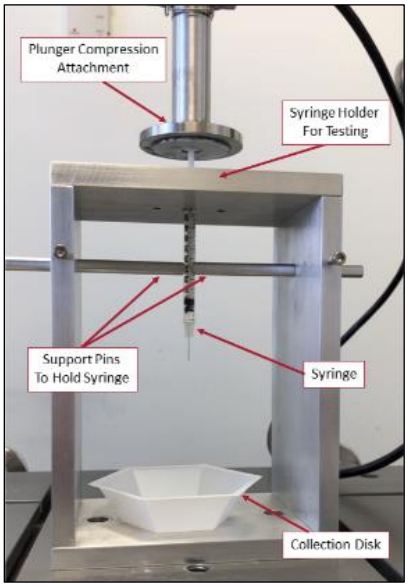

Figure 17: Instron set-up for injection force testing.

5.1.5 Short-Term Dissolution of Hydrogels in PBS

A dissolution study was performed in PBS to quantify the rate of dissolution of F127/CS hydrogels, as the dissolution rate of these hydrogels was unknown. This process was not required for the CS-MA hydrogels because the formulation had been previously used and short-term dissolution of these hydrogels was not a concern.

This process was performed in accordance with the protocol outlined in Appendix H. A volume of 500 µL of F127/CS hydrogel was fully gelled in a hot block at 37°C and the weight was recorded. Pre-warmed PBS (1 mL) was then added to the hydrogel and allowed to sit in the hot block for 2 h. At the 2 h mark, the PBS was aspirated off, the hydrogel was weighed, and 1 mL of fresh PBS was added back to the hydrogel. This process was repeated for time points 4 h, 8 h, 10 h, 12 h, 24 h, 28 h, 32 h, 36 h, 48 h, 52 h, 56 h, and 60 h, or until the hydrogel had completely dissolved. Results of this study can be found in Section 5.2.3.

5.1.6 Dimethyl-Methylene Blue Assay of Hydrogels

The DMMB Assay was used to quantify CS leaching from hydrogels that did not face short-term dissolution limitations. This resulted in the team conducting DMMB Assays on 20 µL and 50 µL CS-MA hydrogels.

Individual CS-MA samples were placed in a 24-well plate and 1 mL of PBS was added to each well. Over the course of 7 days, the PBS supernatant of each CS-MA sample was collected and stored at 4°C and replaced with new PBS. To quantify CS in the PBS supernatant, a standard curve was created from a 500 µg/mL CS solution using a serial dilution method. To a 96-well plate, 20 µL of standard and sample were added, followed by the addition of 200 µL of the DMMB solution. The visible light absorbance at 525 nm was measured using a Molecular Devices SpectraMax M2 Multilabel Microplate Reader with a 5 second pre-shake. The detailed protocol for the DMMB assay was adapted from a 2014 Bio-Protocol and is outlined in Appendix I. Results of this study for each formulation run can be found in Section 5.4.2.

5.1.7 Drug Loading and Release Studies of Hydrogels

The team conducted DNR loading and release studies on hydrogels that did not face short-term dissolution limitations, resulting in the team conducting these studies on the CS-MA hydrogels only. The detailed protocol for the drug loading and release studies can be found in Appendix J.

This process was completed using 20 µL and 50 µL CS-MA hydrogels at concentrations of 10% and 20%. The 50 µL hydrogels were used to test injection force and a load and release study was performed on them to understand the effect of hydrogel size on its drug loading and release properties.

For this study, three hydrogels containing 20% CS-MA and three hydrogels containing 10% CS-MA were made. For drug loading, adsorption from solution was used. The hydrogels were submerged in 1 mL of 500 μg/mL DNR in water, and the hydrogels were loaded for 3 days. After the hydrogels were loaded, they were removed from the loading solution and placed in lo-bind microcentrifuge tubes for the release study. The loading was calculated using Equation 2. The pre-absorbed solution refers to the loading solution of concentration 500 μg/mL, while the post-adsorbed solution refers to the supernatant solution in each well.

[pre-adsorbed concentration (μg/mL) – post-adsorbed concentration (μg/mL)] x 1 mL = mass loaded (μg) **(Equation 2)**

For the drug release studies, hydrogels were placed in 1 mL of PBS (pH 7.4) at 37°C in a humid environment. Drug concentration was evaluated using UV/vis spectrophotometry at regular intervals. A standard curve was created before using a Molecular Devices SpectraMax M2 Multilabel Microplate Reader spectrophotometer to determine the concentration of a sample solution of unknown concentration. After the supernatant sample was collected, the entire volume of PBS solution was exchanged with fresh PBS to maintain a continuous sink state. The methodology for drug loading and release studies was followed for both 20 μL and 50 μL hydrogels. The results of this study can be found in Section 5.4.3.

5.2 F127 Design Verification Results

5.2.1 F127/CS Fabrication and Gelation Time

Various F127 and CS concentrations/formulations were analyzed and a summary of the behaviors of each of these concentrations can be found in Table 16.

Table 16: Summary of gelation behaviors for carious F127/CS concentrations. Where V stands for variable, L for liquid, G for gelled, -- for not applicable, and X for yes.

Formulation		State at...		Reversal?		Comments
F127 %	**CS %**	**Room Temp**	**37°C**	**Room Temp**	**If No, 4°C**	
10	0	L	L	--		
15	0	L	G	X		
15	5	L	L	--		
15	8	L	L	--		
15	10	L	L	--		
16	0	L	G	X		
16	0.5	L	G	X		
16	1	L	G	X		
16	2	L	G	X		
16	3	L	G	X		
17	0	L	G	X		
17	2	V	G	V	X	
17	3	G	G		X	
18	0	V	G	V	X	
18	0.5	L	G	X		
18	1	L	G	X		
18	2	V	G		X	
18	3	V	G		X	
18	5	G	L		X	
18	8	G	L	--	--	Reversed thermosensitive properties
18	10	L	L	--	--	Reversed thermosensitive properties
20	0	G	G		X	
20	0.5	G	G		X	
20	1	G	G		X	
20	2	G	G		X	
20	5	G	G		X	

5.2.2 Injection Forces

Upon verification of gelation of F127 formulations and their stability across 4℃, 25℃ (room temperature), and 37℃ (body temperature) the formulations were subjected to injection force testing. Before the addition of CS into the F127 hydrogel formulations, preliminary injection force testing was completed on F127 formulations with 0% CS. The F127 concentrations evaluated for injection forces included 15%, 16%, and 20%; the data can be seen in Figure 18. Following testing of these hydrogels the maximum injection force and the average injection force across the plateau were evaluated (see Table 17).

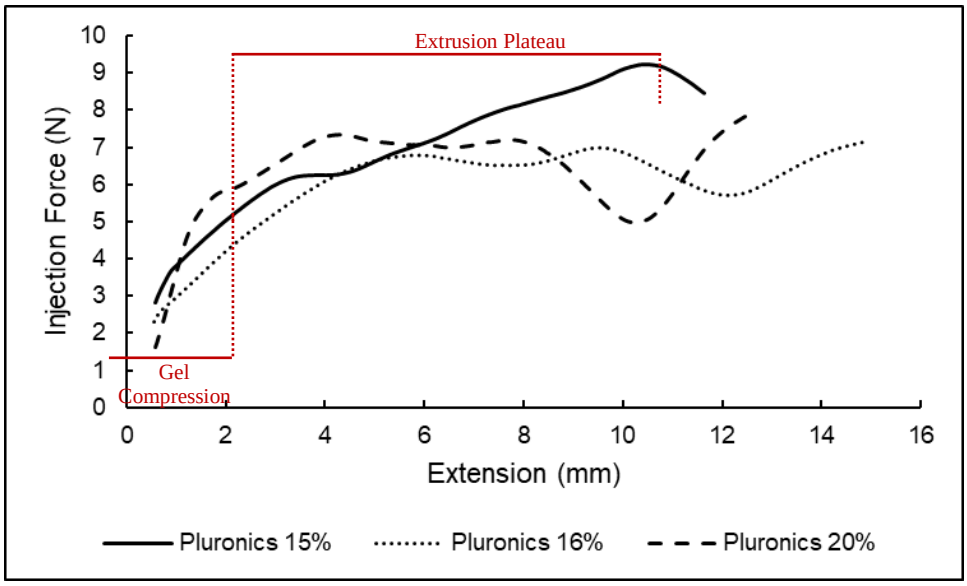

Figure 18: Results of injection force testing for F127 hydrogels at 15%, 16%, and 20%.

Table 17: Summary of maximum injection force and average injection force during testing for F127 formulas at 15%, 16%, 20%.

F127 Formulation	Maximum Injection Force (N)	Average Injection Force (N)
15%	9.23	7.67
16%	7.18	6.58
20%	7.96	6.61

The F127 hydrogels of 15%, 16%, and 20% were further analyzed via a single factor ANOVA test in excel to see if the increase in F127 concentration resulted in a statistically significant difference in the required force for extrusion. Through this ANOVA test a p-value of 0.38 was reported, indicating statistically similar average injection forces between formulations. This concluded that an increase of F127 concentration did not result in an increased injection force. This allowed the team to explore more concentration combinations of F127/CS to ensure a proper formulation for desired gelation and injection force testing.

Due to the instability of gelation of hydrogel formulations 15% and 17% -20% F127 doped with CS, these formulations were not considered for injection force testing. Rather, the team investigated 16% F127 formulations with 2% and 3% CS. These formulations were then compared against a 16% F127 formulation with 0% CS which may be seen in Figure 19. The maximum injection force and average injection force across the plateau of each formulation was found and reported in Table 18.

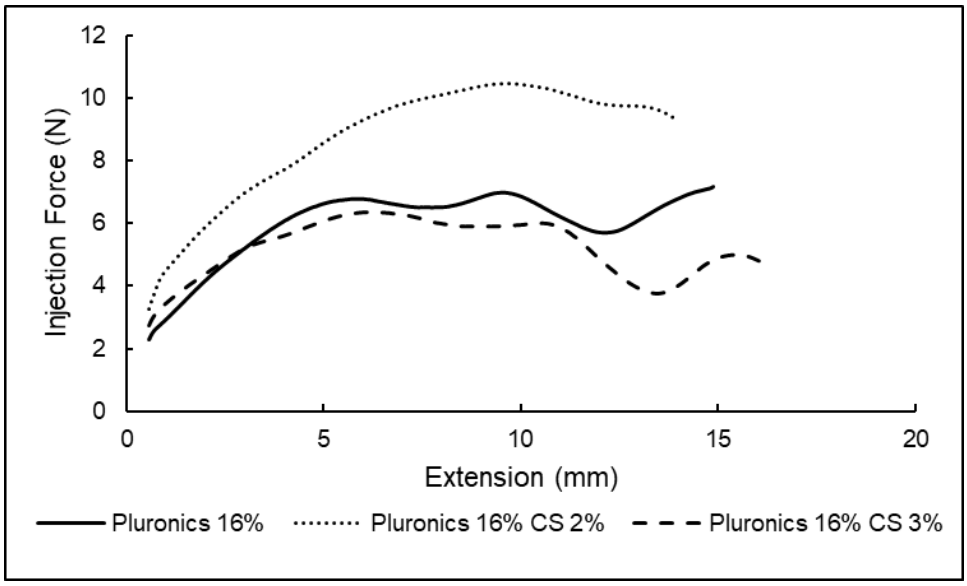

Figure 19: Results of injection force testing for F127/CS hydrogels at 16%/0%, 16%/2%, 16%/3%.

Table 18: Summary of maximum injection force and average injection force during testing for F127/CS hydrogels at 16%/0%, 16%/2%, 16%/3%.

F127/CS Formulation	Maximum Injection Force (N)	Average Injection Force (N)
16% / 0%	7.1	6.53
16% / 2%	10.48	9.61
16% / 3%	6.35	5.42

By testing various F127 hydrogels, including those with CS content, the team was able to draw conclusions regarding the use of thermosensitive polymers for injectable DDS. F127 hydrogels with the addition of CS were further validated for product dissolution through additional testing to determine its DDS capabilities.

5.2.3 Short-Term Dissolution Study

A short-term dissolution study was performed to understand how the F127 hydrogels would behave in PBS as assays and drug loading/release studies require insolubility in PBS. This study was performed on 500 µL hydrogels for formulations 16, 18, and 20% F127 with 0%, 0.5%, and 1% CS. All 9 formulations were completely dissolved after 28 h in PBS, and it was concluded that an increased F127 concentration resulted in a slower dissolution rate whereas an increased CS concentration resulted in a faster dissolution rate (Figure 20). Based on the dissolution study, none of the formulations tested would remain insoluble for the entirety of a 7-day DMMB assay or a 30-day drug load/release study.

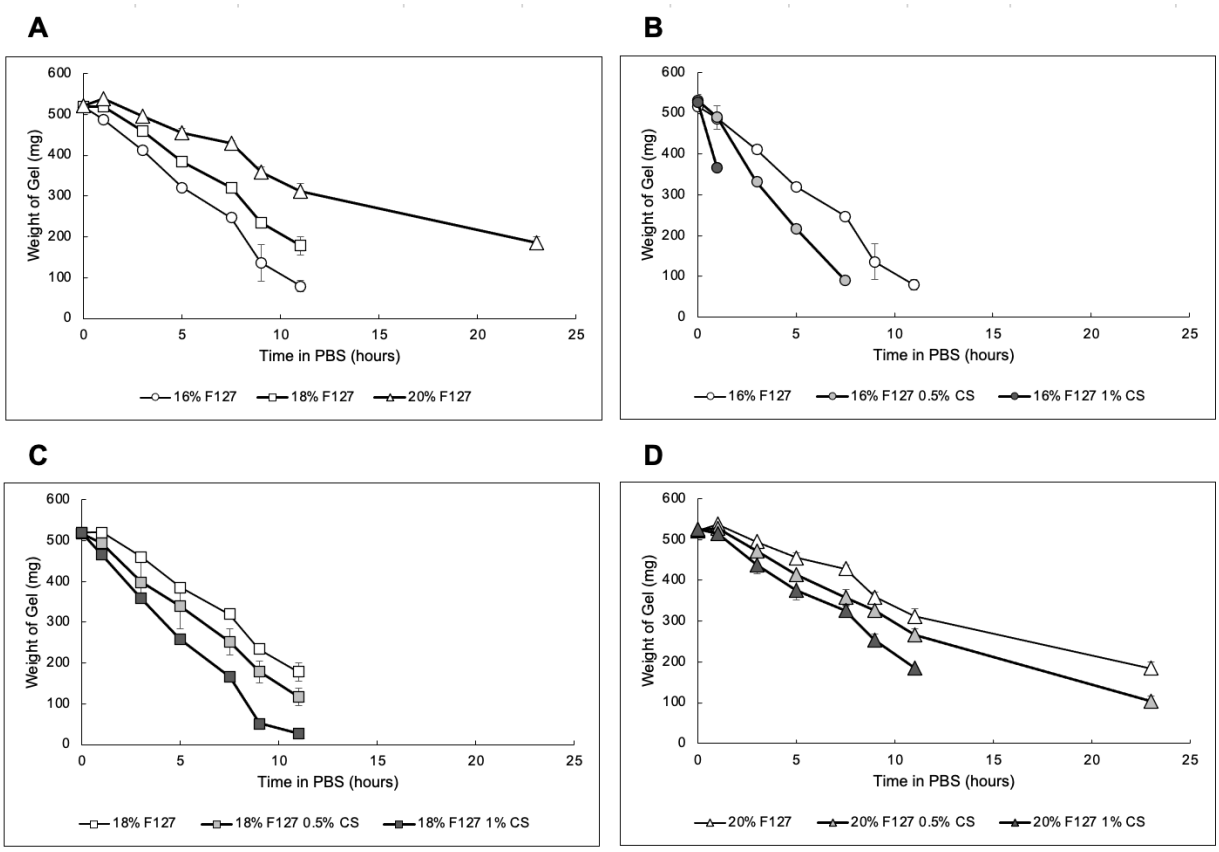

Figure 20: Results of dissolution study for (A) 16%, 18% and 20% F127 concentration, (B) 16% F127 at 0%, 0.5%, and 1% CS, (C) 18% F127 at 0%, 0.5%, and 1% CS, and (D) 20% F127 at 0%, 0.5%, and 1% CS.

5.3 PNIPAM Hydrogel Design Verification Results

5.3.1 PNIPAM-CS Fabrication and Gelation

PNIPAM was conjugated to CS at a 1:1 molar ratio. Three different concentrations of this PNIPAM-CS mixture were then analyzed and a summary of the behaviors of each of these concentrations can be found in Table 19.

Table 19: Summary of gelation behaviors for various PNIPAM-CS concentrations, where L stands for liquid.

Formulation	State at…		Comments
PNIPAM-CS %	Room Temp	37°C	
10	L	L	
20	L	L	
33	L	L	

5.4 4 h CS-MA Hydrogel Design Verification Results

5.4.1 Injection Force Testing

To begin testing and validation of the hydrogels generated by the team, the current CS-MA hydrogel system developed by the Coburn lab was tested at 20% concentration with varying methacrylation time. The CS-MA hydrogels for the Coburn lab tested included 4 h, 8 h, and 24 h methacrylated CS-MA as it was previously found that varying the methacrylation times of CS can alter the mechanical properties of the hydrogels (Ornell et al., 2019). Shown in Figure 21 is the data generated from injection force testing.

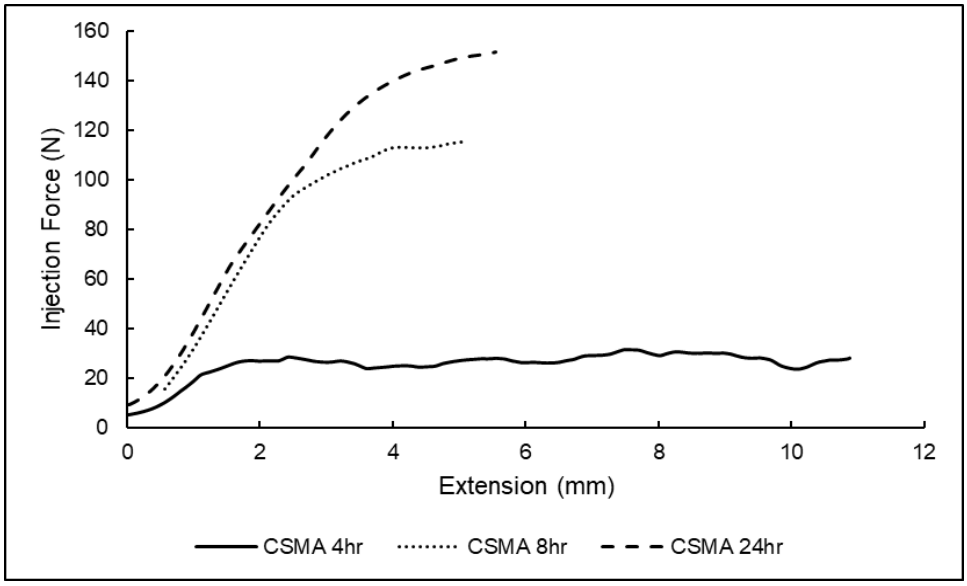

Figure 21: Injection force testing of 20% CS-MA Hydrogels with 4 h, 8 h, and 24 h methacrylation time.

Table 20: Summary of maximum injection force and average injection force during testing for 20% CS-MA hydrogels with 4 h, 8 h, and 24 h methacrylation time.

CS-MA Formulation	Maximum Injection Force (N)	Average Injection Force (N)
20% 4 h	30.73	27.17
20% 8 h	122.07	110.57
20% 24 h	151.51	142.91

Through this testing, it was confirmed that the force needed to inject the hydrogel was dependent on the methacrylation time. The longer the methacrylate time, the more the CS was modified with acrylate groups, which attributes to the increase in injection force needed for extrusion of the hydrogel. As shown in Figure 22 and Table 20, the 24 h CS-MA has the highest injection force of 142.91 N whereas 4 h CS-MA hydrogels resulted in a maximum injection force

of 27.17 N which falls within the team's defined specification of an injectable hydrogel system. From this outcome, the team decided to further investigate the difference in injection forces between 5%, 10%, and 20% 4 h CS-MA by running six 50 μL hydrogels at the specified weight percent. A comparison of these outcomes may be seen in Figure 22. This data was further quantified by the average and maximum injection force required in Table 21, respectively.

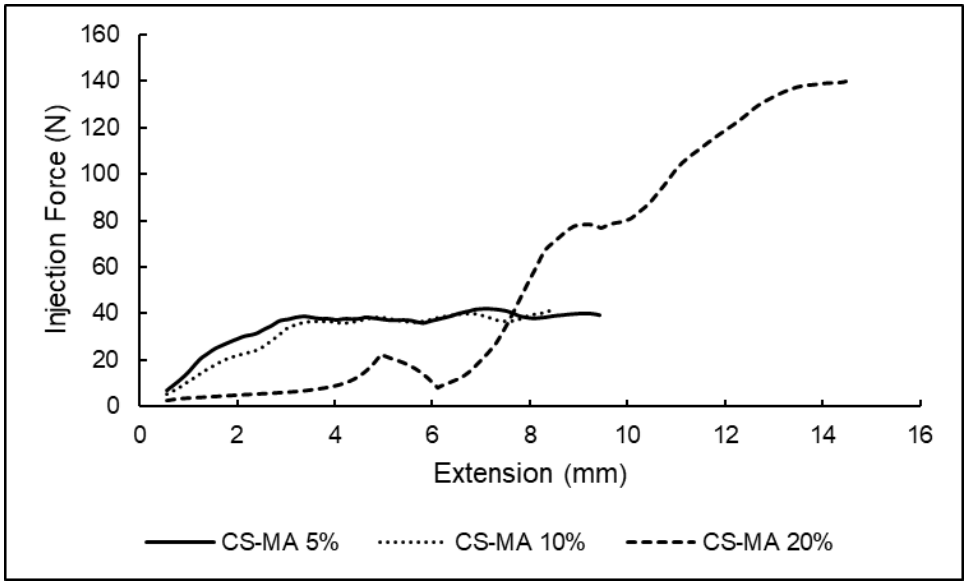

Figure 22: Injection force testing of 5%, 10%, and 20% CS-MA hydrogels.

Table 21: Summary of maximum injection force and average injection force during testing for 5%, 10%, and 20% CS-MA hydrogels with 4 h methacrylation time.

CS-MA Weight %	Maximum Injection Force (N)	Average Injection Force (N)
5%	41.83	38.52
10%	41.58	37.74
20%	135.95	124.59

Due to its mechanical and DDS properties, the team decided to move forward with the 10% 4 h CS-MA hydrogel formulation for additional studies. To test the reproducibility of injection force required for extrusion, two additional batches of six 10% 4 h CS-MA hydrogels were produced. The two additional sets made total three sets of 6 hydrogels, to compare all samples, the samples within the sets, and the variance between the sets. Figure 23 displays the outcomes of all samples run broken into their respective sets.

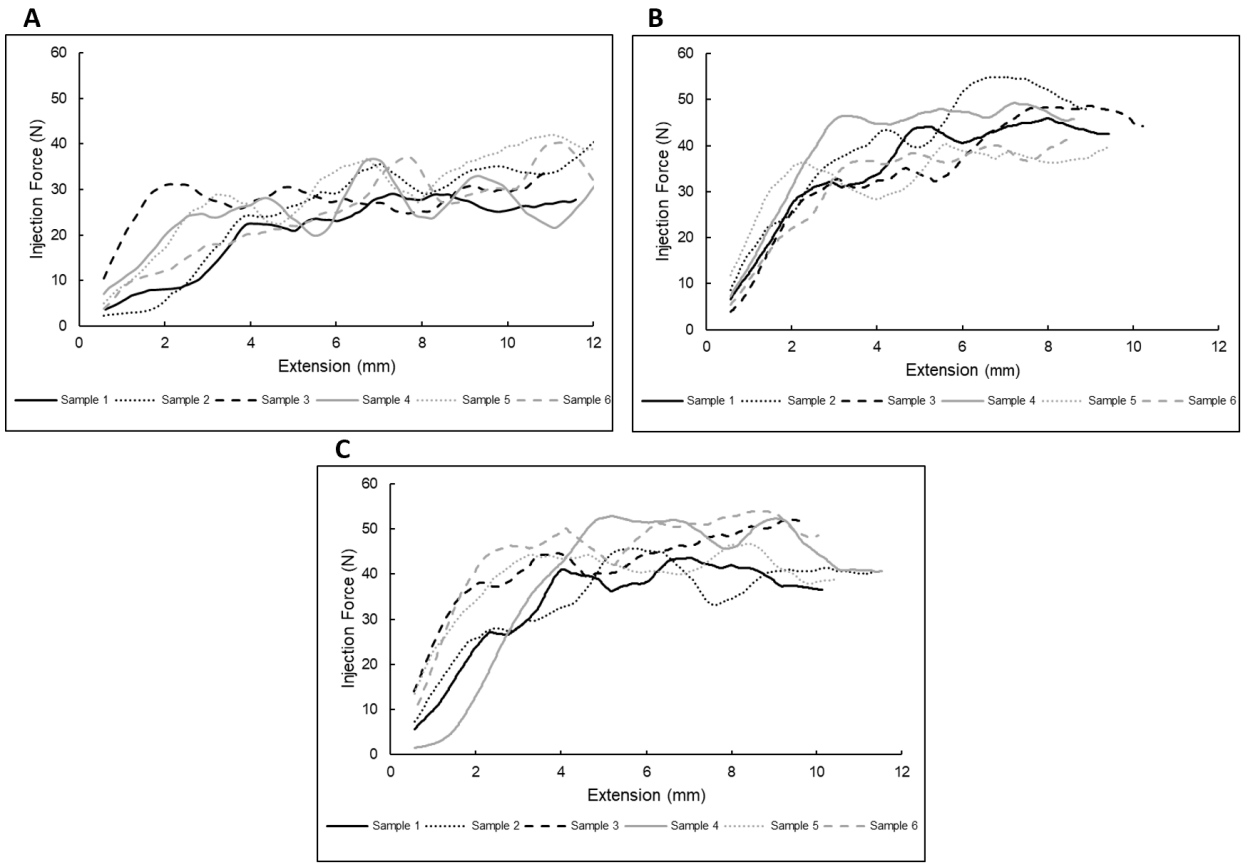

Figure 23: Injection force testing of 10% 4 h CS-MA hydrogels (A) representative of trial 1, (B) representative of trial 2, (C) representative of trial 3. The three sets show varied results between both samples and sets samples and sets.

These samples were further quantified to understand if the average injection force across the plateau fit within 5% of the average between samples. Each average injection force was tested to see if it was within 5% of the trial average and the average of all samples. Table 22 shows the average used for the 5% variance test, and the number of samples that fit within for each run of the test. This test of variance showed that between the samples in the trials and the total amount of samples there was a significant variance, thus concluding that the system does not have a reproductible injection force.

Table 22: Summary of 5% variance test for 10% 4 h CS-MA.

Comparison	Average	# Within 5%	# Of Total Samples
Trial 1	30.23	0	6
Trial 2	41.76	2	6
Trial 3	44.27	2	6
All Samples	38.75	4	18

Following these results, the team chose to further investigate how the loading of the 10% 4 h CS-MA hydrogel system with DNR may affect the injection forces needed to extrude the hydrogel. In Figure 24, the six loaded hydrogels ran can be seen as well as a comparison between a representative sample of the loaded 10% CS-MA group versus a sample from the unloaded 10% CS-MA hydrogels. The injection forces obtained highlight a significant increase in injection force required when compared against the hydrogels without the addition of DNR. Table 23 reports the maximum and average injection force of the trails shown in Figure 24B, this data shows that the injection force required for the 10% 4 h CS-MA hydrogels loaded with DNR resulted in double the force required for extrusion when compared to unloaded hydrogels.

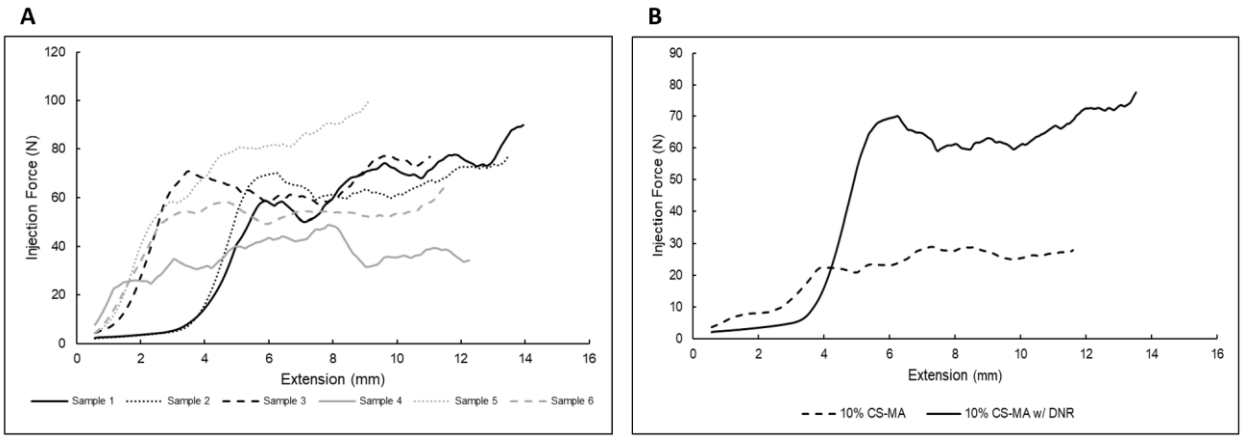

Figure 24: (A) Injection force testing of six DNR loaded 10% 4 h CS-MA hydrogel samples. (B) Comparison of injection force profiles of hydrogels without DNR and loaded with DNR.

Table 23: Summary of maximum injection force and average injection force during testing for DNR loaded 10% CS-MA Hydrogels with 4 h methacrylation time.

CS-MA Trial	Maximum Injection Force (N)	Average Injection Force (N)
10%	41.58	37.74
10% CS-MA w/ DNR	77.56	65.89

5.4.2 DMMB Assay

A DMMB assay was completed on 20 µL and 50 µL 4 h CS-MA hydrogels, at CS-MA concentrations of 10% and 20%. Both volumes of hydrogels were compared using the same standard curve to determine the CS concentration, which was collected in triplicates, as shown in Figure 25. The absorbance readings were averaged, and each average was subtracted by 0.2159, the absorbance of the known 0 µg/mL, to account for the background absorbance reading due to the DMMB dye with PBS. These absorbances are displayed in Table 24. The calculated absorbances and known concentrations were then used to create a standard curve, as shown in Figure 26. The data point for 500 µg/mL was deemed an outlier due to its location past the CS saturation point. A linear line of best fit was created, in which the y-intercept was forced to 0, resulting in an R^2 value of 0.994. The equation yielded from this curve was rearranged to equate for concentration when absorbance was input, as shown in Equation 3, and that final equation was used when making estimations for CS leached from the CS-MA hydrogels.

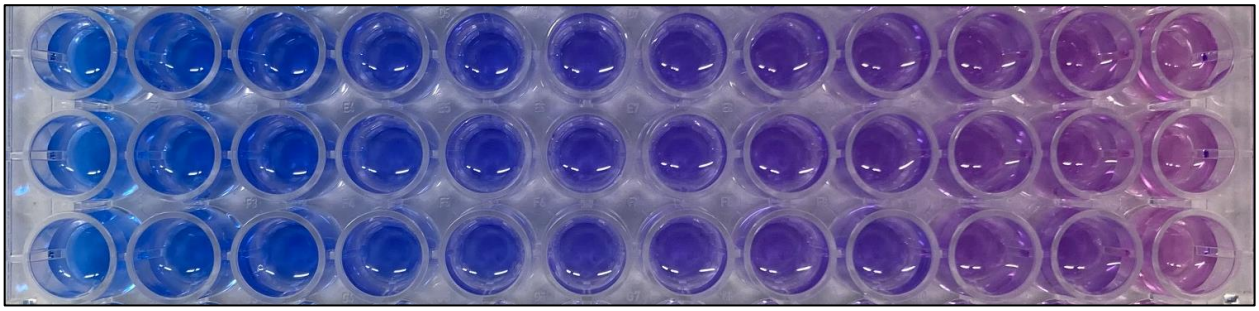

Figure 25: DMMB assay plate of standard curve using known CS solution from 0 µg/mL (leftmost) to 500 µg/mL (rightmost), completed in triplicate.

Table 24: CS standard curve data using PBS.

Conc (µg/mL)	0	25	50	75	100	125	150	175	200	225	250	500
SC 1	0.2208	0.2636	0.2961	0.3232	0.3709	0.4122	0.4335	0.4657	0.4739	0.4976	0.5079	0.5489
SC 2	0.2120	0.2453	0.2931	0.3255	0.3737	0.4033	0.4428	0.4816	0.4930	0.5030	0.5379	0.5502
SC 3	0.2149	0.2451	0.3003	0.3289	0.3696	0.4026	0.4395	0.4499	0.4512	0.5088	0.5478	0.5535
Ave	**0.2159**	**0.2513**	**0.2965**	**0.3259**	**0.3714**	**0.4060**	**0.4386**	**0.4657**	**0.4727**	**0.5031**	**0.5312**	**0.5509**
Final	**0.0000**	**0.0354**	**0.0806**	**0.1100**	**0.1555**	**0.1901**	**0.2227**	**0.2498**	**0.2568**	**0.2872**	**0.3153**	**0.3350**

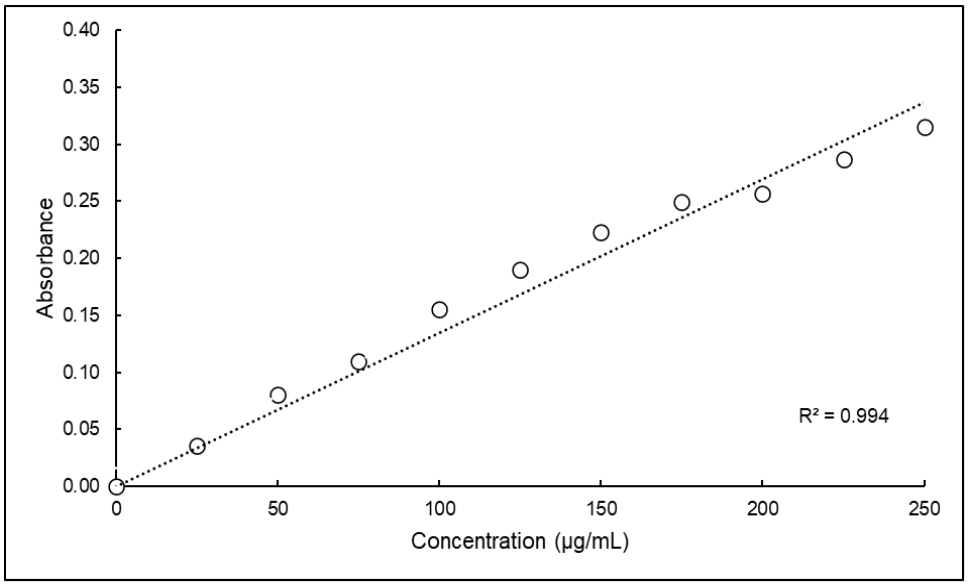

Figure 26: CS standard curve using PBS.

$y = 0.0013x \rightarrow \mathbf{x = \frac{y}{0.0013}}$; where: y = absorbance, x = concentration **(Equation 3)**

A DMMB assay was completed using 20 µL 4 h CS-MA hydrogels at concentrations of 10% and 20%. The 10% CS-MA formulation was run in triplicate, while the 20% CS-MA formulation only had two samples due to excessive hydrogel breakage. Readings were background subtracted and then averaged to give a single absorbance reading for each formulation over the 7-day study. The absorbance readings for 20 µL formulations, with the average and standard deviation of each, are shown in Table 25.

Table 25: 20 µL CS-MA hydrogels absorbance readings.

All values were background subtracted 0.2159, the absorbance of the known 0 µg/mL									
Time (Days)	**10% 1 Abs**	**10% 2 Abs**	**10% 3 Abs**	**10% AVG**	**10% STD**	**20% 1 Abs**	**20% 2 Abs**	**20% AVG**	**20% STD**
1	0.0236	0.0195	0.0226	**0.0219**	**0.0021**	0.0295	0.0203	**0.0249**	**0.0065**
2	0.0097	0.0176	0.0128	**0.0134**	**0.0040**	0.0259	0.0177	**0.0218**	**0.0058**
3	0.0131	0.0145	0.0109	**0.0128**	**0.0018**	0.0220	0.0135	**0.0178**	**0.0060**
4	0.0113	0.0108	0.0160	**0.0127**	**0.0029**	0.0205	0.0206	**0.0206**	**0.0001**
5	0.0217	0.0189	0.0125	**0.0177**	**0.0047**	0.0199	0.0267	**0.0233**	**0.0048**
6	0.0175	0.0200	0.0109	**0.0161**	**0.0047**	0.0209	0.0093	**0.0151**	**0.0082**
7	0.0365	0.0302	0.0446	**0.0371**	**0.0072**	0.0374	0.0167	**0.0271**	**0.0146**

From the absorbance readings, estimated concentrations were interpolated using Equation 3. These estimated concentrations are displayed in Table 26, with the average and standard deviation of each, and represent the amount of CS that was leached in that day's sample.

Table 26: 20 µL CS-MA hydrogels estimated CS concentration.

Time (Days)	10% 1 Conc (µg/mL)	10% 2 Conc (µg/mL)	10% 3 Conc (µg/mL)	10% AVG (µg/mL)	10% STD (µg/mL)	20% 1 Conc (µg/mL)	20% 2 Conc (µg/mL)	20% AVG (µg/mL)	20% STD (µg/mL)
1	17.50	14.46	16.76	**16.24**	**1.59**	21.88	15.06	**18.47**	**4.83**
2	7.19	13.05	9.49	**9.91**	**2.95**	19.21	13.13	**16.17**	**4.30**
3	9.72	10.75	8.08	**9.52**	**1.35**	16.32	10.01	**13.17**	**4.46**
4	8.38	8.01	11.87	**9.42**	**2.13**	15.21	15.28	**15.24**	**0.05**
5	16.10	14.02	9.27	**13.13**	**3.50**	14.76	19.80	**17.28**	**3.57**
6	12.98	14.83	8.08	**11.97**	**3.49**	15.50	6.90	**11.20**	**6.08**
7	27.07	22.40	33.08	**27.52**	**5.35**	27.74	12.39	**20.06**	**10.86**

A DMMB assay was completed with 50 µL 4 h CS-MA hydrogels at concentrations of 10% and 20%, where each concentration was run in triplicate, and readings were completed by diluting each day's sample by 50% with PBS. This was done to prevent the oversaturation such that accurate readings may be gathered using a spectrophotometer. Readings were background subtracted and then averaged to give a single absorbance reading for each formulation over the 7-day study. The absorbance readings for 50 µL formulations, with the average and standard deviation of each, are shown in Table 27.

Table 27: 50 µL CS-MA hydrogels absorbance readings.

All values were background subtracted 0.2159, the absorbance of the known 0 µg/mL										
Time (Days)	**10% 1 Abs**	**10% 2 Abs**	**10% 3 Abs**	**10% AVG**	**10% STD**	**20% 1 Abs**	**20% 2 Abs**	**20% 3 Abs**	**20% AVG**	**20% STD**
1	0.0500	0.0407	0.0491	**0.0466**	**0.0051**	0.0417	0.0506	0.0498	**0.0474**	**0.0049**
2	0.1635	0.1516	0.1004	**0.1385**	**0.0335**	0.1118	0.1142	0.1090	**0.1117**	**0.0026**
3	0.0645	0.0605	0.0525	**0.0592**	**0.0061**	0.0665	0.0668	0.0618	**0.0650**	**0.0028**
4	0.0597	0.0786	0.0411	**0.0598**	**0.0188**	0.0494	0.0524	0.0472	**0.0497**	**0.0026**
5	0.0451	0.0416	0.0520	**0.0462**	**0.0053**	0.0342	0.0438	0.0458	**0.0413**	**0.0062**
6	0.0602	0.0464	0.0496	**0.0521**	**0.0072**	0.0414	0.0459	0.0569	**0.0481**	**0.0080**
7	0.0441	0.0496	0.0316	**0.0418**	**0.0092**	0.0369	0.0383	0.0655	**0.0469**	**0.0161**

From the absorbance readings, estimated concentrations were interpolated using Equation 3, and doubled to account for PBS dilution. These estimated concentrations are displayed in Table 28, with the average and standard deviation of each, and represent the amount of CS that was leached in that day's sample.

Table 28: 50 µL CS-MA hydrogels estimated CS concentration.

Time (Days)	10% 1 Conc (µg/mL)	10% 2 Conc (µg/mL)	10% 3 Conc (µg/mL)	10% AVG (µg/mL)	10% STD (µg/mL)	20% 1 Conc (µg/mL)	20% 2 Conc (µg/mL)	20% 3 Conc (µg/mL)	20% AVG (µg/mL)	20% STD (µg/mL)
1	74.17	60.38	72.84	**69.13**	**7.61**	61.86	75.06	73.87	**70.26**	**7.30**
2	242.54	224.89	148.94	**205.45**	**49.74**	165.85	169.41	161.69	**165.65**	**3.86**
3	95.68	89.75	77.88	**87.77**	**9.06**	98.65	99.09	91.68	**96.47**	**4.16**
4	88.56	116.60	60.97	**88.71**	**27.81**	73.28	77.73	70.02	**73.68**	**3.87**
5	66.90	61.71	77.14	**68.58**	**7.85**	50.73	64.97	67.94	**61.22**	**9.20**
6	89.30	68.83	73.58	**77.24**	**10.71**	61.41	68.09	84.41	**71.30**	**11.83**
7	65.42	73.58	46.88	**61.96**	**13.68**	54.74	56.82	97.16	**69.57**	**23.92**

The estimated CS concentrations for each 20 µL and 50 µL 4 h CS-MA hydrogel formulation is visualized in Figure 27. The 50 µL CS-MA hydrogels exhibited higher CS concentrations than the 20 µL CS-MA hydrogels for each day. Additionally, both 50 µL CS-MA hydrogel formulations experienced an unexpected burst of CS leaching on Day 2 due to an inability for hydrogel samples to fully swell in the cutoff syringe setup.

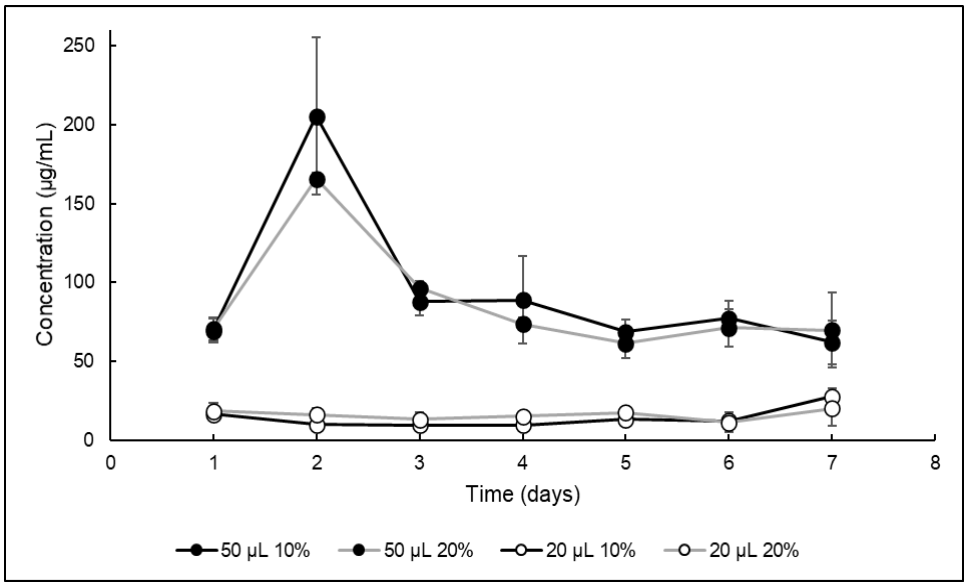

Figure 27: CS concentrations of 20 µL and 50 µL CS-MA hydrogels.

The estimated concentrations for each 20 µL and 50 µL 4 h CS-MA hydrogel formulation was utilized to calculate the percentage of the CS content that was leached over the 7-day study. These calculations were completed based on the 1 mL PBS samples collected each day of the

study, which allowed for CS concentrations to be multiplied by 1 to get the amount of CS leached in each sample, in µg. The known quantity of CS in each hydrogel formulation: 2000 µg (20 µL 10% CS-MA), 4000 µg (20 µL 20% CS-MA), 5000 µg (50 µL 10% CS-MA), and 10000 µg (50 µL 20% CS-MA), were then compared to produce a percentage of the total CS leached each day. These percentages were summed, and Figure 28 visualizes the cumulative percent of CS leached over time for each hydrogel formulation.

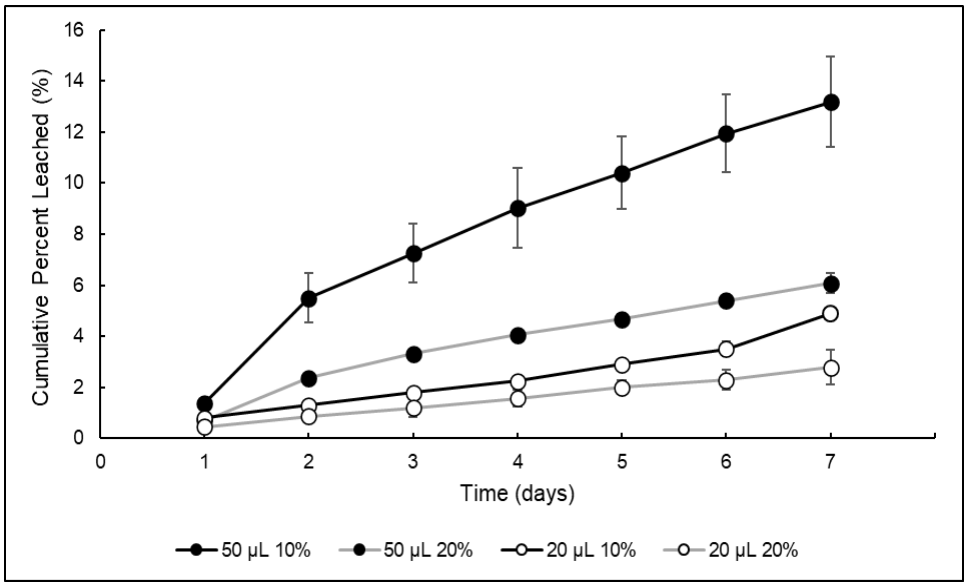

Figure 28: CS leached from CS-MA hydrogels over time.

Over the 7-day study, the cumulative percentage of CS leached varied slightly for each hydrogel formulation: 4.89% (20 µL 10% CS-MA), 2.79% (20 µL 20% CS-MA), 13.18% (50 µL 10% CS-MA), and 6.08% (50 µL 20% CS-MA). A linear line of best fit was placed for each formulation and the equations were utilized to estimate how long it would take each formulation to reach 100% CS leached, as shown in Figure 29. Day 1 was excluded when creating these lines to account for bursting behaviors previously noted in the 50 µL CS-MA hydrogel formulations. Based on the line of best fit equations, the length of time, to the nearest day, that it would take for 100% CS leached for each formulation is: 148 days (20 µL 10% CS-MA), 262 days (20 µL 20% CS-MA), 63 days (50 µL 10% CS-MA), and 136 days (50 µL 20% CS-MA), concluding that all evaluated hydrogel formulations would maintain insolubility for at least 30 days.

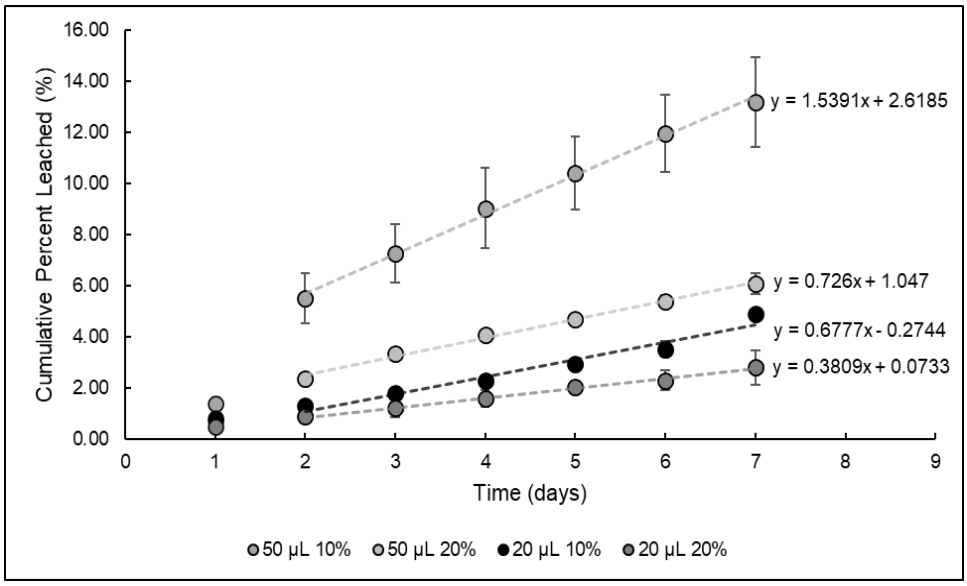

Figure 29: Line of best fit of each CS-MA hydrogel formulation for CS leached over time.

5.4.3 Drug Loading and Release Studies

The team completed drug loading and release studies on 4 h CS-MA hydrogels. The DNR loaded into each hydrogel was determined by light absorbance values of the post-loading supernatant on the spectrophotometer and then converted to concentration using a standard curve, which was created to quantitively associate the absorbance readings to DNR concentration (1.56-200 µg/mL). By conducting a serial dilution of the DNR loading solution (500 µg/mL), the standard curve created can be seen in Figure 30. Then, the concentration of DNR (µg/mL) in the samples was quantified using Equation 4.

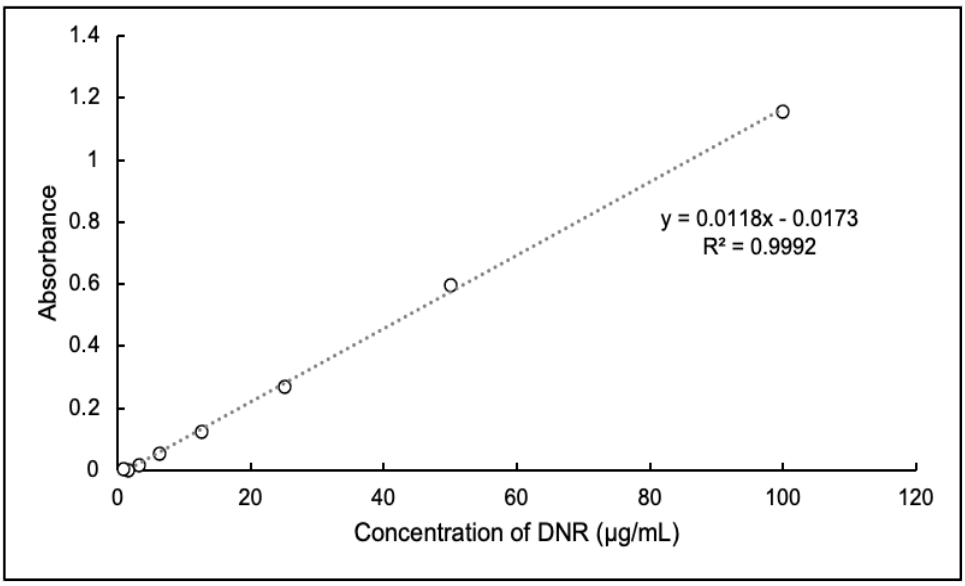

Figure 30: Standard curve of the light absorbance per DNR concentration.

$$\text{Concentration of DNR } \left(\frac{\mu g}{mL}\right) = \frac{\text{Light absorbance value}}{\frac{\text{Absorbance}}{\mu g/mL}\ (\text{slope of standard curve})} \quad \textbf{(Equation 4)}$$

To understand if hydrogel size would affect drug loading, the amount of drug-loaded in 20 µL and 50 µL hydrogels (N = 3; n = 3,6) can be seen in Figure 32. This was visually confirmed due to the color change from the loading solution from bright orange to a nearly colorless solution after 3 days of loading, shown in Figure 31. In addition to the plot, t-tests were performed to determine if changing CS-MA concentration and hydrogel size would significantly affect the loading of DNR. In both cases, the *p* was calculated to be lower than 0.05 (0.0018 and 0.0030, respectively), meaning that there was a statistical difference in the loading of hydrogels when changing size and concentration of CS-MA. This means that these changes directly impact DNR loading, which is directly related to the higher the concentration of CS-MA and surface area in the hydrogels, as more carboxyl groups are available for the drug to bind to. In other words, hydrogels with higher concentration of CS-MA and bigger size loaded more DNR, as expected. However, since nearly all the drug was loaded into the hydrogels, we cannot make conclusions regarding the maximum drug loading capacity in both 20 µL or 50 µL hydrogels.

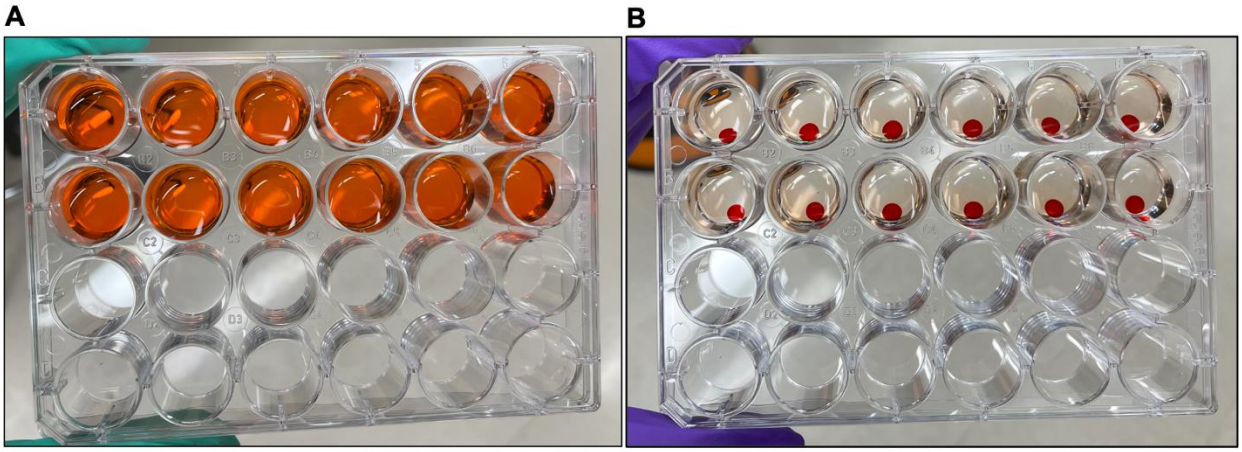

Figure 31: Drug loading study conducted with CS-MA hydrogels, with (A) representing day 0 and (B) representing day 3.

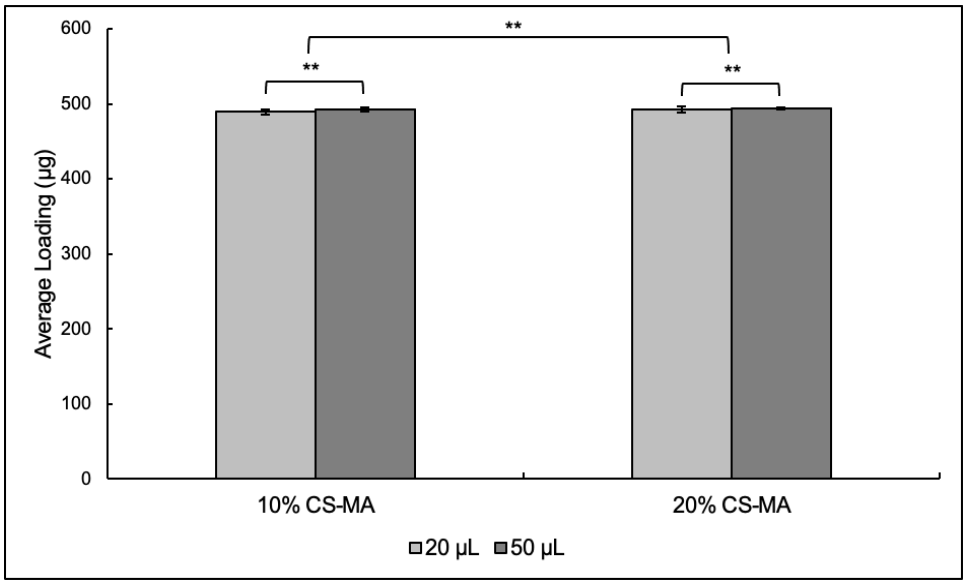

Figure 32: Daunorubicin loading of 20 µL and 50 µL hydrogels at 10% and 20% CS-MA concentration. Data are presented as mean ± standard deviation of three independent experiments. Asterisks indicate statistical differences between the indicated (**$p < 0.05$).

Moreover, the amount of drug loaded for across three trials of 20 µL 10% 4 h CS-MA hydrogels (N = 3; n = 3,6) can be seen in Figure 33. From 1 mL of the 500 µg/mL loading solution, in which each hydrogel was submerged for 3 days, the average amount of drug-loaded between all 3 trials was 486.7 ± 2.60 µg. To confirm reproducibility of loading between the different trials, an ANOVA test was conducted. The *p* was calculated to be 0.22, which is higher

than 0.05, meaning that there's no significant difference in the loading of hydrogels in different trials.

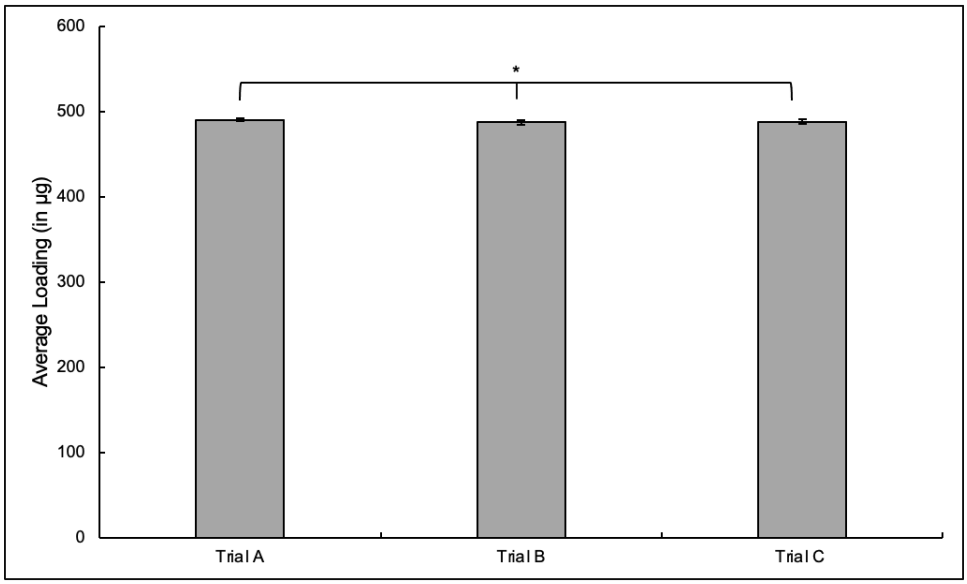

Figure 33: Daunorubicin loading of 20 µL 10% CS-MA hydrogels. Data are presented as mean ± standard deviation of three independent experiments. Asterisks indicate statistical differences between the indicated (*$p > 0.05$).

The release profile of the different formulations of hydrogels studied can be seen in Figure 34. 50 µL 10% 4 h CS-MA hydrogels were not able to withstand, without dissolving, the release study for 30 days, as intended. The fabrication process of the 50 µL hydrogels is hypothesized to be the reason for this, as they were made in syringe posts instead of the parafilm, leading to them being easily broken down when transferred to the well-plate. In reference to the other formulations, significant conclusions were drawn. Firstly, 20 µL 10% 4 h CS-MA hydrogels released an average of 68.4% of the drug loaded, while 20 µL 20% CS-MA hydrogels released 64.1%, over 30 days. On the other hand, 50 µL 20% CS-MA hydrogels released an average of 66.7% over the course of 30 days. Finally, for these 4 hydrogel formulations, almost 40% of the drug was released in the first 10 days of the study, with the remaining drug being released in a sustained manner until the termination of the study.

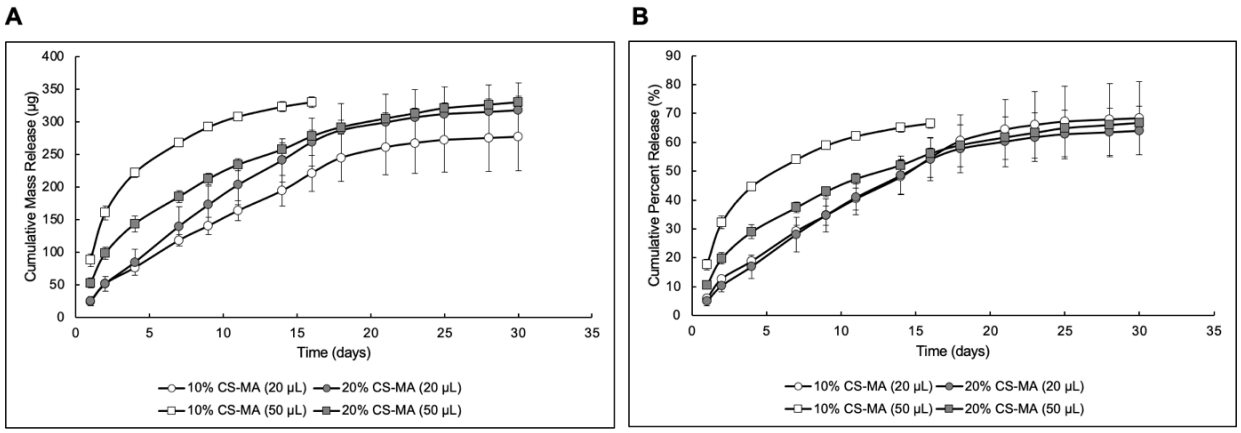

Figure 34: DNR release profile for 20 µL and 50 µL hydrogels formulated at two different concentrations (10% and 20%). Data are presented as mean ± standard deviation of three independent experiments. (A) Cumulative mass released in µg from hydrogels over a period of 30 days, or until hydrogel dissolved in PBS solution. (B) Cumulative percent (%) release of DNR from hydrogels taking into consideration amount of drug loaded.

VI. Final Design and Validation

The project has developed and executed various experiments and tests on the three design approaches to achieve a successful final design. However, to complete the design it must first be validated. This section will offer a detailed overview of how the initial goals were met by the final design and will also briefly cover what role industry standards play in the design process for the current phase of the final design.

6.1 Final Design Overview

The final design for a water-insoluble, injectable CS-based hydrogel DDS is a 20 µL 10% 4 h CS-MA hydrogel. To create this DDS, CS-MA was first fabricated using the established protocol, outlined in Appendix E. The product of this process was utilized to fabricate CS-MA hydrogels, using an adapted version of the protocol used in Professor Coburn's lab, found in Appendix F. This fabrication process required the use of CS-MA, ultrapure water, and a 10% Irgacure® 2959 stock at a ratio of 1:100. Gelation of the hydrogels took place under UV light, in the form of droplets, and took approximately 15 minutes to gel completely. The hydrogels were then swelled for at least 3 days, before further experimentation took place.

The first experiment run on this hydrogel formulation was injection force testing according to the protocol in Appendix G, though for this test 50 µL hydrogels were utilized to ensure an adequate quantity of hydrogel in the syringe. This experiment was completed using an Instron E1000 with a 2 kN load cell (Catalog # 2527-129) with a custom-made compression fixture to hold 0.5 mL syringe with a needle length of 0.5 in and needle size of 28 G, as shown in Figure 17. Furthermore, it was run using a compression based Bluehill script, at a rate of 4 mm/min and measurements of extension and load taken every 250 ms. The experimentation on this hydrogel formulation resulted in an average unloaded injection force of 38.75 N, between three trials, and an average loaded injection force of 65.89 N, in one trial.

The second experiment completed was a DMMB assay, using the protocol outlined in Appendix I. This required daily PBS supernatant samples over 7 days, and the DMMB assay was run using a Molecular Devices SpectraMax M2 Multilabel Microplate Reader with a 5 second pre-shake, at a visible light absorbance of 525. Using average absorbance readings of 3 samples, on a known standard curve, average concentrations were calculated for each day, and these concentrations were utilized to calculate the percentage of the CS content released over the 7-day

study, based on a known CS quantity of 2000 ug in each hydrogel. The cumulative percentage of the CS released over the course of the study was 4.89%, equating to a 100% CS release timeline of approximately 148 days.

The third and final experiment completed on the 20 μL 10% 4 h CS-MA hydrogels was a drug loading and release study, using the protocol found in Appendix J. This required 3 days of drug loading using 1 mL of 500 μg/mL DNR in water, and release took place at 37°C over 30 days and evaluation utilized UV/vis spectrophotometry. Additionally, a standard curve was created using a Molecular Devices SpectraMax M2 Multilabel Microplate Reader spectrophotometer to determine the concentration of a sample solution of unknown concentration. For drug loading, the average amount of drug that loaded within across three trials was 486.7 μg, with a statistical *p* value of 0.22, thus meaning no statistically difference between loading of hydrogels in different trials. For this same formulation, the release profile over 30 days was 68.4% of the drug that was loaded, with approximately 40% releases in the first 10 days and the remaining drug being released in a sustained manner over time.

6.2 Impact of Final Design

6.2.1 Economics

This work is aimed at improving the current DDS for delivery of chemotherapeutic agents. The current gold standard treatment includes intravenous delivery of the agent that systemically enters the blood stream and require numerous treatment rounds.

It is difficult at this time to estimate a final cost of this system; however, it is likely that there will be increased costs due to the need to manufacture the product, perform clinical trials, and the addition of new materials. However, although there is no way of knowing the final cost of this intratumorally delivered DDS, the new drug delivery system would hopefully reduce expenses for patients. The sustained delivery of the hydrogel DDS would reduce the amount of necessary in-person treatments and the localized approach would limit systemic side effects. This reduced visitation would be beneficial for patients in terms of the cost of transportation to and from appointments as well as the hotel stays, and appointment fees and the reduced systemic side effects would reduce costs associated with treatment of off-target complications.

6.2.2 Environmental Impact

While in the R&D phase, the large-scale environmental impacts are not yet of concern. However, it is important to recognize these concerns to ensure that this treatment method is not having adverse effects on the environment. Environmental impacts can be discussed by breaking down components of this device. Key components include CS-MA, DNR, insulin syringe, PBS, Ethanol, glycidyl methacrylate, acetone, and disposable labware. These components are used in small quantities and disposed of according to lab standards so there is no environmental concern. Another environmental concern with the fabrication process is lyophilization to make CS-MA, as this is an energy heavy process which has negative environmental impacts.

6.2.3 Societal Influence

As of today, the societal influence of this project's work is negligible. The goal of the project was to create an injectable hydrogel DDS and test the finished result. Because the team did not conduct any of the experiments on humans, and the system did not go through clinical trials, there is very little effect on this front. However, if the proposed work is further enhanced and built to better assist present neuroblastoma treatment options, the social impact will be significant. To begin with, the impact will be significant due to the extensive testing required to bring the product to the patient's bedside. The societal impact will be substantial if the technology is proven to be successful and superior to present treatment options for neuroblastoma. Therefore, the effectiveness of this project's work, as well as who and what it influences, will ultimately determine its societal impact.

6.2.4 Political Ramifications

Because of the basis of this project's work, it has no political implications in the project's current phase or substantial possible effect in the future. The project's ultimate goals can only potentially improve existing treatments. The only political repercussion of this initiative to consider is that a better alternative to neuroblastoma treatment originates in the United States and is utilized in other countries. This factor, however, is only relevant once the product has progressed from the experimental stage to a more developed product that is closer to the market.

6.2.5 Ethical Concern

Drug delivery is an emerging field in biomedical engineering, with many laboratories and institutions focusing on developing new advancements. With the growth of this field comes additional concerns, like ethical considerations, which can be overlooked. During the process of research and development, ethics may be considered during clinical testing to validate the product safely and effectively. For this project, studies were completed *in vitro* to design and characterize a DDS. None of the tests completed require human or animal subjects. This project was to develop and design a new type of polymeric drug carrier for further research. Additionally, as researchers, data and tests should be completed with care to ensure that the results are not intentionally falsified, and to appropriately show efficacy of the drug carries. There is no conflict of interest to be reported regarding this project. The research team is one entity, with no connections to third parties that have financial stakes on the results.

6.2.6 Health and Safety Issue

For the scope of this project, the health and safety concerns are applicable to individuals who come into contact with the DDS: fabricators, administers, and patients. The fabrication processes used to develop the DDS does not pose any danger to the operators, however standard lab practice and caution should be used when synthesizing CS-MA. Although, upon the addition of DNR or other chemotherapeutic agents into the system, there is a posed risk. DNR is a commonly administer chemotherapeutic that is handled in clinical settings for the administration to cancer patients. With this being said, the use and exposure to the loaded DDS would require necessary safety precautions and protocols be followed, similar to the safety protocols taken by administrators when delivery chemotherapeutic agents. Additionally, through continued research and preclinical testing the validation of this product would be thoroughly verified before patient administration. This produce is still in development and far from clinical translation testing, it is still important to note that the health and safety issues would be inspected to ensure they are at a minimum due to strict government regulations.

6.2.7 Manufacturability

The project does have some manufacturability concerns. In general, the manufacturing world favors automation, and at current, creating this hydrogel requires intensive time and management. Since the project is still in an exploratory phase, this is not a high priority item, but

in the future scale-up of the DDS fabrication should be considered. Additionally, while the DDS requires limited materials for fabrication, some materials are costly and may not be favorable for manufacturing scale-up.

6.2.8 Sustainability

The project has a low sustainability impact, as little to no materials are in the hydrogel DDS fabrication process. What little is lost, is insignificant and of no substance. Additionally, the main material used that may impact the biological world is CS, in the form of CS-MA. CS is usually naturally derived from animals such as sharks and cows, as it is abundant in the ECM. While this does present some sustainability concerns, the benefits of using CS for this DDS outweigh the disadvantages. Also, while it is usually naturally sourced, CS has the capacity to be fabricated synthetically in a lab, so this is also a future option to further increase the sustainability of the DDS.

VII. Discussion

7.1 Pluronic F127

From the injection force testing performed, the team was able to conclude that by adjusting F127 concentration the mechanical properties of the hydrogel were not significantly altered. As shown in Figure 18, increasing the F127 concentration shows some difference between the injection forces required, but upon running an ANOVA test the team concluded that there was no significant change in the required injection force needed for extrusion. From this conclusion, varying the concentration of F127 within the hydrogels did not become a limiting factor for the team. Additionally, by adding CS to the F127 hydrogel formulation there was no significant change observed in required injection force. As seen in Figure 19, the injection force for 16%/2% and 16%/3% F127/CS were similar in range to the 16% F127 with no CS. This was further quantified by completing an ANOVA test to compare the average injection force required to extrude 16%, 16%/2%, and 16%/3%. From this statistical analysis it was found that by increasing the concentration of CS in a 16% F127 hydrogel that there was a statistically significant difference between the samples in comparison to the 16% F127 hydrogels. This helped the team determine that CS can affect the hydrogels material properties when it is added into F127 hydrogels.

Regarding the dissolution and gelation studies of F17, significant conclusions were drawn. Based on literature, F127 concentration was varied between 15-20% and CS content was varied between 0.5-3%. As a result, there are two primary takeaways. Firstly, increasing F127 concentration increased solution viscosity and lowered LCST, resulting in concentrations of over 17% F127 gelling at room temperature and becoming unusable. Increasing F127 concentration also increased dissolution rate of the gelled solution in PBS. Moreover, the presence of CS influenced thermal gelation and dissolution rate. Increasing the CS concentration while keeping the F127 concentration constant increased the viscosity of the solution state and faster dissolution rate in PBS. It was determined that none of the formulations evaluated remained insoluble for the duration of a 7-day DMMB assay or a 30-day drug load/release trial, which are specifications determined in Functions 3 and 4, respectively.

7.2 PNIPAM

Limited PNIPAM was able to be purchased and very few experiments were able to be performed due to project budget and time constraints. One formulation of PNIPAM-CS at a 1:1 ratio was tested at three different concentrations (10%, 20% and 33%). All three formulations were a viscous liquid at room temperature and became less viscous when raised to 37°C. In addition to the change in viscosity, a reversible color change from clear/cloudy to white was observed when each of the concentrations were raised to body temperature. Due to a lack of time and resources to perform additional testing, PNIPAM was ruled out as an option for this MQP.

7.3 CS-MA Hydrogels

7.3.1 Injection Force Testing

As the team began the CS-MA hydrogel approach, many formulations were tested in an attempt to obtain a hydrogel that has an injection force ≤ 38 N, fitting Function 1 as discussed in Section 3.3.1. All injection force data was collected using 50 µL hydrogels, to ensure an adequate quantity of hydrogel in the syringe. Upon testing, the team evaluated the effects of methacrylation time on injection force but completed injection force testing on 20% 4 h, 8 h, and 24 h CS-MA. From this testing, it was concluded that 8 h and 24 h CS-MA had a high injection force, not fitting in the 38 N parameters, as both formulations resulted in an injection force over 100 N. The team found that the hydrogel formulation of 20% 4 h CS-MA resulted in an injection force of 27.17 N, fitting Function 1, so only 4 h CS-MA formulations were considered further. When running this experiment, the team used a batch of 4h CS-MA that was synthesized in 2019 (Batch no. 009), which resulted in significantly lower injection forces in comparison to our later tests, in which the team used Batch no. 031 synthesized in 2022.

From this conclusion, the team investigated the effects of weight percent on the force required for extrusion by testing 5%, 10%, and 20% 4 h CS-MA hydrogels. From this testing the team concluded that 20% 4 h CS-MA hydrogels result in a high injection force greater than 100 N, thus not fitting Function 1. Additionally, the team found that 5% and 10% resulted in an average injection force of 38.52 N and 37.74 N respectively, resulting in very similar injection force profiles.

For the final studies, the team evaluated 10% 4 h CS-MA hydrogels in three sets (N=6, n=3) to understand the behaviors of these hydrogels further. Through these studies it was

discovered that many of the injection force profiles varied from one another, including those within the same set, which is further expanded on later. With this variation, there were some hydrogels with an average of 30 N and others with an average of 40 N, thus not only showing a lack of reproducibility, but also showing that some hydrogels do not result in an injection force that fits Function 1. The reported averages of the three sets are: 30.23 N, 41.76 N, and 44.27 N, respectively. This reflects that two of the three sets ultimately resulted in injection forces above 38 N, thus not fitting Function 1.

Upon running three set of six 10% 4 h CS-MA hydrogels, 18 total, it was found that many of the samples showed significant variance in average force required for extrusion. When running the three sets of hydrogels, each set average was calculated, and the sample averages were tested to determine if they were within 5% variability, as shown in Section 5.4.1. During these tests it was found that less than or equal to, two of the hydrogels fit within 5% of the average for each individual set. Furthermore, the average for all eighteen samples were calculated to later test if all the samples fit within 5% of the cumulative average. The average of these samples was 38.75N to extrude the hydrogels, and upon running the test to determine variance only four of the eighteen fit within the criteria. This showed that only 22% of the hydrogels fit within that defined 5% range. According to Function 2, defined in Section 3.3.2, the hydrogels must have a reproducible injection force across sets, specifically within a 5% range. From the conclusions made during injection force testing, the current 10% 4 h CS-MA design showcase significant variance of forces required for extrusion, thus not completing Function 2.

Following these tests, the team also investigated the effects of loading DNR into the hydrogels before extrusion, on the hydrogel's injection force profile. From this test it was found that the average injection force of loaded hydrogels to be 65.89 N. The loading of the hydrogels resulted in an increase in injection force needed, approximately two times the injection force required for unloaded 10% 4 h CS-MA hydrogels. The loaded hydrogels resulted in an injection force higher than 38 N, thus not fitting Function 1.

7.3.2 DMMB Assay

Due to conclusions made through injection force testing, only 4 h CS-MA formulations were utilized when running DMMB assays, at hydrogel sizes of 20 µL and 50 µL, and CS-MA concentrations of both 10% and 20%. In general, it was found that 50 µL CS-MA hydrogels exhibited higher CS concentrations and greater cumulative percentages of CS leached over time.

The team linked this result to two potential reasons. First, there was increase in surface area of the larger hydrogels, especially because the 50 µL hydrogels faced extensive breakage when moved from the cutoff syringe set-up to the 24-well plate; each sample was broken into 3 or more fragments. In comparison, the 20 µL hydrogels were at most 2 fragments. This increase in surface area likely contributed to an increase in CS leached. Second, as previously noted, the 50 µL CS-MA hydrogels experienced a burst of CS leached on Day 2. While the definite reason for this is unknown, it is hypothesized that the 50 µL CS-MA hydrogels were not completely swelled by Day 0 of the DMMB assay due to lack of space for water in the cutoff syringes. This led to the hydrogels taking in water at the start of the study and bursting on Day 2, which would skew the results of the 50 µL hydrogel CS leaching data. For this reason, 20 µL 4 h CS-MA hydrogels were favored when further analyzing the DMMB assay.

For the 20 µL samples, the difference in CS leached from the 10% and 20% 4 h CS-MA hydrogels was minimal. The cumulative percentage of CS leached over the 7-day study was 4.89% for the 10% samples, and 2.79% for the 20%. This equates to a 100% CS leach time of approximately 148 days for 10% samples, and 262 days for 20% samples. This estimate is a "worst case scenario," in which the leaching profile does not plateau, but it can provide an idea of when all CS would leach, and theoretically when the hydrogel would dissolve if left as the only limiting factor. Based on this analysis, both 20 µL 4 h CS-MA hydrogel formulations would maintain insolubility for at least 30 days, thus meeting Function 3, as discussed in Section 3.3.3. Though the 20% 4 h CS-MA hydrogels samples had a slightly better CS leaching rate, it is inconsequential when noting how little CS the 10% 4 h CS-MA hydrogels samples also leached, so either formulation is recommended based on the DMMB assay.

7.3.3 Drug Loading and Release

The average amount of DNR loaded per mg of 10% 4 h CS-MA hydrogels was 486.7 µg. With this information, the variability of the amount of drug loaded in the hydrogels was calculated. The standard deviation represents 0.53% of the average drug loaded between all trials, confirming a less than 5% variability. The loading was reproducible, with no significant difference between the quantity of DNR being absorbed into the hydrogels during the incubation duration. Overall, these findings meet the requirements for drug loading detailed in Function 5.

Regarding the release of 10% 4 h CS-MA hydrogels, significant conclusions were drawn. On day 1, there was a burst release of 23.6 µg of DNR, which accounts for approximately 6% of

the total drug loaded into the hydrogel. The release profile for the hydrogels became linear around day 9, with a release rate of approximately 13.2 μg/day. Moreover, the release profile of 4 h 10% CS-MA hydrogels is comparable to prevalent literature, as 40.4% of the drug loaded was released in the first 10 days of the study followed by a sustained release of DNR. This hydrogel behavior is comparable to previous literature showing *in vitro* drug release profiles that were effective *in vivo* by slowing tumor growth (Chiu et al., 2014). Ideally, these hydrogels are designed to release approximately 250 μg (half of the drug loaded in this study) at first to trigger a fast tumor response, followed by a sustained release to aid with the slowing of tumor regrowth. Therefore, these findings confirm that the hydrogels can deliver a chemotherapeutic drug at a sustained rate overtime, which is determined in Function 4.

VIII. Conclusions and Recommendations

8.1 Thermosensitive CS Hydrogels

F127 and PNIPAM were explored as potential co-polymers for the formulation of thermosensitive hydrogels doped with CS. As verified by the injection force testing on F127, this decreased viscosity at room temperature allowed for ideal injection forces less than 12 N. However, a dissolution study with F127 in PBS showed that none of the hydrogel formulations would be able to remain insoluble for the entirety of a 7-day DMMB assay or a 30-day drug load/release study. This study also concluded that increased CS resulted in an increased dissolution rate whereas increased F127 resulted in a decreased dissolution rate. Because of this finding of dissolution in PBS, F127 was deemed a poor solution and the team would not recommend future exploration of F127 for the scope of this project.

PNIPAM was also explored as a potential co-polymer due to its prevalence in related literature with other polysaccharides; however, due to budget and time constraints very few experiments were able to be run. The protocol adapted from literature called for a 1:1 molar ratio of polysaccharide to PNIPAM resulting in nearly equal weight percent between PNIPAM and CS. This formulation resulted in a solution that became less viscous and underwent a color change when raised to 37°C. Previous studies with F127 showed that increased CS resulted in instability with gelation so as a next step the team would recommend a fabrication method with less CS. Additionally, when raised from room temperature to 37°C the solution underwent a color change from clear and cloudy to white, indicating some form of a phase change. As a next step the team would recommend experimentation to determine the properties of this solution and determine whether a precipitant or particulate suspension was formed that may be capable of the desired drug carrier properties.

8.2 10% 4 h CS-MA Hydrogels

A 10% 4 h CS-MA hydrogel that met three of the five outlined functions was successfully fabricated. This hydrogel proved to maintain insolubility in PBS, allow for sustained drug release, and allow for reproducible drug loading. Additionally, the formulation proved to be capable of an injection force within acceptable range; however, this injection force was not reproducible between batches. To further this research the team has made three primary

recommendations for future work: injection forces on loaded material, pre-extrusion of material, and cytotoxicity studies.

To gain more representative data on the material that would be extruded, the team recommends that injection forces be run on hydrogels loaded with the chemotherapeutic in addition to the injection forces on unloaded material. Preliminary testing showed that this made a significant impact on the injection force profile (Figure 24B). In the future we would recommend targeting a loaded hydrogel injection force less than 38 N and ideally less than 12 N.

To further decrease this injection force and improve reproducibility the team recommends pre-extrusion of the hydrogel through a needle. Preliminary testing was performed by extruding the gel through a 28 G 0.5 in 0.5 mL syringe into a collection plate and then loading an identical syringe with the pre-extruded material. This experimentation was performed with the loaded hydrogel referenced in Figure 24 and proved to have a more stable injection force profile within the acceptable range as seen in Figure 35. To do this, the team has designed a CAD model that would be used with the current injection fixture as the fixture is not tall enough to directly extrude into a new syringe (Figure 36). This design would allow for the design to be placed under the current fixture and for the hydrogel to be extruded into the top chamber of the design. After extrusion, the design would be moved from under the current fixture, and the bottom chamber would be placed into the new syringe. The middle plate would be slid across to allow for the material from the top chamber to enter the bottom chamber, and finally the plunger stick from the syringe would be used to push the material through the design, into the new syringe. The CAD drawing for this design can be found in Appendix K.

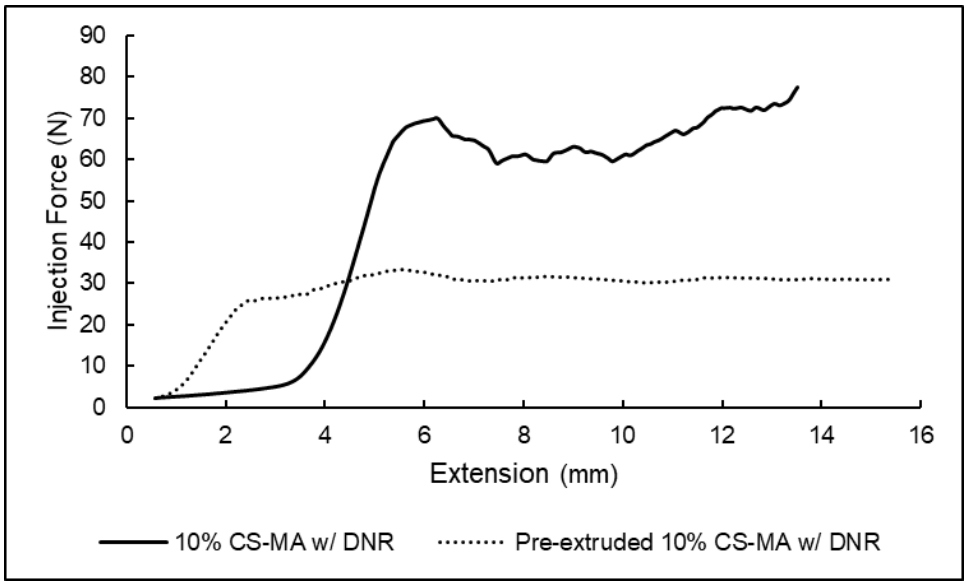

Figure 35: Comparison of injection force profiles of hydrogels loaded with DNR, and hydrogels loaded with DNR that were pre-extruded once.

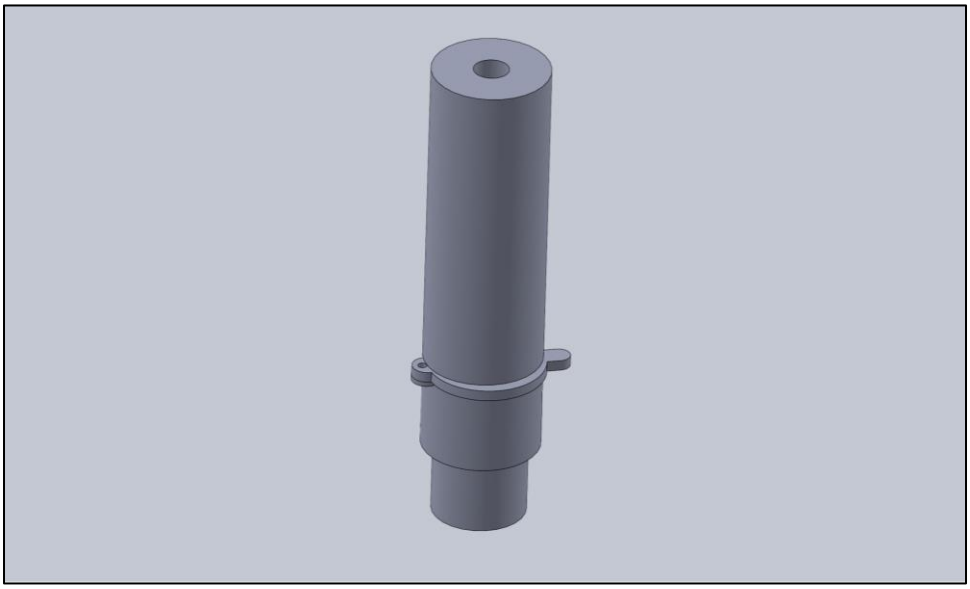

Figure 36: CAD model for pre-extrusion technique.

To prove efficacy of this design the team would recommend running cytotoxicity studies consistent with those already used in the Coburn lab. Previous studies with similar models have shown that this chemotherapeutic is effective in killing cells; however, we recommend studies to confirm that the CS based drug carrier does not also elicit cell death (Ornell et al., 2019). Finally, the team would recommend drug release studies on the extruded material to understand how this difference in hydrogel shape and surface area would impact the release profile.

VI. References

Andrei, M., Turturica, G., Stanescu, P. O., & Teodorescu, M. (2016). Thermosensitive injectable hydrogels from poly(N-isopropylacrylamide)–dextran aqueous solutions: Thermogelation and drug release properties. *Soft Materials*, *14*(3), 162-169. https://doi.org/10.1080/1539445X.2016.1172317

Betancourt, T., Pardo, J., Soo, K., & Peppas, N. A. (2010). Characterization of pH-responsive hydrogels of poly(itaconic acid-g-ethylene glycol) prepared by UV-initiated free radical polymerization as biomaterials for oral delivery of bioactive agents [https://doi.org/10.1002/jbm.a.32510]. *Journal of Biomedical Materials Research Part A*, *93A*(1), 175-188. https://doi.org/https://doi.org/10.1002/jbm.a.32510

Bishnoi, M., Jain, A., Hurkat, P., & Jain, S. K. (2016). Chondroitin sulphate: a focus on osteoarthritis. *Glycoconjugate Journal*, *33*(5), 693-705. https://doi.org/10.1007/s10719-016-9665-3

Brunet-Maheu, J. M., Fernandes, J. C., de Lacerda, C. A., Shi, Q., Benderdour, M., & Lavigne, P. (2009). Pluronic F-127 as a cell carrier for bone tissue engineering. *J Biomater Appl*, *24*(3), 275-287. https://doi.org/10.1177/0885328208096534

Chiu, B., Coburn, J., Pilichowska, M., Holcroft, C., Seib, F. P., Charest, A., & Kaplan, D. L. (2014). Surgery combined with controlled-release doxorubicin silk films as a treatment strategy in an orthotopic neuroblastoma mouse model. *British Journal of Cancer*, *111*(4), 708-715. https://doi.org/10.1038/bjc.2014.324

Chu, C. M., Rasalkar, D. D., Hu, Y. J., Cheng, F. W. T., Li, C. K., & Chu, W. C. W. (2011). Clinical presentations and imaging findings of neuroblastoma beyond abdominal mass and a review of imaging algorithm. *The British journal of radiology*, *84*(997), 81-91. https://doi.org/10.1259/bjr/31861984

Clinic, M. (2021). Chemotherapy for Neuroblastoma. https://www.cancer.org/cancer/neuroblastoma/treating/chemotherapy.html

Coburn, J. M. Free Radical Crosslinking of a Polymer with a Methacrylate Group. In.

Daley, E. L. H., Coleman, R. M., & Stegemann, J. P. (2015). Biomimetic microbeads containing a chondroitin sulfate/chitosan polyelectrolyte complex for cell-based cartilage therapy [10.1039/C5TB00934K]. *Journal of Materials Chemistry B*, *3*(40), 7920-7929. https://doi.org/10.1039/C5TB00934K

Davidoff, A. M. (2012). Neuroblastoma. *Seminars in Pediatric Surgery*, *21*(1), 2-14. https://doi.org/https://doi.org/10.1053/j.sempedsurg.2011.10.009

Fajardo, A. R., Fávaro, S. L., Rubira, A. F., & Muniz, E. C. (2013). Dual-network hydrogels based on chemically and physically crosslinked chitosan/chondroitin sulfate. *Reactive and Functional Polymers*, *73*(12), 1662-1671. https://doi.org/https://doi.org/10.1016/j.reactfunctpolym.2013.10.003

Fan, D.-y., Tian, Y., & Liu, Z.-j. (2019). Injectable Hydrogels for Localized Cancer Therapy [Review]. *Frontiers in Chemistry*, *7*(675). https://doi.org/10.3389/fchem.2019.00675

Gilbert, J. C., Hadgraft, J., Bye, A., & Brookes, L. G. (1986). Drug release from Pluronic F-127 gels. *International Journal of Pharmaceutics*, *32*(2), 223-228. https://doi.org/https://doi.org/10.1016/0378-5173(86)90182-1

Gioffredi, E., Boffito, M., Calzone, S., Giannitelli, S. M., Rainer, A., Trombetta, M., Mozetic, P., & Chiono, V. (2016). Pluronic F127 Hydrogel Characterization and Biofabrication in

Cellularized Constructs for Tissue Engineering Applications. *Procedia CIRP*, *49*, 125-132. https://doi.org/https://doi.org/10.1016/j.procir.2015.11.001

Henrotin, Y., Mathy, M., Sanchez, C., & Lambert, C. (2010). Chondroitin sulfate in the treatment of osteoarthritis: from in vitro studies to clinical recommendations. *Therapeutic advances in musculoskeletal disease*, *2*(6), 335-348. https://doi.org/10.1177/1759720X10383076

Huang, P., Song, H., Zhang, Y., Liu, J., Zhang, J., Wang, W., Liu, J., Li, C., & Kong, D. (2016). Bridging the Gap between Macroscale Drug Delivery Systems and Nanomedicines: A Nanoparticle-Assembled Thermosensitive Hydrogel for Peritumoral Chemotherapy. *ACS Applied Materials & Interfaces*, *8*(43), 29323-29333. https://doi.org/10.1021/acsami.6b10416

Insitute, N. C. (2021). Neuroblastoma Treatment (PDQ®)–Patient Version. https://www.cancer.gov/types/neuroblastoma/patient/neuroblastoma-treatment-pdq

Johnsen, J. I., Dyberg, C., & Wickström, M. (2019). Neuroblastoma—A Neural Crest Derived Embryonal Malignancy [Review]. *Frontiers in Molecular Neuroscience*, *12*(9). https://doi.org/10.3389/fnmol.2019.00009

Kang, H., Liu, H., Zhang, X., Yan, J., Zhu, Z., Peng, L., Yang, H., Kim, Y., & Tan, W. (2011). Photoresponsive DNA-Cross-Linked Hydrogels for Controllable Release and Cancer Therapy. *Langmuir*, *27*(1), 399-408. https://doi.org/10.1021/la1037553

Keutgen, X. M., Ornell, K. J., Vogle, A., Lakiza, O., Williams, J., Miller, P., Mistretta, K. S., Setia, N., Weichselbaum, R. R., & Coburn, J. M. (2021). Sunitinib-Loaded Chondroitin Sulfate Hydrogels as a Novel Drug-Delivery Mechanism for the Treatment of Pancreatic Neuroendocrine Tumors. *Annals of Surgical Oncology*. https://doi.org/10.1245/s10434-021-10245-1

LabX. (n.d.). *https://www.labx.com/product/kinematica-polytron-pt-mr-2100*. LabA. https://www.labx.com/product/kinematica-polytron-pt-mr-2100

Li, Q., Wang, D.-a., & Elisseeff, J. H. (2003). Heterogeneous-Phase Reaction of Glycidyl Methacrylate and Chondroitin Sulfate: Mechanism of Ring-Opening−Transesterification Competition. *Macromolecules*, *36*(7), 2556-2562. https://doi.org/10.1021/ma021190w

Li, Y., Cao, J., Han, S., Liang, Y., Zhang, T., Zhao, H., Wang, L., & Sun, Y. (2018). ECM based injectable thermo-sensitive hydrogel on the recovery of injured cartilage induced by osteoarthritis. *Artificial Cells, Nanomedicine, and Biotechnology*, *46*(sup2), 152-160. https://doi.org/10.1080/21691401.2018.1452752

Liang, Y., Zhao, X., Ma, P. X., Guo, B., Du, Y., & Han, X. (2019). pH-responsive injectable hydrogels with mucosal adhesiveness based on chitosan-grafted-dihydrocaffeic acid and oxidized pullulan for localized drug delivery. *Journal of Colloid and Interface Science*, *536*, 224-234. https://doi.org/https://doi.org/10.1016/j.jcis.2018.10.056

Liu, M., Song, X., Wen, Y., Zhu, J.-L., & Li, J. (2017). Injectable Thermoresponsive Hydrogel Formed by Alginate-g-Poly(N-isopropylacrylamide) That Releases Doxorubicin-Encapsulated Micelles as a Smart Drug Delivery System. *ACS Applied Materials & Interfaces*, *9*(41), 35673-35682. https://doi.org/10.1021/acsami.7b12849

Loaisa, L. S. V., Rahman, M. M. M., Sabillon, F. E. B., & Suqui, K. B. (2018). *A Fabrication System for Chondroitin Sulfate Methacrylate Particles for Drug Release*. https://digital.wpi.edu/show/12579t91m https://digital.wpi.edu/show/6h440v17j

Ma, H., He, C., Cheng, Y., Li, D., Gong, Y., Liu, J., Tian, H., & Chen, X. (2014). PLK1shRNA and doxorubicin co-loaded thermosensitive PLGA-PEG-PLGA hydrogels for osteosarcoma treatment. *Biomaterials*, *35*(30), 8723-8734. https://doi.org/https://doi.org/10.1016/j.biomaterials.2014.06.045

Marinello, J., Delcuratolo, M., & Capranico, G. (2018). Anthracyclines as Topoisomerase II Poisons: From Early Studies to New Perspectives. *International Journal of Molecular Sciences*, *19*(11). https://doi.org/10.3390/ijms19113480

Matthay, K. K., Maris, J. M., Schleiermacher, G., Nakagawara, A., Mackall, C. L., Diller, L., & Weiss, W. A. (2016). Neuroblastoma. *Nature Reviews Disease Primers*, *2*(1), 16078. https://doi.org/10.1038/nrdp.2016.78

McGowan, J. V., Chung, R., Maulik, A., Piotrowska, I., Walker, J. M., & Yellon, D. M. (2017). Anthracycline Chemotherapy and Cardiotoxicity. *Cardiovascular Drugs and Therapy*, *31*(1), 63-75. https://doi.org/10.1007/s10557-016-6711-0

Muzzarelli, R. A. A., Greco, F., Busilacchi, A., Sollazzo, V., & Gigante, A. (2012). Chitosan, hyaluronan and chondroitin sulfate in tissue engineering for cartilage regeneration: A review. *Carbohydrate Polymers*, *89*(3), 723-739. https://doi.org/https://doi.org/10.1016/j.carbpol.2012.04.057

Network, L. S. High-Pressure Homogenization. https://homogenizers.net/pages/ac-high-pressure-homogenization

Nimmano, N., Somavarapu, S., & Taylor, K. M. G. (2018). Aerosol characterisation of nebulised liposomes co-loaded with erlotinib and genistein using an abbreviated cascade impactor method. *International Journal of Pharmaceutics*, *542*(1), 8-17. https://doi.org/https://doi.org/10.1016/j.ijpharm.2018.02.035

Ornell, K. J., Lozada, D., Phan, N. V., & Coburn, J. M. (2019). Controlling methacryloyl substitution of chondroitin sulfate: injectable hydrogels with tunable long-term drug release profiles [10.1039/C8TB03020K]. *Journal of Materials Chemistry B*, *7*(13), 2151-2161. https://doi.org/10.1039/C8TB03020K

Oroojalian, F., Babaei, M., Taghdisi, S. M., Abnous, K., Ramezani, M., & Alibolandi, M. (2018). Encapsulation of Thermo-responsive Gel in pH-sensitive Polymersomes as Dual-Responsive Smart carriers for Controlled Release of Doxorubicin. *Journal of Controlled Release*, *288*, 45-61. https://doi.org/https://doi.org/10.1016/j.jconrel.2018.08.039

Otte, J., Dyberg, C., Pepich, A., & Johnsen, J. I. (2021). MYCN Function in Neuroblastoma Development [Review]. *Frontiers in Oncology*, *10*(3210). https://doi.org/10.3389/fonc.2020.624079

Pezeshki-Modaress, M., Mirzadeh, H., Zandi, M., Rajabi-Zeleti, S., Sodeifi, N., Aghdami, N., & Mofrad, M. R. K. (2017). Gelatin/chondroitin sulfate nanofibrous scaffolds for stimulation of wound healing: In-vitro and in-vivo study [https://doi.org/10.1002/jbm.a.35890]. *Journal of Biomedical Materials Research Part A*, *105*(7), 2020-2034. https://doi.org/https://doi.org/10.1002/jbm.a.35890

Pinto, N. R., Applebaum, M. A., Volchenboum, S. L., Matthay, K. K., London, W. B., Ambros, P. F., Nakagawara, A., Berthold, F., Schleiermacher, G., Park, J. R., Valteau-Couanet, D., Pearson, A. D. J., & Cohn, S. L. (2015). Advances in Risk Classification and Treatment Strategies for Neuroblastoma. *Journal of clinical oncology : official journal of the American Society of Clinical Oncology*, *33*(27), 3008-3017. https://doi.org/10.1200/JCO.2014.59.4648

Polymers, N. PLGA-PEG-PLGA. https://www.nanosoftpolymers.com/product/plga-peg-plga/

Qin, X.-H., Ovsianikov, A., Stampfl, J., & Liska, R. (2014). Additive manufacturing of photosensitive hydrogels for tissue engineering applications. *BioNanoMaterials*, *15*(3-4), 49-70. https://doi.org/doi:10.1515/bnm-2014-0008

Shin, M., Matsunaga, H., & Fujiwara, K. (2010). Differences in accumulation of anthracyclines daunorubicin, doxorubicin and epirubicin in rat tissues revealed by immunocytochemistry. *Histochem Cell Biol*, *133*(6), 677-682. https://doi.org/10.1007/s00418-010-0700-3

Shriky, B., Kelly, A., Isreb, M., Babenko, M., Mahmoudi, N., Rogers, S., Shebanova, O., Snow, T., & Gough, T. (2020). Pluronic F127 thermosensitive injectable smart hydrogels for controlled drug delivery system development. *Journal of Colloid and Interface Science*, *565*, 119-130. https://doi.org/https://doi.org/10.1016/j.jcis.2019.12.096

Society, A. C. (2021a). Chemotherapy Side Effects. https://www.cancer.org/treatment/treatments-and-side-effects/treatment-types/chemotherapy/chemotherapy-side-effects.html

Society, A. C. (2021b). *Neuroblastoma Risk Groups*.

Society, A. C. (2021c). *Treatment of Neuroblastoma by Risk Group*. https://www.cancer.org/cancer/neuroblastoma/treating/by-risk-group.html

Taha, A., Ahmed, E., Ismaiel, A., Ashokkumar, M., Xu, X., Pan, S., & Hu, H. (2020). Ultrasonic emulsification: An overview on the preparation of different emulsifiers-stabilized emulsions. *Trends in Food Science & Technology*, *105*, 363-377. https://doi.org/https://doi.org/10.1016/j.tifs.2020.09.024

Thomas E Robinson, E. A. B. H., Aniruddha Bose, Elizabeth A. Cornish, Jun Y. Teo, Neil M. Einstein, Liam M. Grover, Sophie C. Cox. (2020). Filling the Gap: A Correlation Between Objective and Subjective Measures of Injectability. *Advanced Healthcare Materials*, *9*(1901521), 9. https://doi.org/10.1002/adhm.201901521

Trigg, R. M., & Turner, S. D. (2018). ALK in Neuroblastoma: Biological and Therapeutic Implications. *Cancers*, *10*(4), 113. https://doi.org/10.3390/cancers10040113

van der Graaf, S., Schroën, C. G. P. H., & Boom, R. M. (2005). Preparation of double emulsions by membrane emulsification—a review. *Journal of Membrane Science*, *251*(1), 7-15. https://doi.org/https://doi.org/10.1016/j.memsci.2004.12.013

Wang, L.-F., Shen, S.-S., & Lu, S.-C. (2003). Synthesis and characterization of chondroitin sulfate–methacrylate hydrogels. *Carbohydrate Polymers*, *52*(4), 389-396. https://doi.org/https://doi.org/10.1016/S0144-8617(02)00328-4

Wang, P., Chu, W., Zhuo, X., Zhang, Y., Gou, J., Ren, T., He, H., Yin, T., & Tang, X. (2017). Modified PLGA–PEG–PLGA thermosensitive hydrogels with suitable thermosensitivity and properties for use in a drug delivery system [10.1039/C6TB02158A]. *Journal of Materials Chemistry B*, *5*(8), 1551-1565. https://doi.org/10.1039/C6TB02158A

Wood, J. D. (2004). Sympathetic Innervation. In L. R. Johnson (Ed.), *Encyclopedia of Gastroenterology* (pp. 484-485). Elsevier. https://doi.org/https://doi.org/10.1016/B0-12-386860-2/00680-8

Xu, X., Liu, Y., Fu, W., Yao, M., Ding, Z., Xuan, J., Li, D., Wang, S., Xia, Y., & Cao, M. (2020). Poly(N-isopropylacrylamide)-Based Thermoresponsive Composite Hydrogels for Biomedical Applications. *Polymers*, *12*(3), 580. https://doi.org/10.3390/polym12030580

Yang, Y., Wang, J., Zhang, X., Lu, W., & Zhang, Q. (2009). A novel mixed micelle gel with thermo-sensitive property for the local delivery of docetaxel. *J Control Release*, *135*(2), 175-182. https://doi.org/10.1016/j.jconrel.2009.01.007

Yu, L., Ci, T., Zhou, S., Zeng, W., & Ding, J. (2013). The thermogelling PLGA–PEG–PLGA block copolymer as a sustained release matrix of doxorubicin [10.1039/C2BM00159D]. *Biomaterials Science*, *1*(4), 411-420. https://doi.org/10.1039/C2BM00159D

Zhao, L., Liu, M., Wang, J., & Zhai, G. (2015). Chondroitin sulfate-based nanocarriers for drug/gene delivery. *Carbohydrate Polymers*, *133*, 391-399. https://doi.org/https://doi.org/10.1016/j.carbpol.2015.07.063

Zou, X. H., Foong, W. C., Cao, T., Bay, B. H., Ouyang, H. W., & Yip, G. W. (2004). Chondroitin Sulfate in Palatal Wound Healing. *Journal of Dental Research*, *83*(11), 880-885. https://doi.org/10.1177/154405910408301111

VII. Appendices

Appendix A: Pairwise Comparison Chart

Table 29: Design objectives and sub-objectives PWC chart.

		Consistent Product			User Friendly		Competitive Drug Carrier Properties			Industrial Scalability		Sum
		Reproducible Injection Force	Reproducible Gelation Time	Maintain Insolubility	Safe to Handle	Acceptable Injection Force	Sustained Drug Release	Physiologically Safe Material Degradation	Reliable Drug Loading	Capacity for Sterilization	Consistent Syringe Filling	
Consistent Product	Reproducible Injection Force		1	0.5	1	0	0.5	1	0.5	1	1	6.5
	Reproducible Gelation Time	0		0	0.5	0	0	1	0	1	1	3.5
	Maintain Insolubility	0.5	1		1	0.5	0.5	1	0.5	1	1	7
User Friendly	Safe to Handle	0	0.5	0		0	0	0.5	0	1	0.5	2.5
	Acceptable Injection Force	1	1	0.5	1		1	1	0.5	1	1	8
Competitive Drug Carrier Properties	Sustained Drug Release	0.5	1	0.5	1	0		1	0.5	1	1	6.5
	Physiologically Safe Material Degradation	0	0	0	0.5	0	0		0	1	0.5	2
	Reliable Drug Loading	0.5	1	0.5	1	0.5	0.5	1		1	1	7
Industrial Scalability	Capacity for Sterilization	0	0	0	0	0	0	0	0		0.5	0.5
	Consistent Syringe Filling	0	0	0	0.5	0	0	0.5	0	0.5		1.5

Table 30: Design constraints PWC chart.

	Money	Time	Material Availability	Equiptment Availability	CS Compatability	***Sum***
Money		**1**	**0.5**	**0.5**	**0.5**	**2.5**
Time	**0**		**0**	**1**	**0.5**	**1.5**
Material Availability	**0.5**	**1**		**1**	**0.5**	**3**
Equiptment Availability	**0.5**	**0**	**0**		**0**	**0.5**
CS Compatability	**0.5**	**0.5**	**0.5**	**1**		**2.5**

Appendix B: Final Design Selection Matrix

Table 31: Final design selection matrix.

Sub-Objective		Weight	*Thermosensitive Hydrogel*			Low-Methacrylation CS-MA Hydrogels	*Microbeads*	
			F127	PNIPAM	PLGA-PEG-PLGA		High Pressure Homogenizer	Microfluidics
Consistent Product	Reproducible Injection Force	6.5	1	1	1	1	1	0.5
	Maintain Insolubility	7	0.5	1	1	1	1	1
User Friendly	Acceptable Injection Force	8	1	1	1	0.5	0.5	0.5
Comparable Drug Carrier Properties	Sustained Drug Release	6.5	1	1	1	1	1	1
	Reliable Drug Loading	7	1	1	1	1	1	1
Sub-Objective Score		**35**	**31.5**	**35**	**35**	**31**	**31**	**27.75**
Constraint								
Money		2.5	1	0.5	0	1	0	0
Time		1.5	1	1	1	1	1	0
Material Availability		3	1	1	0	1	1	1
Equipment Availability		0.5	1	1	1	1	0.5	0.5
CS Compatability		2.5	0.5	1	0.5	1	1	1
Constraint Score		**10**	**8.75**	**8.75**	**3.25**	**10**	**7.25**	**5.75**
Total Score		**45**	**40.25**	**43.75**	**38.25**	**41**	**38.25**	**33.5**

Appendix C: Pluronic F127 Hydrogel Fabrication Protocol

Adapted from:

https://www.ncbi.nlm.nih.gov/pmc/articles/PMC3075891/

https://pubmed.ncbi.nlm.nih.gov/15763618/

https://doi.org/10.1016/j.jcis.2019.12.096

Making 15%, 18% and 20% F127 hydrogels

1. Perform calculations to ensure you have the right amount of F127. An example calculation can be seen below.
2. Weight the desired amount of F127 using an analytical balance.
3. Add the weighed amount of F127 to the calculated amount of deionized water in flat-bottomed screw-capped glass vials.
4. Gently mix with magnetic stirrers for 24 h at 4°C until all the F127 granules are completely dissolved, and a clear solution is obtained.
5. Remove glass vials from the cold room and let them sit for at least 12 h at 25°C (room temperature).

Doping F127 hydrogels in CS

Method 1: Mixing CS and F127 together

1. Perform calculations to ensure that the correct amount of CS is being added in conjunction with F127. An example calculation can be seen below.
    - For this experiment, the density of water is assumed to be 1 g/mL.

$$\frac{0.4\ g\ F127}{2\ g\ H_20} = 0.2$$

$$\frac{0.1\ g\ CS}{2\ g\ H_20} = 0.05$$

2. Weight the desired amount of F127 and CS using an analytical balance.
3. Add the weighed amount of F127 and CS to the calculated amount of deionized water in flat-bottomed screw-capped glass vials.
    - From the example calculation above, 0.4 g of F127 and 0.1 g of CS would be added to 1.5 g (or mL) of deionized water. The amount of water is determined by

subtracting the total amount of powdered material added from the amount of water used in the calculations (in this case, 2 mL).

4. Gently mix with magnetic stirrers for 24 h at 4°C until all the F127 granules and CS powder are completely dissolved, and a clear solution is obtained.
5. Remove glass vials from the cold room and let them sit for at least 12 h at 25°C (room temperature).

Method 2: Adding CS after mixing

1. Perform calculations to ensure that the correct amount of CS is being added in conjunction with F127. The same calculation as method 1 should be used.
    - For this experiment, the density of water is assumed to be 1 g/mL.
2. After F127 solution has been dissolved, add the weighed amount CS to solution at 4°C.
3. Gently mix solution with magnetic stirrers at 4°C until solution is completely dissolved.
4. Remove glass vials from the cold room and let them sit for at least 12 h at 25°C (room temperature).

Appendix D: Protocol for PNIPAM-CS Synthesis

PNIPAM-CS Conjugation

1. Bring 500 mM MES buffer stock to 100 mM concentration and pH 6.5.
    a. (ex) For a final volume of 125 mL: add 75 mL of ultrapure water to 25 mL of the 500 mM stock; adjust pH, then bring to a final volume of 125 mL.
2. Dissolve the desired amount of EDC, NHS, and CS in 100 mM MES buffer solution, such that the molar ratio of carboxyl group of CS/EDC/NHS is 1:1:1, and there are 0.2 moles of PNIPAM per 1 mole of disaccharide in CS. Allow to mix on a stir plate at 4°C for 15 minutes.
3. Dissolve 1 g of PNIPAM in the MES buffer solution from step 2 to a final concentration of 20 mg/mL. Allow to mix on a stir plate at 4°C for 24 hours.
4. After 24 h, aliquot approximately 30 mL of the solution into 3.5 kD dialysis tubing. Cut tubes to approximately 25 cm, with excess for sealing. Use dialysis clips to seal both ends, ensuring that all air is removed.
5. Place tubes into a 4000 mL beaker and fill with DI water. Prevent tubes from falling to the bottom of the beaker by fastening one end of each tube to a long bar and rest bar across the top of the beaker.
6. Add a large stir bar to the beaker and place it on a stir plate at 4°C.
7. Replace the DI water regularly for 3 days to ensure fresh dialysis as the salts release through the dialysis tubing.
    a. On Day 1, replace the DI water at least 3 times.
    b. For Day 2 and 3, replace the DI water twice, in the morning and afternoon.
    c. ***CAUTION*** The dialysis tubes should never be completely full, as this can cause bursting. While the tubes will swell a significant amount, if there are ever at risk of bursting, realiquot the solution into an additional tube for dialysis duration.
8. Once dialysis is completed, aliquot 30 mL of the solution into 50 mL conical tubes, with a KimWipe secured over the top with a rubber band, instead of its cover.
9. Freeze the solution in the conical tubes, and then lyophilize the solution for 5 days.
    a. The lyophilized solution can then be stored in the freezer.

PNIPAM-CS Hydrogel Formulation

1. Weight the desired amount of PNIPAM-CS using an analytical balance.
2. Add the weighed amount of PNIPAM-CS to the calculated amount of PBS in an Eppindorf tube.
3. Allow PNIPAM-CS solution to dissolve in PBS at 4°C for approximately 30 minutes, or until completely dissolved.
4. Aliquot desired volumes into new Eppendorf tubes and perform gelation studies in hot block at 37°C.

Appendix E: Protocol for CS-MA Synthesis

1. Dissolve 5 g CS into 45 mL ultrapure water in round bottom flask with cap.
    a. This takes some time to ensure all the powder is dissolved. Add the ultrapure water to the round bottom flask and get stirring then add the CS powder. If you do this slowly, you might minimize clumping, which will make dissolution easier.
2. Add 32.5 mL GMA 97%, 100 ppm MMEQ inhibitor (Sigma 151238).
3. Adjust the pH to 3.5 using 1.5 M HCL.
4. React at 60°C in oven, w/ stirring (3 cm stir bar; use the Corning stir plate on the lowest setting – otherwise it will throw the stir bar off and not mix correctly), light protected, time depends on length of reaction needed (typically ranges 2-24 h).
5. Precipitate with acetone (500 mL), gently pour down the side.
6. Carefully pour off acetone so that precipitate is left at the bottom (if poured correctly it should remain as a large piece in the bottom of the beaker, some small pieces/cloudy liquid may come off, try to retain larger pieces).
7. Wash with acetone (250 mL) by pouring new acetone onto precipitate then removing carefully.
8. Let dry at RT overnight (light protected).
9. In a 50 mL beaker, resuspend in 25 mL H2O + 10 mL ultrapure water beaker rinse (light protected).
    a. This takes some time to dissolve. Mix on a stir plate until dissolved. Perturbing the clumps with a 200 uL pipette tip helps.
10. Dialyze minimum 48 h against ultrapure water with 6 water bath changes (Morning, Midday, Afternoon, depending on when you start) (light protected) (I recommend 7-8 in of tubing x 2 and splitting a 5 g reaction into 2 tubes, take care to make sure it does not explode).
11. After dialysis, transfer content of tubing into a 500 mL beaker.
12. Transfer the content of the beaker into 50 mL conical tubes.
    a. For a 5 g batch, you will have about 240 mL (8 x 30 mL per tube).
13. Centrifuge at 2,500 rpm for 5 minutes. Rinse 500 mL beaker with ultrapure water.
14. Transfer the content of the centrifuged 50 mL conical tubes into the rinsed 500 mL beaker.

15. Rinse the 50 mL conical tubes with ultrapure water.
16. Transfer to content of the 500 mL beaker back into the rinsed 50 mL conical tubes, maximum 30 mL per tube.
17. Freeze at -80°C overnight.
18. Lyophilize minimum 72 h (light protected) (at -25°C, 210 mTorr or on side arm 4th floor lyo)
19. Store at -20°C after lyophilization.

Appendix F: Protocol for CS-MA Hydrogels

Making CS-MA Hydrogel Solution:

1. Calculate weight of CS-MA necessary to achieve the desired concentration and volume of hydrogel.
2. Weigh out CS-MA directly into a microcentrifuge tube. Any centrifuge appropriate in size (i.e. 1.7 mL tubes or 15 mL conical tubes can be used here on the quick/short settings as RPM is not important).
3. Weigh out minimal amount of (<10 mg) as you will need very little.
4. Add the calculated volume of ultrapure water to the CS-MA.
5. Invert the tube, top over bottom multiple times to dissolve the CS-MA. You may also gently shake and tap on the countertop to facilitate dissolution. Continue with this process until no noticeable clumps are present.
    a. If necessary, use a glass aspiration pipette to break up and clumps of CS-MA in the bottom of the tube.
6. Centrifuge at maximum speed for 2 minutes to separate any undissolved materials.
    a. If there appears to be a large amount of undissolved materials, pipette up and down to try to dissolve further.
7. Use 70% ethanol to make a 10% Irgacure® 2959 solution. Vortex to dissolve, ensure no Irgacure® 2959 is stuck on the sides of the tube.
8. Add 10% Irgacure® 2959 solution to the CS-MA solutions at a ratio of 1:100 for 4 h CS-MA solutions (10 µL Irgacure® 2959 stock to 1 mL CS-MA solution) and 1:50 to 8 h and 24 h CS-MA solutions (20 µL Irgacure® 2959 stock to 1 mL CS-MA solution).
9. Pipette up and down until well mixed (Note: dispose of extra Irgacure® 2959 after hydrogels are complete).
    a. Critical Step: The CS-MA solution is viscous. If the Irgacure® 2959 is homogeneous distributed in the solution, you will not get consistent hydrogel formation. Therefore, use a pipette setting about 20% less than the volume of CS-MA solution to pipette up and down and ensure well mixing (use positive displacement pipettors to minimize CS-MA solution loss).

10. Centrifuge at maximum speed for 2 minutes to separate any undissolved materials.
    a. Critical step: undissolved materials will be trapped within the hydrogel. Undissolved materials will interfere with light exposure.

Gelling and swelling of 20 μL Gels

1. Pipette the 20 μL for each hydrogel onto a clean flat surface.
2. Place the droplets under a Portable luminere UV light for 10 minutes (make sure the droplets are lined up in a straight line directly under the light so that they get evenly exposed and are as close vertically to the lamp as possible).
3. If the droplets have gelled after 10 minutes carefully removed them from the surface with a clean razorblade, wash 3 times with ultrapure water and place them in ultrapure water to swell for approximately 3 days.

Gelling and swelling of 50 μL Gels:

1. Pipette the 50 μL for each hydrogel into a cutoff syringe set-up.
2. Place the syringes under a Portable luminere UV light for 10 minutes (make sure the droplets are lined up in a straight line directly under the light so that they get evenly exposed and are as close vertically to the lamp as possible).
3. If the solution has gelled after 10 minutes, wash 3 times with ultrapure and suspend them in ultrapure water to swell for approximately 3 days, in the syringe set-up.

Appendix G: Protocol for Instron Testing

Adapted from:

Instron Training Checklist

Compression Testing Method- Keely Nistler

Generation of Bluehill Method:

1. In Bluehill start by creating a testing method and choose the compression test option
2. Within the General tab select SI for units
3. In the Calculations tab select Peak Max/Min
4. To designate the collection data for testing select the following in the Test tab:
    1. Start by using start button
    2. Test: 4 mm/min rate
    3. End of Test: Measurement Event- Extension (Measure the height of the hydrogel using calipers each time of testing and input here)
    4. Data: Take data every 250 ms
5. In the Console tab select the following:
    1. Set Live Display to Extension and Load
    2. Set a Soft Key for zeroing extension
6. For the Workspace tab select the following:
    1. Results 1: Max Load, and Specimen Label
    2. Graph 1: Extension v. Load
    3. Raw Data, Time, Extension, and load
    4. Layout: Graph and Result table
7. To select the information being exported use the Export tab to select the following:
    1. File settings: Set the location where the file should be saved to
    2. Export results
    3. Export raw data (and include the specimen label and test rate)
8. Int the Prompted Test tab select the following:
    1. Choose “Before Specimen” and “After Specimen”
        1. In “Before Specimen” select specimen label
        2. In the test menu: select “rate”

9. In the “Before Test” put: “Make sure to zero extension and load”

Testing Hydrogels for Injection force:

1. Upon entering, check in the Instron room that the Instron is on. If not, turn on to warm up for 15 minutes. During this time also sign in into the logbook
2. Before entering the Instron room to test, preload the syringes with the hydrogels to test for the day
3. Once the Instron has warmed up, follow these step (taken from the Instron Training Checklist)
4. Make sure the Instron is in Vertical position for Instron testing
5. Start the Instron Console software
6. Make sure to select proper commissioning files for the orientation of the Instron.
    1. Click the double arrow in the bottom left of the Console bar
    2. Click the wrench
    3. Click yes, you are sure you want to continue
    4. Click the Pink Electropuls tab
    5. Select the commission tab on the left side bar
    6. Select vertical commissioning, next, and okay
7. Attach the 2 kN load cell (attached to machine, place the data cable in the head in the proper position)
8. Calibrate the load cell by going to “Load” in the console, selecting “Calibration”, “Calibration Wizard”
    1. Keep all default values and move through the menu.
    2. Select “Auto Calibrate and press start”
    3. Following calibration make sure you “Lock Calibration” and “Save Calibration” with a file name with the appropriate inputs as follows “date.load cell.initials”
9. On the Instron, move the actuator into position (make sure to place into I mode), to the bottom black line
10. Within both “Load” and “Position” tabs in the console go to “Primary Limits” and enable the limits
11. Open Bluehill and select the MQP Compression Test Protocol from the team flash drive
    1. If messages come up select “no” to move forward

12. Measure the height of the gel before loading in the box and input into the extension measurement control in the Protocol pink tab
13. Load the sample into the syringe testing box as follows:
    1. If on the Instron, remove the bottom silver plate with an Alen wrench so the dark grey platform is left.
    2. Place the syringe (28 G, 0.5 mL, 0.5 in) into the hole in the top of the syringe box
    3. Place the finger holds of the syringe underneath the washers on the top of the box and tighten the bolts to hold the syringe in place
14. On the Instron, attach the Syringe Compression hold with a pin and safety lock
15. Place the Syringe box on the Instron and lower the actuator into position so the plunger is placed in the hole of the syringe compression hold
    1. Move the body of the Instron if necessary, with the black switch on the controls box
16. One in place zero the extension and balance the load cell
17. Input proper specimen labels and run the tests necessary
18. Remove the sample and box from the Instron when finished **(Before Exporting Data, Closing Bluehill, and Closing the console)**
19. In a new folder on the flash drive make sure to save the protocol before finishing the test.
20. Select Finish test and select “no” for running more samples
21. Check the flash drive and make sure the data from the test was saved
    1. If needed look through the computer to find the exported files
22. Close the Instron Console

Notes:

1. Remember to always take proper safety precautions and wear proper PPE or Goggles
2. If you need to stop the machine in an emergency, hit the red button on the actuator. In order to start it again after this, you will need to turn the button to release it.
3. Do not store your results on the computer. Copy them on to an external device and delete them off of the computer and empty the recycling bin.
4. All accessories for the Instron must remain in the Instron room - be careful not to walk away with any pieces.

5. Always clean up after yourself, wipe down all surfaces with 70% ethanol and put items back in their place.
6. If you experience any problems with the Instron, report them IMMEDIATELY

Appendix H: Protocol for Short-Term Dissolution of Hydrogels in PBS

Adapted from:

https://www.ncbi.nlm.nih.gov/pmc/articles/PMC3075891/#!po=50.5435

Dissolution Protocol:

1. Record the weight of a 1.5 mL Eppendorf tube.
2. Pipette 500 µL of F127 and/or CS solution into 1.5 mL Eppendorf tube.
3. Allow the sample to gel fully in the hot block at 37°C.
4. Record the weight of the 1.5 mL Eppendorf tube plus the hydrogel for time 0.
5. Add 0.5 mL of pre-warmed PBS into the Eppendorf tube with F127 and/or CS and allow it to remain in hot block until next time point.
6. After 2 h remove the Eppendorf tube from the hot block, aspirate off the PBS and record the weight of the Eppendorf tube plus the hydrogel.
7. Replace the aspirated PBS with 0.5 mL of fresh pre-warmed PBS.
8. Repeat this process at time points: 1 h, 3 h, 5 h, 7 h, 9 h, 11 h, 23 h, 27 h, 31 h, 35 h, 47 h, 51 h, 55 h, and 59 h. Or until the gel has completely dissolved.

Appendix I: Protocol for DMMB Assay

Adapted from:

https://www.researchgate.net/publication/308759000_Dimethylmethylene_Blue_Assay_DMMB

Reading pH of DMMB Solution:

1. Read pH of solution; it should be approximately 3.

Notes: Protect from light and do not use it if precipitate is present.

Preparing DMMB samples from hydrogels

1. Place one CS-MA gel in each well of a 24-well plate.
2. Add 1 mL of PBS to each sample and place the well plate in a dark, secure area.
3. Once daily, replace the 1 mL of PBS in each sample.
    a. Save the PBS from each day and ensure adequate labeling to differentiate samples. Store at 4°C for later evaluation.
4. After 7 days, remove the samples from the dark area.

Running of the DMMB Assay:

1. Prepare a solution of CS. Dissolve 10 mg (0.01 g) CS in 1 mL of ultrapure water. Dilute to 0.5 mg/mL (500 µg/mL) by adding 0.05 mL (50 µL) of the stock and 0.95 mL (950 µL) ultrapure water.
2. Using a 96-well plate, pipet the CS solution, with PBS when required, to make a standard curve according to the table below. Each aliquot should have a total volume of 20 µL.

Standard #	Standard (µg/mL)	Vol (µL) 500µg/mL Standard	Vol PBS (µL)	Vol DMMB (µL)
1	0	0	20	200
2	25	1	19	200
3	50	2	18	200
4	75	3	17	200
5	100	4	16	200
6	125	5	15	200
7	150	6	14	200
8	175	7	13	200
9	200	8	12	200
10	225	9	11	200
11	250	10	10	200
12	500	20	0	200

3. Pipet 20 µL of each day's PBS sample from the CS-MA hydrogels into the same 96 well plate.
4. Add 200 µL of DMMB solution to the standard curve aliquots and each sample.
5. Immediately place the plate into a spectrophotometer with a 525 nm filter set and a 5 second pre-shake to read the absorbance.

Notes: The DMMB-GAG complex results in the formation of turbidity, which begins to precipitate after approximately 10 minutes. For this reason, absorbance measurements should be completed immediately after solutions are prepared.

Appendix J: Protocol for DNR Loading and Release Studies

Drug Loading

1. Retrieve DNR powder from the fridge. Let it warm up at room temperature for 1 to 2 minutes to avoid condensation.
2. Weigh 5 mg of DNR using an analytical balance. Use chemical resistance gloves when doing so.
3. Prepare a 5 mg/mL stock solution by adding the weighed amount of DNR to the desired amount of deionized water. Be extremely careful and pipette slowly.
4. Perform a 1:100 dilution, from 5 mg/ml to 500 µg/ml. This will be the loading solution used for the experiment.
5. Retrieve a 24-well plate for the hydrogels to be transferred to. Add 1 mL of loading solution per well and let the hydrogels load for 2 days (48 h).
6. Store remaining solutions in the fridge.

Drug Release

1. Perform a serial dilution as described below.

Dilutions with Deionized Water

Start with:	Dilution process
500 µg/mL (loading solution)	200 µL loading solution + 300 µL deionized water
200 µg/mL	250 µL previous dilution+ 250 µL deionized water
100 µg/mL	250 µL previous dilution+ 250 µL deionized water
50 µg/mL	250 µL previous dilution+ 250 µL deionized water
25 µg/mL	250 µL previous dilution+ 250 µL deionized water
12.5 µg/mL	250 µL previous dilution+ 250 µL deionized water
6.25 µg/mL	250 µL previous dilution+ 250 µL deionized water
3.125 µg/mL	250 µL previous dilution+ 250 µL deionized water
1.56 µg/mL	250 µL previous dilution+ 250 µL deionized water
0.78 µg/mL	250 µL previous dilution+ 250 µL deionized water

Dilutions with PBS

Start with:	Dilution process
500 µg/mL (loading solution)	200 µL loading solution + 300 µL PBS
200 µg/mL	250 µL previous dilution+ 250 µL PBS
100 µg/mL	250 µL previous dilution+ 250 µL PBS
50 µg/mL	250 µL previous dilution+ 250 µL PBS
25 µg/mL	250 µL previous dilution+ 250 µL PBS
12.5 µg/mL	250 µL previous dilution+ 250 µL PBS
6.25 µg/mL	250 µL previous dilution+ 250 µL PBS
3.125 µg/mL	250 µL previous dilution+ 250 µL PBS
1.56 µg/mL	250 µL previous dilution+ 250 µL PBS
0.78µg/mL	250 µL previous dilution+ 250 µL PBS

2. Retrieve 24-well plate with loaded hydrogels and transfer them to lo-bind. Add 1 mL of PBS solution to each tube.
3. Place tubes in the incubator for the designated time of the release study.
4. Retrieve 3 microcentrifuge tubes and perform a 1:10 dilution with loading solution. For each tube, add 30 µL of loading solution and 270 µL of deionized water.
5. Prepare the plate as shown below.

	1	2	3	4	5	6	7	8	9	10	11	12
A	500	1.56	200	0.78	L1							
B	200	0.78	100	PBS	L2							
C	100	H_20	50	PBS	L3							
D	50	H_20	25		DL1							
E	25		12.5		DL2							
F	12.5		6.25		DL3							
G	6.25		3.125									
H	3.125		1.56									

L = loading solution; DL = diluted loading solution

6. To read how much drug was released during each round, place the plate in the spectrometer and use the software available on the computer to perform the reading. The wavelength setting for DNR should be 486 nm.
7. When done using the machine, close the drawer and exit out of the software before turning machine off.
    1. Clean all the plates used in the release study using a 1 ml pipette to transfer the liquid to the waste bottle. Rinse the 96-well plate 3 times using deionized water. Place the well plate in the oven upside down for no more than 24 hours to dry out.

Appendix K: Pre-Extrusion Funnel Drawing

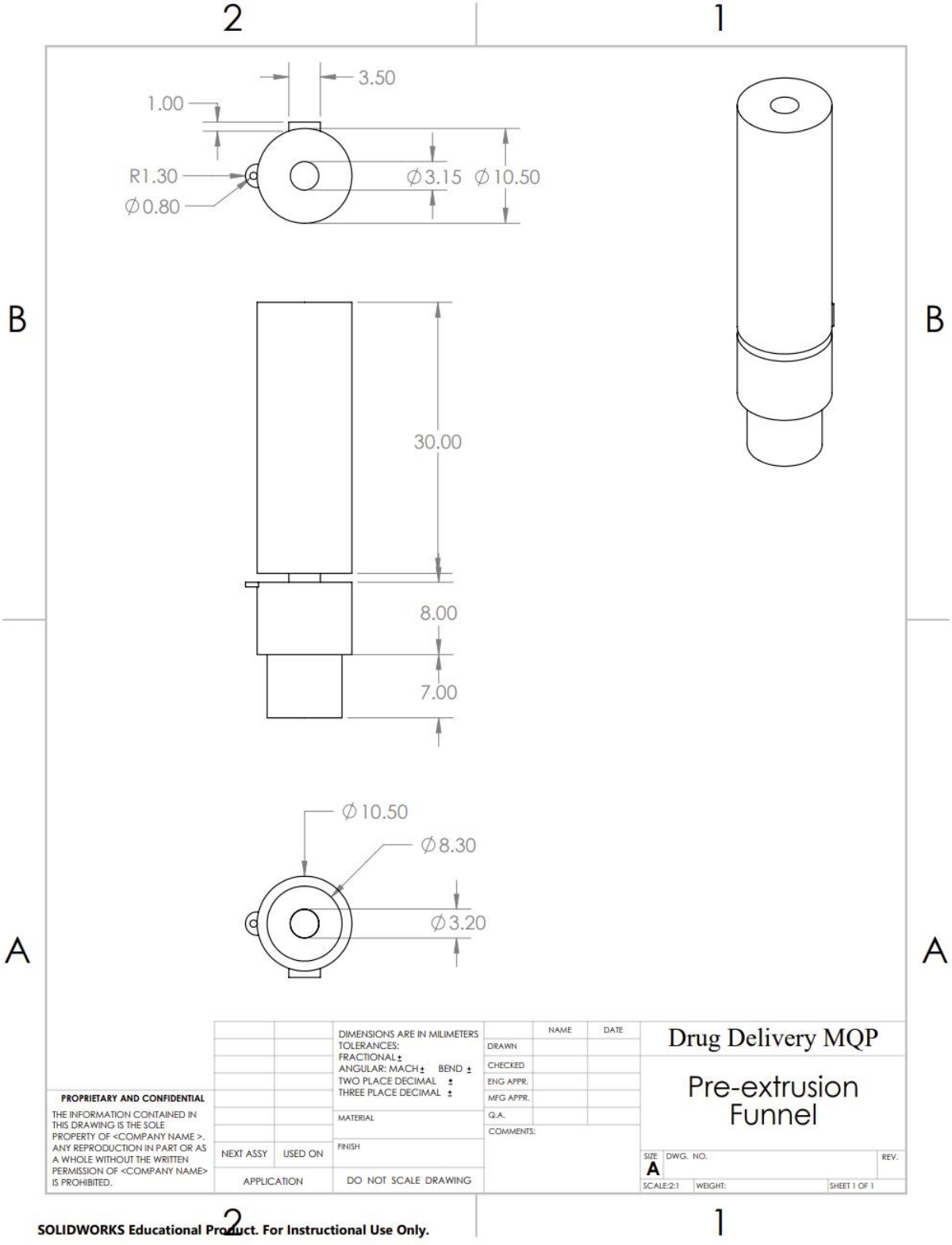

Figure 37: Pre-extrusion funnel engineering CAD drawing.